ANTI-VIRAL RNAi AND ITS SUPPRESSION IN PLANTS

A Thesis

by

JESSICA J. CIOMPERLIK

Submitted to the Office of Graduate Studies of
Texas A&M University
in partial fulfillment of the requirements for the degree of

MASTER OF SCIENCE

August 2008

Major Subject: Plant Pathology

ANTI-VIRAL RNAi AND ITS SUPPRESSION IN PLANTS

A Thesis

by

JESSICA J. CIOMPERLIK

Submitted to the Office of Graduate Studies of
Texas A&M University
in partial fulfillment of the requirements for the degree of

MASTER OF SCIENCE

Approved by:

Chair of Committee,	Herman B. Scholthof
Committee Members,	Karen-Beth G. Scholthof
	Hisashi Koiwa
Head of Department,	Dennis C. Gross

August 2008

Major Subject: Plant Pathology

ABSTRACT

Anti-viral RNAi and Its Suppression in Plants. (August 2008)
Jessica J. Ciomperlik, B.S., Texas A&M University
Chair of Advisory Committee: Dr. Herman B. Scholthof

As a defense against viral infection, plants are thought to use RNA-induced silencing complexes (RISCs) to target and cleave viral RNA. To counteract this, some viruses have evolved proteins to inhibit RISC-mediated activity, thus ensuring continued virulence. This research focused on the study and analysis of the anti-viral RNAi response to various viruses in plants to gain an understanding of how the plant defense operates on the molecular and biochemical levels. *Nicotiana benthamiana* plants were infected with *Tomato bushy stunt virus* (TBSV) and *Tobacco rattle virus* (TRV). These plants were subjected to column chromatography methods, and fractions contained a virus-specific ribonuclease activity, co-eluting with small interfering RNAs (siRNA), that was shown to be sensitive to inhibition with EDTA and enhanced by the addition of divalent metal cations. This ribonuclease activity co-purified with proteins that contained a domain from the hallmark RISC protein Argonaute family. To further study host responses to viral infection, monocots were infected with *Panicum mosaic virus* (PMV) and satellite panicum mosaic virus (SPMV) and also were subjected to column chromatography following infection. Preliminary studies show that fractions contained ribonuclease activity as well as siRNAs and proteins containing an Argonaute domain. Additionally, silencing suppressors have been directly implicated in interfering with RNAi pathways in plants. Studies involving *Agrobacterium*- and virus-vectored cDNA to express green fluorescent protein (GFP) were used to establish that co-introduced suppressors of RNAi can extend the production of a foreign protein for enhancement of biotechnological applications. It was found that the hordeivirus protein γb contributes to enhancement of expression for the foreign protein GFP early in the

infection, while the potyvirus protein HcPro and tombusvirus protein P19 enhance and extend protein production later in the infection.

ACKNOWLEDGEMENTS

In working toward my master's degree, I am fortunate to have several people whom I would like to acknowledge here.

Many, many thanks to Dr. Herman Scholthof, my advisor, for allowing me to work in his laboratory, as well as for his encouragement, advice, and especially patience. My appreciation goes to Dr. Karen-Beth Scholthof for her support, discussions, and literature recommendations. Thank you to Dr. Hisashi Koiwa for experimental design advice and manuscript comments.

I would like to convey my gratitude to my labmates. Thank you to Rustem Omarov for his mentorship, advice, and for teaching me most of the laboratory techniques used here - without him this thesis would not have been possible. Many thanks to Yoshimi Yamamura, Yi-cheng Hsieh (John) and Dong Qi (Tony) for their encouragement, general lab advice, and leadership by example (and a special thanks to John for the healthy plants!). I am grateful to Bonnie Seaberg, Anthany Everett, Christa Chavez, Kristina Twigg, Malika Shamekova, Shuga Manabayeva, Veria Alvarado, and Vanessa Vaughn for their support and conversations. I would also like to express my appreciation to the faculty, staff, and students of Plant Pathology for their encouragement.

Additionally, I thank my parents, brother, family, and friends - Kelly, Karla, Cass, Zachary, Frankie, Sonia, Brandon, Shaw, and others - for their unfailing support and enthusiasm.

Thanks, you guys!

TABLE OF CONTENTS

CHAPTER Page

LIST OF FIGURES

Page

Page

LIST OF TABLES

Page

CHAPTER I
INTRODUCTION AND SYSTEMS

Introduction

Following infection with a virus, some plants can 'clear' viral material from upper, new plant tissue, and remain resistant to a second infection. This phenomenon was first observed in a *Tobacco ringspot virus* infection of tobacco (Wingard, 1928), but only recently ascribed to RNA interference (RNAi) (Baulcombe, 2004). RNAi is a conserved pathway that post-transcriptionally silences RNA by recognition of target RNA. Double-stranded RNA (dsRNA) serves as the trigger for the RNAi pathway upon cleavage into duplexed small interfering RNAs (siRNAs) or hairpin microRNAs (miRNAs), which act in either a sequence-specific manner to target and degrade ssRNAs, or to guide methylation of specific nucleotide sequences. Fire, Mello and colleagues first described the RNAi pathway using *Caennorhabditis elegans* (Fire et al., 1998; Baulcombe, 2004). Due to wide conservation across many species, RNAi has also been described as co-suppression of homologous genes in petunia plants, quelling in the fungus *Neurospora crassa*, and as RNAi in *Drosophila melanogaster,* mammalian and human cells (Romano and Macino, 1992; Hammond et al., 2001; Liu et al., 2004).

Virus-infected plants form a convenient platform to elucidate the so far incomplete understanding of the biochemical complexities of RNA effector complexes (Omarov et al., 2007; Pantaleo et al., 2007). This is particularly important in studying plant-microbe interactions, especially while considering the frequently-used technique of virus-induced gene silencing (VIGS) (Burch-Smith et al., 2004). This work will center on the siRNA branch of the RNAi pathway, as all viruses produce RNA within plants, rather than the endogenous miRNA pathway in plants.

Because *D. melanogaster* and human RNAi pathways have been studied the most intensely, models are based on what is known from these systems. The most commonly accepted RNAi model is described in Fig. 1.1. For this, dsRNA in the cell is either transcribed directly from DNA by RNA synthesis from complementary strands, or

---

This thesis follows the style of The Plant Cell.

can accumulate in the cell via viral infection or by artificial introduction (Filipowicz, 2005). These dsRNAs are cleaved into smaller segments by a member of the Dicer protein family before being loaded into a RNA-induced silencing complex (RISC) (Fig. 1.1), which is postulated to be a high-molecular weight complex composed of several proteins. Proteins described in other systems as contributing to RISC include one or more loading proteins, proteins from the Argonaute (Ago) family, and possibly a protein from the Dicer family (Song and Joshua-Tor, 2006; MacRae et al., 2007; Tomari et al., 2007). Ago proteins are the catalytic effector unit of RISC, and as such, is a signature protein of this pathway (Hammond et al., 2001; Baumberger and Baulcombe, 2005). It must be mentioned that while there are similarities, RNAi processes are not identical in different species. Along these same lines, RNAi and RISCs for plants might share some common elements with other systems, but may also have specific properties.

For the general postulated pathway, there are several concepts regarding how a duplexed siRNA is loaded onto the RISC and converted into an ssRNA able to associate with long ssRNA for targeting. Possibilities include interaction of the siRNAs with the RISC proteins themselves forcing apart the siRNA duplex to allow association with the Ago protein (Tomari and Zamore, 2005), or that RNA helicase A might be involved to unwind the siRNA duplex, rendering it an active siRNA, as seen in the human cell model (Robb and Rana, 2007). Yet other theories speculate that the spare siRNA strand may be discharged from the RISC in a manner similar to that of the later cleavage of long ssRNA, leaving 11 and 12 nucleotide (nt) strands (Leuschner et al., 2006). While it was previously thought that this process required ATP, this is not the case (Hannon, 2002).

The Ago family of proteins can be divided into two subgroups based on their similarity to Ago1 or Piwi found in *Arabidopsis thaliana* or *Drosophila*, respectively. Two protein domains, Piwi-Argonaute-Zwille (PAZ) and Piwi, are always found associated with this family of proteins, in addition to the N-terminal domain and middle domain (Song and Joshua-Tor, 2006). The Ago Piwi domain is thought to have an RNase H-type fold (Liu et al, 2004) containing an Mg^{2+} ion to catalyze the cleavage of target RNA (Tomari and Zamore, 2005). The PAZ domain (Baulcombe, 2004), also found in

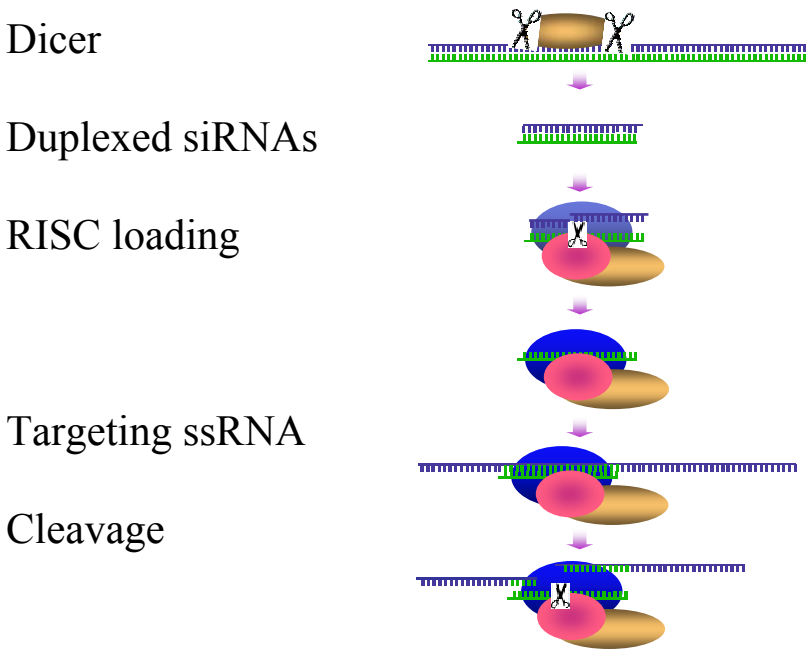

Fig. 1.1 Proposed model of anti-viral RNAi in plants, based on the previously acknowledged proteins from other model systems. Long dsRNAs are recognized by Dicer and cleaved into 21-nt duplexed siRNAs. These siRNA duplexes are loaded onto RISCs, and the passenger strands are released. The active RISC then targets ssRNA in the host homologous to the siRNA for cleavage.

Dicer, recognizes the 2-nt overhangs on duplex siRNAs (Meister et al., 2004) and is a highly-conserved 130 amino acid sequence (Carmell and Hannon, 2004). The crystal structure for an Ago protein from *Pyrococcus furiosus*, an archeabacterium, shows that the PAZ domain is located across a positively charged 'groove' in the protein. It binds the 3' end of the guide siRNA, and the position of the PAZ domain facilitates cleavage via Piwi domain of the long ssRNA upon presumable association with the bound guide siRNA (Song and Joshua-Tor, 2006). As there are several Ago proteins contributing to different types of RNAi, the specific role that the many Ago proteins fulfill is still under investigation (Meister et al., 2004; Toila and Joshua-Tor, 2007).

Once RISC is loaded, the incorporated siRNA allows for sequence-specific binding to a target ssRNA (Fig. 1.1). Cleavage of the target RNA then occurs in a manner similar to that of RNase H, 10-nt in from the 5'- end of the bound siRNA (Ameres et al., 2007). An Ago protein of about 150 kDa has been isolated from *Arabidopsis thaliana* chromatography fractions possibly indicating that only the Ago protein and associated siRNA are required for ribonuclease activity (Baumberger and Baulcombe, 2005). This, considered with other data, suggests that while the holoRISC (before activity) may contain multiple proteins, only the Ago protein is necessary for cleavage activity and that this exact protein varies between species and possibly even functions of RNAi.

During a viral infection, it is hypothesized that viral RNAs are cleaved into duplex siRNAs by a Dicer-like protein. Following this, these siRNAs then associate with a RISC-like complex to form an active, anti-viral RISC that can subsequently be purified using column chromatography methods and studied in vitro. Experiments toward the elucidation of the proteins involved in the RNAi pathway following viral infection of *Nicotiana benthamiana* with *Tomato bushy stunt virus* (TBSV) have shown evidence of RISC-like activity (Omarov et al., 2007). For these experiments, proteins from infected plant tissue are separated using column chromatography and subsequently analyzed for ribonuclease activity. For instance, viral RNA transcripts are added to plant fractions to assay for activity; fractions exhibiting such activity will degrade the exogenously added RNA. Currently, the composition of the anti-TBSV RISC is not known, nor is it clear whether other viruses activate a similar anti-viral RISC. Therefore, a major aim of this project was to further purify the anti-viral RISC and better characterize potential RISC-

contributing proteins. TBSV, *Tobacco rattle virus* (TRV), and the monocot-infecting *Panicum mosaic virus* (PMV) and satellite panicum mosaic virus (SPMV) (Scholthof et al., 1999b) will be compared to examine how different plant viruses might affect an RNAi pathway.

Interestingly, viruses have evolved mechanisms that overcome or impede the RNAi pathway by encoding silencing suppressor proteins, though these proteins often have other functions in addition to their roles in silencing suppression (Scholthof, 2005). This is a widely used manner of host defense evasion, and there are myriad suppressors and modes of action (Silhavy and Burgyan, 2004; Voinnet, 2005). For instance, some silencing suppressors produce proteins to interact with the siRNAs after generation by Dicer, before the duplex is incorporated into the RISC. This method is used by the P19 protein from tombusviruses, where dimers interact with the sugar-phosphate backbone on the siRNAs in a sequence unspecific manner to sequester the siRNAs away from RISCs (Fig. 1.1). HcPro is a silencing suppressor encoded by potyviruses. It has been suggested that HcPro possibly modifies the function of plant Dicer-like enzymes that generate duplexed siRNAs (Mlotshwa et al., 2005) due to accumulation of long dsRNAs in the plant. However, HcPro has been shown to associate with duplexed siRNAs (Lakatos et al., 2006), indicating that it might also function at that step in the RNAi pathway. The γb protein, from hordeiviruses, displays a cysteine-rich motif at the C-terminal region, to which RNA binding and anti-silencing actions are attributed (Yelina et al., 2002; Bragg and Jackson, 2004). The veritable arms-race between the host defense proteins and viruses is well established with silencing suppressor proteins encoded not only from plant viruses, but also animal and insect viruses (Chao et al., 2005; Bennasser and Jeang, 2006; Hemmes et al., 2007).

It has been shown that suppression of RNA silencing can increase the yield of co-introduced foreign gene expression because the suppressors protect all mRNA, including foreign mRNA, from silencing (Voinnet et al., 2003). To explore the interference of RNAi by suppressors for potential use for biotechnology, part of this work sought to extend non-native protein production in plants. This included the examination of the effect of silencing suppressors singly and in combination, on the expression of a co-introduced green fluorescent protein (GFP) cDNA. For this, I used the well-characterized

silencing suppressors P19 from TBSV, HcPro from the potyvirus *Tobacco etch virus* (TEV), and the γb protein from *Barley stripe mosaic virus* (BSMV), with the goal of maximizing the length of time that GFP is produced either from a co-inoculated T-DNA, or expressed by a virus vector. My hypothesis was that as the silencing suppressors act at different steps in the RNAi pathway, their use in combination will provide expression of GFP for a longer length of time than inoculation with a single silencing suppressor or with GFP alone.

Systems

The following section provides background and details on the techniques used in the research Chapters II, III, and IV.

Viruses used

TBSV is a positive-sense, single stranded RNA virus, and the type member of the *Tombusviridae* family. An icosahedral capsid of T=3 is made up of 180 coat protein (CP) subunits, and particles are about 33 nm in diameter. These hold a 4.8 kb genome with 5 open reading frames (ORFs) that do not have a 5'-cap or 3' -poly-A tail (Fields et al., 2007) (Fig. 1.2A). The 5' proximal genes *p33* and *p92* encode the replicase proteins through direct genomic translation. The *p33* ORF has an amber (UGA) stop codon which can be readthrough for production of P92, though a 20-fold greater amount of P33 is present in infected cells (Scholthof et al., 1995b). Subgenomic RNAs (sgRNA) are used to produce the remaining 3 proteins (Fig. 1.2A). sgRNA1 contains the *p41* ORF for production of the viral coat protein. The coat protein (P41) of TBSV is not required for virus movement through certain hosts (Scholthof et al., 1993), and can be replaced or dispensed with to utilize TBSV as a virus vector (Scholthof et al., 1996). However, it has been determined that CP is required for systemic virus spread in pepper, and contributes to systemic infections even in hosts where it is not required (Desvoyes and Scholthof, 2002; Qu and Morris, 2002; Turina et al., 2003).

P22 and P19 are both produced from sgRNA2, albeit from separate ORFs. P22 is the cell-to-cell movement protein of TBSV in compatible hosts, and has been shown to be phosphorylated, membrane- and cell-wall associated, bind to RNA, and most likely

assist in the formation of a ribonucleoprotein complex that moves a replicating virus through plasmodesmata without the need for encapsidation (Desvoyes et al., 2002; Scholthof, 2005). Additionally, it is thought that P22 interacts with specific host proteins to facilitate this movement, as shown via association with HiFi22, a host factor, in a yeast-two hybrid screen (Desvoyes et al., 2002).

P19 is translated from the nested ORF on sgRNA2 by a leaky scanning mechanism, where the ribosome preferentially initiates translation of P19 versus P22 due to the optimal start codon context (Scholthof et al., 1999a; Scholthof, 2006). While P19 is not required for infection of all hosts (some experimental *Nicotiana* species), it is necessary in others for a systemic infection for instance, *Capsicum annuum (*pepper), and *Spinacia oleracea*, (spinach) (Scholthof et al., 1995a), and has been implicated as a pathogenicity factor with involvement in local and systemic infections (Turina et al., 2003). It is now known that P19 acts as a suppressor of gene silencing by dimerizing and isolating duplexed siRNAs following their production by Dicer, preventing their incorporation into RISCs (Voinnet et al., 1999; Qiu et al., 2002; Park et al., 2004; Omarov et al., 2006; Scholthof, 2006).

While the natural host range of TBSV is limited to a few dicotyledonous plant species, the experimental host range is very broad though infection is sometimes limited to the site of entry (Yamamura and Scholthof, 2005). TBSV does not infect *Arabidopsis.* The virus is transmitted mechanically, for instance, by wounding or rub-inoculation, and through the soil. Systemic infections typically consist of stunted growth of the infected plant, followed by a general wilting phenotype, resulting in death of susceptible hosts within a week of infection (Fig 1.2B). Hosts with non-systemic infections display local lesions and necrotic tissue. When passaged several times using infected tissue, particularly in a laboratory setting, it is not uncommon for RNA viruses like TBSV to form defective interfering RNAs (DIs), which consist of short segments of internal and terminal, usually distant, segments of the viral genome. For TBSV, DIs usually consist of 4 segments from conserved regions of the genome. DIs are thought to be generated as the viral replicase complex ‘skips’ and consequently does not replicate certain regions of the genome (Scholthof et al., 1995c; White, 1996; Yamamura and Scholthof, 2005).

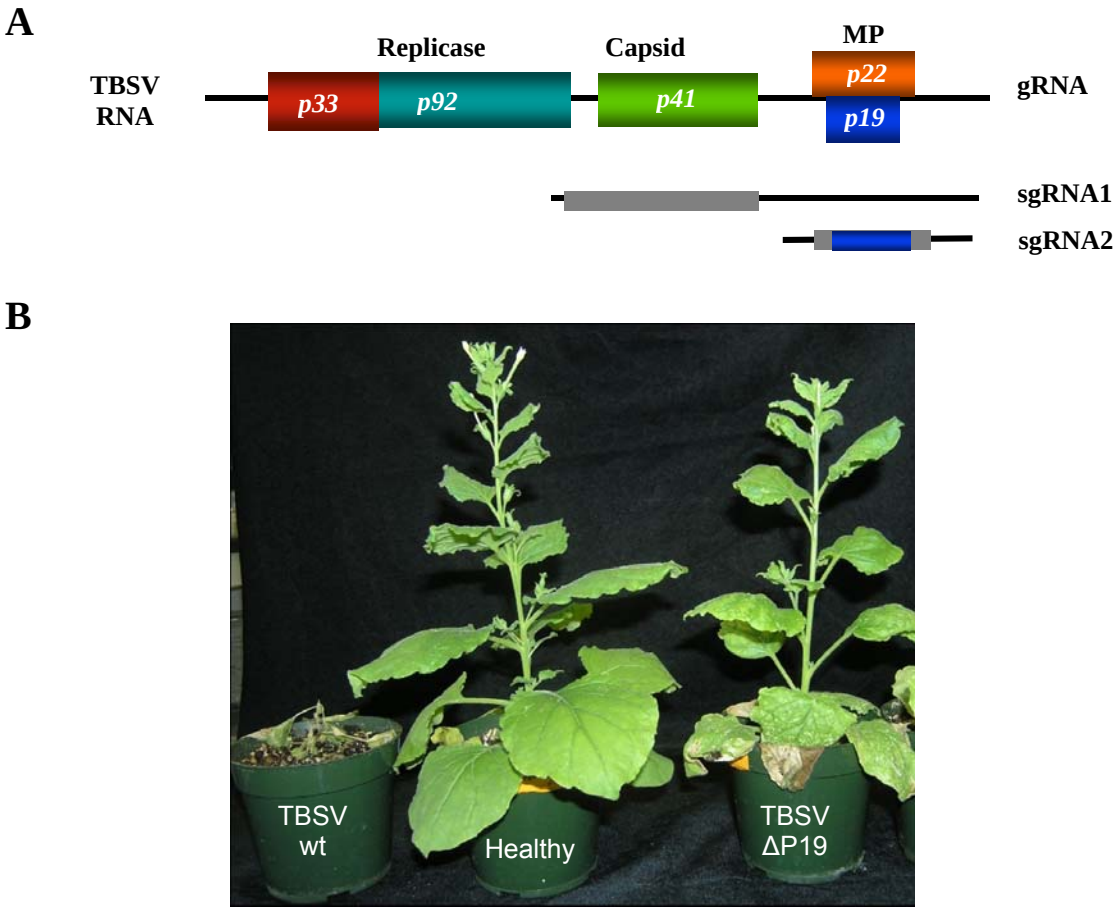

Fig 1.2 *Tomato bushy stunt virus* (TBSV) genome and infected plants. A.) TBSV is a positive-sense, single-stranded RNA virus that encodes 5 ORFs and produces 5 proteins. P33 and P92, expressed from the genomic RNA directly, encode for replicase proteins. P41 is the capsid protein, expressed from subgenomic (sgRNA)1. sgRNA2 encodes P22, the virus movement protein, and P19, a protein shown to have multiple functions, though the best known is as a silencing suppressor. B.) TBSV-infected *N. benthamiana* infected with TBSV and a TBSV mutant (Δ19), which does not produce the silencing suppressor. Following infection with wild type (wt) TBSV (left), plants succumb to vascular wilting symptoms, followed by a lethal necrosis about a week post inoculation. When plants are infected with the mutant deficient for the silencing suppressor protein P19 (right), the plant displays a 'recovery' phenotype, and eventually clears the infection. The center plant is a healthy control. (Plant panel used with permission of Dr.Yi-Cheng (John) Hsieh, TAMU)

TBSV offers an unparalleled model for the study of RNAi in plants. The virus is well adapted to a laboratory setting, with infectious cDNA clones available (Yamamura and Scholthof, 2005; Qiu and Scholthof, 2007), and symptoms are readily visible in hosts. A large amount of ss- and ds- RNAs are produced in planta, to the level of visibility when separated by agarose gel electrophoresis followed by staining with ethidium bromide after total RNA extraction. These dsRNAs would provide ample substrate for Dicer-generation of siRNAs. TBSV virus mutants not producing the silencing suppressor P19 (TBSV ΔP19) (Omarov et al., 2006; Qiu and Scholthof, 2007), instead of causing a lethal infection in the plant, display minor symptoms culminating in eventual clearance of the infection (Fig 1.1B). This recovery is due to RNAi (Omarov et al., 2006), and it was shown that this TBSV mutant is a useful tool for studying anti-viral RNAi-effector complexes (Omarov et al., 2007).

Tobacco rattle virus (TRV) is the type member of the *Tobravirus* genus. It has a bipartite, positive-sense ss-RNA genome (Fig 1.3A). The positive-sense RNAs are encapsidated in rod-shaped particles. RNA1 is about 6.8 kb, with 4 ORFs, and a tRNA-like 3'-terminus. There is a 5' non-coding region of about 255 nts directly upstream of the 5' proximal gene, which encodes a 134 kDa protein with methlytransferase and nucleotide-binding/helicase characteristics (Hull, 2002). ORF1 also has a leaky stop codon to produce a 194 kDa replicase protein. The TRV MP is encoded by gene 1a, which produces a 29 kDa protein, probably via a subgenomic RNA. The final gene on RNA1, 1b, produces a 16 kDa protein with a cysteine-rich N-terminal region from ORF 4. The 16 kDa protein can be incorporated into a complex, possibly with host proteins, which has a high molecular mass when detected by western blotting and localizes to the nucleus. Additionally, deletion of 1b (the 16kDa protein) decreases viral accumulation in *N. benthamiana* protoplasts and whole plants for the TRV isolate PpK20, while having no effect for another isolate, SYM (MacFarlane, 1999). RNA 1 can replicate and move through the plant without RNA 2, though virions will not be formed. The 16 kDa protein encoded by RNA1 is thought to act as a weak silencing suppressor, implicated in both TRV infections and as expressed from a *Potato virus X* viral vector (Martin-Hernandez and Baulcombe, 2008). As TRV invades and infects meristematic tissue, it is speculated

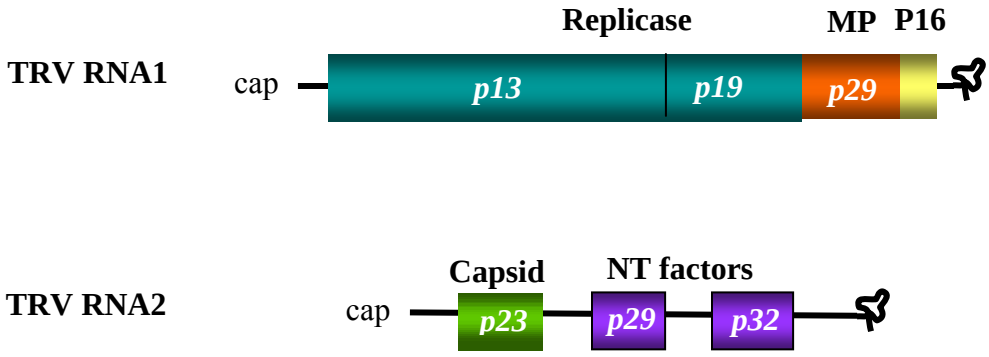

Fig. 1.3 *Tobacco rattle virus* (TRV) genome. TRV is a bipartite, positive sense single-strand RNA virus. TRV RNA1 encodes 4 ORFs, the first and second of which is expressed from the genomic RNA, and produce the 134 kDa and 194 kDa replicase proteins. The third ORF is expressed from a subgenomic RNA, and encodes a 29kDa MP, and the fourth ORF, on subgenomic RNA 1b, is a 16 kDa protein that has recently been implicated as a silencing suppressor. TRV RNA II has 3 ORFs, the first of which produces a 23 kDa coat protein (CP), and the other two produce 29kDa and 32 kDa nematode transmission (NT) factors.

that P16 allows for build up of viral RNAs for infection of seeds, though it does not suppress silencing to the level that would interfere with RNAi-sensitive tissue and seed generation, as has been shown for stronger silencing suppressors like TBSV P19 (Martin-Hernandez and Baulcombe, 2008). The exact mechanism of P16-mediated suppression is not known at this time.

TRV RNA2 differs between various isolates of the virus due to the presence of additional genes as well as specific 3'-regions homologous to those found on RNA1. The only gene present in all isolates is the 5'-proximal CP gene, which usually encodes a 22-24 kDa protein (Hull, 2002). This CP is said to strongly resemble the CPs of tobamoviruses and hordeiviruses, though with a larger, 'protruding' C-terminal region, possibly involved in the interaction of viral particles with nematodes during transmission (MacFarlane, 1999). Other genes present are non-structural, transcribed from sgRNAs, and can include proteins necessary for nematode transmission. Further sources of variation between strains of TRV are attributed to the high rate of recombination, both from the 3'homologous region of RNA1, as well as between the 3' regions of RNA2 in different strains of TRV. RNA2 from TRV strain pPk20 encodes two nematode transmission factors, the 29.4 k protein and 32.8 k proteins, and the CP (MacFarlane, 1999). TRV is vectored by nematodes, utilizing proteins encoded by RNA2 for transmission. TRV can also be spread through mechanical inoculation or by vegetative propagation of bulbs. (MacFarlane, 1999; Hull, 2002). It has a wide host range spanning 12 plant families, with over 60 different species reported as hosts. These include important agricultural crops including oats, potato, and tomato (Ratcliff et al., 2001).

TRV is commonly used as a viral vector to stimulate VIGS. These vectors are found to be very stable, able to spread through the entire plant including meristematic tissue, and cause very mild host symptoms (Ratcliff et al., 2001; Burch-Smith et al., 2004). Again, it has a wide host infection range, including plants in the Solanaceae family, like tomato, pepper, *Petunia hybrida* (petunia), *N. benthamiana*, and *Solanum tuberosum* (potato), and has been shown to infect *Arabidopsis* (Burch-Smith et al., 2006), usually vectored in with *Agrobacterium tumefaciens*. It is for this reason that TRV is studied here for isolation of a RISC complex; it stimulates VIGS, therefore must induce an RNAi response with detectable characteristics.

Panicum mosaic virus (PMV) is the type member of the genus Panicovirus. It is a member of the *Tombusviridae* family, and has a narrow host range limited to a few species of Poaceae. PMV is a positive-sense, ss-RNA virus encapsidated in a T=3 iscosahedral capsid. The genomic RNA is 4.3 kb, contains 5 ORFs, and RNAs require no capping or polyadenylation, though the 3' untranslated region of both the genomic RNA and subgenomic RNA contain a translational enhancer (Batten et al., 2006) (Fig. 1.4). The 5' proximal genes are p48 and p112, which are expressed from the genomic RNA directly, and encode replicase proteins (Batten et al., 2006). P112 is produced by readthrough of the amber stop codon of the first ORF (Turina et al., 1998). One sgRNA containing 4 ORFs is also produced, and proteins encoded include P8, P6, the CP (P26), and P15. P8 is produced from the first ORF (Turina et al., 2000). P6 is probably produced by a noncanonical start codon of GUG, as is the CP from a start codon of CUG, possibly mediated by an internal ribosomal entry site (Turina et al., 2000; Batten et al., 2006). P8, P6, and P15 localize to the cell wall, and are thought to be involved in viral movement (Turina et al., 2000).

Satellite panicum mosaic virus (SPMV) is a positive-sense ss-RNA of approximately 824 nts, encapsidated in a T=1 icosahedral particle. It relies on PMV for movement and replication. It contains one ORF with four start codons, at least two of which are used (Omarov et al., 2005); to yield a 17 kDa CP and a truncated 9.4 kDa product (Fig. 1.3B) (Qi and Scholthof, 2008). The CP has been shown to localize to both the cell wall and cytosol, while P9.4 localizes to only the cell wall. P9.4 has been shown to increase host symptom severity for a mixed PMV/SPMV infection (Omarov et al., 2005). While CP is not required for replication and movement of SPMV through the plant, constructs not producing the CP rapidly succumb to defective interfering RNAs (DIs), which inhibit replication of SPMV (Qi and Scholthof, 2008). Mutations to the N-terminal region, rich in arginine, affect RNA binding and virion assembly in addition to generation of DIs. This and other evidence suggest that CP binds PMV and SPMV RNA to form non-virion complexes which move cell-to-cell (Scholthof, 1999; Qi and Scholthof, 2008). Additionally, the CP might interfere with viral silencing suppressors or slow effects of RNAi, as demonstrated by Qiu and Scholthof for *Potato virus X* (PVX)

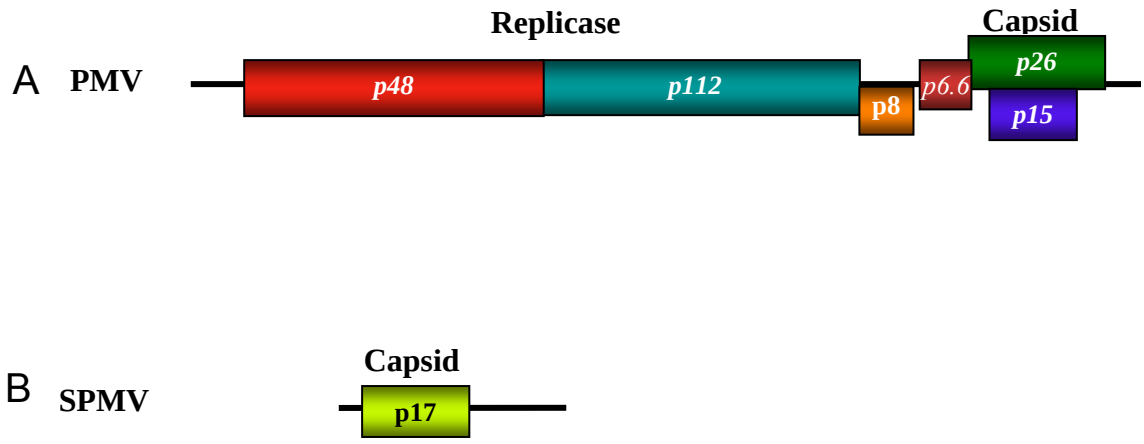

Fig. 1.4 *Panicum mosaic virus* (PMV) and satellite panicum mosaic virus (SPMV) genomes. A.) The PMV genes *p48* and *p112* are expressed from the genomic RNA directly and encode replicase proteins. One subgenomic RNA containing 4 ORFs is also produced, and proteins encoded include P8, P6, the CP, and P15. B.) SPMV produces a 17 kDa protein encoding a CP from genomic RNA directly, although there are 4 ORFs present.

p25, when SPMV is co-expressed from a PVX viral vector. This also enhanced host symptoms caused by that same vector (Qiu and Scholthof, 2004).

Column chromatographic systems

Separation of biological moieties in the crude extracts of virus-infected plants is accomplished for this project utilizing column chromatography. This technique involves the use of a stationary phase media, a column, through which a mobile phase (typically the sample of interest) is applied. Molecules in the mobile phase interact with sites of the stationary phase in various manners, usually by means of characteristic groups present on mobile molecules (Nelson and Cox, 2005), and these interactions are reversible to allow elution, usually in a gradient-related fashion. Several types of chromatography were used in this project. One of these is ion exchange chromatography, in which charged functional groups of mobile phase (sample) molecules interact with oppositely charged groups on the stationary phase – the greater the charge, the more tightly interacting. Gel filtration, or size separation, is another method used; larger molecules in the mobile phase move more slowly through the gel matrix, and subsequently elute in later fractions. Hydroxyapatite chromatography, using a calcium phosphate ceramic, is a 'mixed-media' or 'pseudo-affinity' stationary phase that interacts with both ionic and anionic groups; for instance, the positively charged functional groups of some amino acids, as well carboxylate residues of various proteins. Elution occurs with an increasing gradient of phosphates (Gagnon et al., 1996; Schroder et al., 2005).

The experiments outlined in Chapters II and III use all three described chromatography methods. Early experiments used Sephacryl S200 gel filtration chromatography, and then DEAE anion exchange chromatography was used for the characterization of TBSV and TRV –infected plant antiviral complexes. Hydroxyapatite chromatography was substituted for DEAE anion exchange chromatography with the discovery that fractions containing activity following anion exchange chromatography co-eluted with ribulose 1,5-bisphosphatase (Rubisco). Therefore, hydroxyapatite was used to separate samples and obtain a different elution profile. Gel filtration was used often as a second step of chromatography to further separate proteins present in fractions

containing activity; this type of chromatography had the additional benefit of removing salt and phosphates from the fractions.

Objectives

This work aimed to examine the RNAi pathway in plants for defense against viruses. The objectives included 1) biochemical characterization of an RNAi response against TBSV in *N. benthamiana*, 2) determination of an antiviral response following infection of *N. benthamiana* with TRV, as well as examination of defense elements present following PMV and SPMV infection of a monocot model system, and 3) using agro-infiltration of silencing suppressors HcPro, P19, and γb to measure their effects on the performance of a virus-vectored GFP gene. Supplementary data complementing the first objective also address the rapid method of TBSV virion purification using hydroxyapatite column chromatography.

The research presented in the first chapter of this thesis was undertaken with the intent of biochemically characterizing the antiviral plant defense response in *N. benthamiana* against the plant virus TBSV. To do this, *N. benthamiana* was infected with either wt TBSV or its derivative, TBSV ΔP19, which does not produce the silencing suppressor P19. Following establishment of infection, the plant tissue was harvested, proteins separated using 3 different types of column chromatography, and the fractions assayed for ribonuclease activity, and presence of siRNAs, plus the ribonuclease activity was further characterized by examining the effect of divalent metal cations, and EDTA. Subsequently, active fractions were subjected to further steps of column chromatography to improve protein separation, and those proteins were visualized by staining.
Once these were established, the second chapter sought to characterize *N. benthamiana* responses to another virus, TRV, and further more, to examine if a virus similar to TBSV, PMV together with its satellite SPMV, produced a similar response in a monocot host, proso millet. These responses were examined using the same methods as in Chapter II, namely, biochemical analysis of the proteins present following column chromatography of virus-infected plants. Because RNAi is thought to be a cellular pathway conserved across 3 kingdoms, it was hypothesized that the anti-viral RNAi response for plants would be identical for different viruses, in both dicots and monocot hosts.

The supplementary material for Chapter II found in the appendix characterizes a new method of virion purification by column chromatography. Following hydroxyapatite chromatography of TBSV-infected plants, a distinct band was seen upon electrophoresis of the flowthrough wash from the column. This band was determined to represent the TBSV coat protein, and visualization with electron microscopy showed that this fraction in fact contains a relatively pure high titer of virions that can be used to readily infect plants.

The third chapter aimed to use three RNAi silencing suppressors from viruses, - carried by *Agrobacterium*, to measure the effect on a virus-vectored GFP gene. Silencing suppressors are encoded by viruses to evade the RNAi defense in plants. The goal of the third chapter was to use these silencing suppressors for biotechnology; to enhance and extend the length of production that a virus-vectored foreign gene was produced in planta. Three silencing suppressors, the hordeivirus protein γb, the potyvirus protein HcPro, and the tombusvirus protein P19, which are thought to act at different steps in the RNAi pathway, were expressed singly as well as in combination, vectored by *Agrobacterium*. To establish the system, initial experiments used co-infiltrated *Agrobacterium*-vectored silencing suppressors with an *Agrobacterium*-vectored foreign gene (GFP, here) for production of a visible green signal under UV light. When the system was operational, plants were agro-infiltrated with the silencing suppressors, then infected with a TBSV-derived vector expressing GFP. Expression of GFP was determined both with observation of the visible GFP signal, as well as with western blots for detection of the GFP protein.

The in vitro system for RNAi analysis described above is unique because it has not yet been described for any virus-host system, and offers the advantage of isolating and determining the composition of RISC. Determining the specifics of the RNAi pathway in plants is necessary in order to better understand how this process correlates to described model systems, as well as designing better strategies of protecting plants against viruses, and for the exploitation of the pathway for biotechnology. Additionally, the method of virion purification is much quicker than those traditionally used, and presents a reliable, attractive alternative.

CHAPTER II
BIOCHEMICAL CHARACTERIZATION OF AN RNAi RESPONSE AGAINST TBSV IN *N. BENTHAMIANA*

Introduction

RNAi

RNAi is a conserved pathway that silences RNA by recognition of target RNA. This pathway can be divided into two separate mechanisms. For both, double-stranded RNA (dsRNA) serves as the trigger for the RNAi pathway upon cleavage into duplexed small interfering RNAs (siRNAs) or (usually) host-encoded hairpin microRNAs (miRNAs), which can act in a sequence-specific manner to target and degrade ssRNAs, called post-transcriptional gene silencing (PTGS) (Baulcombe, 2004). Alternatively, these small RNAs guide methylation of specific nucleotide sequences (transcriptional gene silencing, TGS) (Brodersen and Voinnet, 2006). PTGS acts during the growth and development of an organism using endogenous miRNAs or other species of short RNAs, or during the defense of an organism against viral infections, using siRNAs (Baulcombe, 2004). The two pathways (PTGS and TGS) coalesce to use the same cellular machinery to target mRNA for degradation (Filipowicz, 2005).

As mentioned in Chapter I, plants can ‘clear’ viral material from upper, new plant tissue following infection and remain resistant to a second infection. This phenomenon was first observed in a *Tobacco ringspot virus*-infected tobacco plant in 1928 (Wingard, 1928; Baulcombe, 2004), but the occurrence was only recently attributed to RNA interference (RNAi). This is widely conserved across many species/kingdoms; early observations were made in a *Caennorhabditis elegans* system (Fire et al., 1998), and in plants, the RNAi pathway was first termed co-suppression of homologous genes following studies in petunia plants (Napoli et al., 1990). Virus-infected plants form a convenient platform to elucidate the so far incomplete understanding of the biochemical complexities of RNA effector complexes (Omarov et al., 2007; Pantaleo et al., 2007).

While the details can vary between organisms, RNAi is thought to occur as described in Chapter I (Fig. 1). As illustrated in the figure, a member of the Dicer protein

family cleaves dsRNA in the cell. This dsRNA originally is either transcribed directly from DNA by RNA synthesis from complementary strands, or can accumulate in the cell via viral infection as well as by artificial introduction (Filipowicz, 2005). Following cleavage, the dsRNA segments are loaded into a RNA-induced silencing complex (RISC). The following section will describe in some detail what is known about the pathway and mechanisms of RNAi with regard to siRNAs, Dicer, RISC, and how this might be relevant to an anti-viral RNAi.

Key molecules for RNAi are short RNAs, but recent literature suggest that different types of these short RNAs are used toward different ends of the RNAi pathway and as such, are generated in various ways. For production of anti-viral siRNAs, viral double-stranded RNA is produced in the cytoplasm directly, where it is acted upon by a Dicer-type protein. Genes inserted into a viral vector to direct the silencing of endogenous genes are typically designed as inverted repeats which form secondary structures of hairpins, for recognition by a Dicer and subsequent processing into siRNAs. RNA-dependent RNA polymerase 6 (RDRP6) has been implicated in siRNA generation for transitivity in *Arabidopsis*, using RNA templates without 5' caps to generate transcripts (Brodersen and Voinnet, 2006; Moissiard et al., 2007). Transitivity uses single stranded (ss) siRNAs as primers for RNA dependent RNA polymerases, to yield secondary siRNAs up- and downstream from the initial siRNA site, and is said to be responsible for the spread of the systemic silencing signal in plants (Moissiard et al., 2007). Regarding endogenous siRNAs, these are thought to originate from small RNAs produced from hairpins from Dicer like proteins (DCL) other than DCL1, such as DCL2, DCL3, or DCL4 (Deleris et al., 2006; Moissiard et al., 2007). 'True' microRNAs (miRNAs) are thought to be processed by DCL1, and again, act in development and regulation of the plant, specifically in *Arabidopsis* (Zhang et al., 2007).

Plant genome siRNAs are thought to be important in protecting the plant from transposons, and possibly viruses. The particular DCL involved is thought to direct the length of the siRNA (from 21-24 nts) and indirectly specify the Argonaute (Ago) protein with which the siRNAs interacts. This might have significance in instances where certain DCL or Ago proteins are inhibited. Other examples of endogenous siRNAs include transacting siRNAs (ta-siRNAs), which are produced from non-coding regions of the

genome, similar to the mechanism of transitivity, as seen in studies with *Arabidopsis*, though it is likely that other species produce these as well (Brodersen and Voinnet, 2006). These ta-siRNAs are thought to silence genes in trans (Vasquez et al., 2004), with targets separate from the locus of origin (Jones-Rhoades et al., 2006). Similar to ta-siRNAs are natural anti-sense siRNAs (nat-siRNAs), which are produced from overlapping regions of neighboring genes on opposite DNA strands, and target parental gene products, possibly for stress adaptation in the plant (Borsani et al., 2005; Brodersen and Voinnet, 2006). Recent studies suggest that a nat-siRNA is induced by plant infection with the pathogenic bacteria *Pseudomonas syringae*, to target a negative regulator of the plant resistance pathway (Katiyar-Agarwal et al., 2006). This has implications in that not only can viral pathogens trigger RNAi, but the pathway has significance for other types of plant pathogens. Other small RNAs are directed against repeat-associated elements, repeat-associated siRNAs (ra-siRNAs) (Vagin et al., 2006; Gunawardane et al., 2007), as well as against transposons, piwi- interacting RNAs (pi-RNAs), as seen in *Drosophila* (Vagin et al., 2006).

Dicer-type enzymes belong to the ribonuclease III family of endo-ribonucleases, along with eubacteria RNaseIIIs and Drosha proteins. Enzymes in this family range in size from 200 to about 2000 amino acid residues, function in the processing of dsRNA, have characteristic catalytic sites, and leave 2-nt overhangs on their target RNAs (Bernstein et al., 2001; Jaskiewicz and Filipowicz, 2008; Ji, 2008). Dicers are multi-domain enzymes found in nearly all eukaryotes, with varying degrees of complexity determined by the domains present (Jaskiewicz and Filipowicz, 2008). These domains always include the RNase III catalytic domain containing divalent metal ion co-factors and conserved amino acids as well as a dsRNA binding domain, for minimum ribonuclease activity (Ji, 2008). Other domains present can include the PAZ domain (Piwi-Argonaute-Zwille, also found in Argonaute proteins (Cerutti et al., 2000), a helicase/ATPase for some Dicer-type proteins, as well as others. The PAZ domain is shown bind to the 2' nt overhangs of the duplex RNAs, and possibly contributes to transferring siRNAs to Argonaut (Cerutti et al., 2000; Carmell and Hannon, 2004; Ji, 2008). The endonuclease domain dimerizes to form a catalytic groove in the enzyme to hold a dsRNA substrate, as well as having two catalytic sites containing divalent metal

ions, usually Mg^{2+} and Mn^{2+}. These cofactors interact with conserved amino acids and a water molecule to cleave a single strand of duplexed RNA (MacRae et al., 2006; Ji, 2008).

Because Dicer cleaves a dsRNA into an siRNA, two catalytic sites and a total of four Mg^{2+} metal ions are necessary. The distance of the catalytic sites directly influences the size of the small RNA that is produced (MacRae et al., 2006). The dsRNA binding site, while not completely necessary, increases the activity of the enzyme (MacRae et al., 2006). Dicer is common in nearly every organism, in varying forms. *Arabidopsis* has 4 Dicer-like proteins (DCLs), and these are used for production of different small RNAs; DCL1 for miRNAs, DCL2 for siRNAs, DCL3 to generate siRNAs involved in chromatin RNA modification, and DCL4 to produce ta-siRNAs (Xie et al., 2004; Jaskiewicz and Filipowicz, 2008). For activity in the cell, Dicer-type proteins have been shown to associate with other proteins. For humans, this is the TRBP (Chendrimada et al., 2005), Prbp in mice, *Drosophila's* R2D2 (Liu et al., 2003), and HYL1/DRB proteins in *Arabidopsis* (Hiraguri et al., 2005).

A RISC is postulated to be a high-molecular weight complex composed of several proteins. RISC elements have been described in other systems to include one or more loading proteins, proteins from the Ago family, and possibly a protein from the Dicer family (Song and Joshua-Tor, 2006; MacRae et al., 2007; Tomari et al., 2007). The model pathway is based on *D. melanogaster* and human RNAi pathways, because these are the most comprehensively studied. RNAi processes are similar but not identical in various species. Along these same lines, RNAi and RISCs for plants likely share some common elements with other systems, but may also have specific properties.

How do these different components operate together? There are several concepts regarding how a duplexed siRNA or miRNA, upon export from the nucleus, is loaded onto the RISC and converted into an ssRNA able to associate with long ssRNA for targeting. Some model systems implicate Dicer-type proteins as a sort of shuttle for siRNAs, usually called a RISC loading complex (Tomari et al., 2004; Liu et al., 2006), with interacting proteins like *Arabidopsis'* HYL1 from *Arabidopsis*, RDE-4 from *C. elegan*s, and R2D2 from *Drosophila* serve to facilitate the loading of siRNAs (Tabara et al., 2002; Liu et al., 2003; Hiraguri et al., 2005; Liu et al., 2006; Tomari et al., 2007).

A RISC without a bound small RNA is usually referred to as inactivated, or a holoRISC. The orientation in which the small RNA is associated to the Dicer protein might govern the direction that RISC is loaded (Tomari et al., 2004). For *Drosophila*, R2D2 seems to bind to the more thermodynamically stable 5' end of the siRNA, leaving Dicer at the less stable end; this manner of protein/siRNA orientation would allow a sort of directionality for small RNA loading (Schwartz et al., 2003; Tomari et al., 2004; Liu et al., 2006), though other work suggests this might not be a conserved property in other systems (Hong et al., 2008). It is possible that the small RNA binds externally to the Ago protein, then is internalized, and that this might be facilitated by interactions between Dicer and the Piwi domain of Ago (Yuan et al., 2006). Once the small RNA is associated with RISC, several possibilities exist to explain how the duplexed RNA unwinds. Among the earliest theories was that small ssRNAs associate with the Ago protein, without an 'unwinding' step after association. Current theories involve the interaction of small RNAs with the RISC proteins themselves forcing the siRNA duplex apart to allow association with the Ago protein (Tomari and Zamore, 2005) or that RNA helicase A might become involved to unwind the siRNA duplex and render it an active siRNA, shown for the human model (Robb and Rana, 2007). Yet other theories speculate that the spare siRNA strand must be discharged from the RISC in a manner similar to that of the later cleavage of long ssRNA, leaving 11- and 12- nt strands (Leuschner et al., 2006). This process does not require ATP (Hannon, 2002), though siRNA initial binding to RISC is facilitated by phosphorylation (Schwarz et al., 2002).

The catalytic unit of RNAi in all cases is thought to be an Ago protein (Hammond et al., 2001; Song et al., 2004). The Ago family of proteins can be divided into two subgroups based on their similarity to Ago1 or Piwi found in *Arabidopsis* or *Drosophila*, respectively. Two protein domains, Piwi-Argonaute-Zwille (PAZ) and Piwi, are always found associated with this family of proteins, in addition to the N-terminal domain and middle domain. (Song and Joshua-Tor, 2006) In human cell lines, the Piwi domain has been shown to be involved in loading the RISC complex, via a protein-protein interaction between Ago and Dicer (Meister et al., 2004), although this might not be the case for other RISCs. The Ago Piwi domain is thought to have an RNase H-type fold, with a Asp-Asp-Glu/His/Lys amino acid catalytic region (Liu et al., 2004; Hutvagner and Simard,

2008) containing an Mg^{2+} ion to catalyze the cleavage of target RNA (Tomari and Zamore, 2005), rendering products with a 3'-OH and 5'-phosphate (Schwarz et al., 2004). Non-catalytic Piwi domains have a catalytic region with amino acids different than those seen in cleavage-capable Agos (Toila and Joshua-Tor, 2007; Hutvagner and Simard, 2008), though gene repression with animal miRNAs involves binding of miRNAs with non-perfect sequence complementarities (Hutvagner and Simard, 2008).

The PAZ domain, also found in Dicer (Cerutti et al., 2000; Baulcombe, 2004), recognizes the 2-nt overhangs on duplex siRNAs (Meister et al., 2004) and is a highly-conserved 130 amino acid sequence (Carmell and Hannon, 2004). The crystal structure for an Ago protein from *Pyrococcus furiosus*, an archeabacteria, shows that the PAZ domain binds the 3' end of siRNAs, and is located across a positively charged 'groove' in the protein, holding the siRNA for cleavage by the Piwi domain (Song and Joshua-Tor, 2006). As there are several Ago proteins contributing to different types of RNAi, the many roles that these proteins fulfill is still under investigation (Meister et al., 2004; Toila and Joshua-Tor, 2007). It has been shown that in mammalian cell lines, Ago-2 functions as the RNAi endonuclease, and there may be potential differences in the amount of each Ago species per cells (Meister et al., 2004). For *Arabidopsis*, there are 10 known Ago proteins (Hutvagner and Simard, 2008). Ago-1 is said to be the ribonuclease associated with RNAi (Baumberger and Baulcombe, 2005), while studies suggest that Ago-1 and Ago-4 fill this role in *N. benthamiana* (Jones et al., 2006).

Once RISC is loaded, the incorporated siRNA allows for sequence-specific binding to a target ssRNA. Cleavage of the target RNA then occurs in a manner similar to that of RNase H, 10-nt in from the 5' end of the bound siRNA (Ameres et al., 2007). An Ago protein of about 150 kDa has been isolated from *A. thaliana* chromatography fractions, suggesting that only the presence of the Ago protein and associated siRNA (Baumberger and Baulcombe, 2005) are required for activity, while other RISCs range in size from 70 kDa to 500 kDa (Nykanen et al., 2001; Martinez et al., 2002). This, considered with other data, suggests that while the holoRISC (before activity) may contain multiple proteins, only the Ago protein is necessary for cleavage activity and that this exact protein varies between species and possibly even between functions of RNAi, though the human RISC is composed of Ago-2, TRBP, and Dicer (MacRae et al., 2006).

It remains to be determined if Ago-1 is the common plant RNAi ribonuclease (Jones et al., 2006), and if any other proteins are required for minimal RISC ribonuclease activity.

Considering the literature on silencing pathways as it is described in previous papers, my hypothesis is that the anti-viral RISC in plants should be a high molecular weight complex that can be isolated using chromatography procedures. Furthermore, the isolated complex should specifically cleave viral RNA when tested in vitro, contain virus-derived ss-siRNAs, and has biochemical properties and protein composition (including Ago proteins) consistent with RISC. To test this, *Tomato bushy stunt virus* (TBSV) was used to infect *N. benthamiana.* The plant defense response was observed following infection with both wildtype (wt) TBSV, as well a TBSV derivative (TBSV ΔP19) that is deficient for the silencing suppressor protein P19.

Materials and Methods

Inoculation of plants with TBSV and TBSV ΔP19

TBSV and TBSV ΔP19 cDNA were available in plasmids with resistance to Ampicillin for selection purposes, and these were grown overnight in a 37° C incubator, in a broth containing yeast extract, tryptone, salt, and dextrose (Luria broth) (Sambrook et al., 1989) until turbid. The plasmids were then isolated, according to manufacturer's directions (Qaigen, Valencia, CA), and linearized with *Sma*1 (20 µl DNA plasmid, 5 µl 5X Buffer 4, 2 µl *Sma1*, 23 µl sterile ddH2O at 25°). The linearized DNA was then extracted with phenol/chloroform (1:1 vol/vol), vortexed and centrifuged at 10,000 rpm, 4° C in a Beckman F4180 rotor for 20 min. The aqueous layer was removed, 1/10 vol sodium acetate added, plus 2 vol 800 µl ice cold absolute ethanol, and the mixture placed at - 80°C for at least an hour. This was centrifuged to precipitate the linearized DNA. The DNA pellet was then rinsed with 500 µl 70% ethanol, and dried briefly before re-suspending in 50 µl a/c ddH2O. Infectious RNA transcripts were then made using the linearized DNA as a template [1 µl linearized DNA was added to 16 µl did-water, 5 µl 5X transcript buffer, 2.5 µl 5 mM rNTP mix, 2 µl 0.1 mM DTT, 0.25 µl Ribolock RNase inhibitor, and 0.5 µl T7 RNA polymerase (Fermentas, Glen Burnie, MD)]. These transcripts were used to rub-inoculate *N. benthamiana* with RNA-inoculation buffer (50 mM KH_2PO_4, 50 mM Glycine, pH 9.0, 1% celite, 1% bentonite) by lightly rubbing

approximately 20 µl on a leaf.

Column chromatography

For Sephacryl S200 (gel filtration) column chromatography, columns were packed using Sephacryl S200 high resolution resin (Amersham Piscataway, NJ), with 200 mM Tris-HCL, pH 7.4, 5 mM DTT, and the indicated concentration of NaCl. This chapter uses 150 mM NaCl. With DEAE anion exchange column chromatography, about 50 ml MacroPrep DEAE Support (Bio-Rad, Hercules, CA) was packed using 50 mM sodium phosphate buffer, pH7.4. Fractions were eluted off with a NaCl gradient of 0.1 – 1 M NaCl after application of the clarified plant extract, and about 200 ml wash. To pack a hydroxyapatite column for chromatography, about 40 ml hydroxyapatite bio-gel HT (Bio-Rad) in 10 mM sodium phosphate buffer, pH 6.8 was poured into a clean glass column. After the column was loaded and washed extensively with this buffer, the fractions were eluted using a 10 mM - 200 mM or -400 mM (as indicated) increasing sodium phosphate gradient, pH 6.8.

Plants were harvested about 1 week post inoculation. About 40 grams of infected plant tissue was ground with a mortar and pestle in 50 ml of the buffer appropriate for the column specified, and further processed in a blender with 50 ml more buffer. This crude extract was filtered through cheesecloth and centrifuged at 4000 rpm with a Beckman S4180 rotor for 20 min. at 4° C. The supernatant was then filtered through cheesecloth into round-bottomed tubes for centrifugation at 10,000 rpm for 20 min. at 4° C in a Beckman F0630 rotor, when the supernatant was removed and placed on ice until it was loaded on the column.

Once all plant extract had been applied to the column (about 100 ml), it was washed thoroughly, and then proteins eluted off as described above. These fractions were then combined (1 and 2, 3 and 4, 5 and 6, etc.) for ease of manipulation, and stored at -20° C until needed.

Extraction of siRNAs from chromatography fractions

Analysis of 300 µl of each combined fraction was added to a 1.5 ml micro-centrifuge tube, and 30 µl of 10% SDS was added. These fractions were incubated at 60°

C for 20 min. The volume of the sample was brought to 500 µl with sterile dd H2O and 500 µl 1:1 phenol/chloroform was added to each tube. The mix was vortexed, then centrifuged at 10,000 rpm, 4° C in a Beckman F4180 rotor for 20 min. to separate aqueous and inorganic phases. The upper aqueous phase (~350 µl) was removed to a separate mini-fuge tube for each fraction, and 35 µl sodium acetate plus 800 µl ice cold ethanol was added. These were inverted to mix, and incubated at -56° C for at least an hour (preferably overnight). Fractions were then centrifuged at 10,000 rpm, 4° C, for 20 min. to pellet the siRNAs. The supernatant was decanted, and the pellet washed with cold 70% ethanol by centrifuging for 10 min. at 10,000 rpm and 4° C. The supernatant was discarded, and the pellet dried briefly to evaporate the remaining ethanol. The pellet was then re-suspended in siRNA loading dye (1 ml formamide, 500 µl of agarose electrophoresis loading mix), and boiled for 3 min. before being immediately iced. These siRNAs were then loaded into a 17 % acrylamide gel containing 8 M urea, and run at 30-45 volts in 0.5 X TBE (45 mM Tris, 45 mM Boric acid, 1 mM EDTA) until adequate separation occurred. The gel was removed from the SDS-PAGE electrophoresis apparatus (Bio-Rad Mini-PROTEAN tetra cell), and stained with ethidium bromide before visualization with UV. The siRNAs were then transferred to a nylon membrane using a western blot apparatus and 0.5X TBE, at 150 mA for 1 hour. The membrane was subsequently crosslinked with UV (twice on each side, turning with a 90° angle between) using the autolink setting, and the blot stored at 4° before hybridization probing. For extraction of siRNAs from other sources, the sample was brought to a total volume of 300 µl before the addition of 30 µl of 10% SDS, then the extraction proceeded as described above.

Assays for the presence and characterization of ribonuclease activity

Fractions from column chromatography were mixed with either total RNA extracted from virus-infected plants, or with transcripts generated in vitro from linearized viral cDNA as outlined above. To test for activity of ribonucleases, 5 µl of each combined fraction was incubated at room temperature (about 25°C) with 1.5-2 µl RNA for 20 min. Then, 2 µl DNA loading dye was added, and samples were run on a 1% agarose gel, 120 volts, in 1X TBE (90 mM Tris, 90 mM Boric acid, 2 mM EDTA) until

the lower dye band was about ¾ of the way from the front of the gel. These gels were then stained with ethidium bromide for 15 min., and viewed with a UV light box.

To test for inhibition by EDTA or NaCl, the indicated amount of 50 mM or 100 mM EDTA or 5 M NaCl stock solution was added to each fraction before the addition of RNA. To stop a reaction, EDTA was added at the time detailed in the assay, or after 20 min. To determine the effect of divalent metal cations on ribonuclease activity present in the fractions, 50 mM $MgCl_2$ and 50 mM $MnSO_4$ were used in the amount specified by the assay.

Northern blotting and hybridization with radioactive DNA probes

After visualization with UV, 1% agarose gels were usually blotted to a nylon membrane (Osmotics, Westborough, MA) for northern blot analysis using capillary transfer with 10X SCC (1.5 M NaCl and 150 mM sodium citrate, pH 7.0). After transferring at least 12 hours, the membrane was crosslinked with UV light, twice on each side, turning the blot 90° between each repetition. The blot was then incubated 4 hours - overnight in 2X SSPE + 1% SDS (20X SSPE stock contains 3M NaCl, 0.2 M NaH_2PO_4, 26 mM EDTA, pH7.4). The membranes were incubated at 65° for regular RNA assays and 41°C for siRNA blots, on a standard drum rotator. Hybridization probes were made using the appropriate DNA plasmid. For this, 1 µl plasmid or linearized DNA was added to 12 µl a/c ddH20 and 3 µl random primers, boiled for 3 min. and cooled on ice. Then, 2.5 µl EcoPol 5X buffer, 2.5 µl 12 mM mixed dNTPs (without C), 2 µl ^{32}P-dCTP (10 µCi/ µl) and 1 µl Klenow (5,000 U/ml) was added to the cooled probe, and this was incubated for at least an hour at 25°C before boiling again for 3 min. and cooled again on ice. This mixture (about 25 µl) was added to the blot in 2X SSPE+1% SDS, and incubated at the suitable temperature overnight. The blot was then removed from the radio-isotope mixture and washed with about 50 ml 2X SSPE +1% SDS for 20 min., three times, or until 'cool' when signal strength was tested with a Geiger counter (Ludlum Measurements, Sweetwater, TX). The blot was then dried briefly, wrapped in plastic wrap, and exposed to Kodak BioMax X-ray film. The length of exposure varied with radio-isotope signal strength, but typically was done overnight.

SDS-PAGE analysis and western analysis

For SDS-PAGE electrophoresis, samples were typically boiled with a 5X cracking buffer containing SDS, glycerol, and the reducing agent ß-mercaptoethanol, usually with a 3:1 ratio, for 3 min. Then, 30 µl of these boiled samples were loaded into 5% acrylamide SDS-PAGE gels (gel consisting of 3 ml 30% acrylamide stock, 3 ml water, 3.8 ml 1.5 Tris pH 8.8, 100 µl 10% ammonium persulfate, 100 µl 10% SDS and 30 µl TEMED; stacking gel with 600 µl 30% acrylamide, 500 µl Tris pH 6.8, 2.7 ml water, 100 µl 10% ammonium persulfate, 40 µl 10% SDS, and 3.2 µl Temed), and electrophoreised at 90 and 120 volts for 2 hours in 1X running buffer (24.8 mM Tris, 192 mM glycine, 3.5 mM SDS). The gel was then either transferred to a nitrocellulose membrane for western blot analysis, or stained with Coomassie Brilliant Blue R according to standard methods, (Sambrook et al., 1989).

For western blotting, the proteins on the SDS-PAGE gel were transferred to nitrocellulose membrane (Osmotics, Westborough, MA) at 300 mA for an hour, and transfer was verified by staining of the membrane with Ponceau S (Sigma, St. Louis, MO). The membrane was then blocked with 7.5% milk solution (7.5 grams skim milk powder, 1X TBS/Tween-20; 50 mM Tris, 200 mM NaCl, 500 µl Tween-20) for an hour. This was then rinsed for 15 min., 3 times, with about 20 ml TBS-Tween, and the primary antibody added at 1:2,000 dilutions for at least 2 hours. The secondary antibody in 7.5% milk solution was added to each blot following three 15-min. 20 ml TBS-Tween-20 washes, and the blots were developed with 5-Bromo-4-chloro-3-indoyl phosphate p-toludine (BCIP) (66 µl) and Nitrotetrazolium blue chloride (NTB) (33 µl) (Sigma-Aldrich, St. Louis, MO) in alkaline phosphate buffer. The reaction was stopped by rinsing blot with ddH20.

Silver staining ($AgNO_3$) of proteins

Following SDS-PAGE, the gel was removed to a clean dish. The gel was then immersed in fixative solution (30% ethanol with 10% acetic acid) for at least an hour, then rinsed with for 20 min. with water followed by 10 min. in 20% ethanol. Sensitizer solution (0.02% sodium thiosulfate) was then added to the dish for 1 min., and the gel was rinsed with ddH2O 3 times for 20 seconds apiece. Silver nitrate solution (0.2%) was

then used to stain the gel for at least an hour, after which the gel was rinsed for 15 seconds with ddH2O, and incubated in the developer solution [3% sodium carbonate, 2.5 ml sodium thiosulfate stock (1 mg in 100 ml ddH2O) , and 40 µl Formaldehyde] until desired band intensity was observed. At that time, the developer was removed and a stop solution was added for 15 min. (Tris, 25% acetic acid). The stained gel was stored in dd H2O.

Protein immunoprecipitation

About 1 ml of the fractions of interest were incubated with 2 µl P19-specific antiserum for 2 hours, and shaken at room temperature. Then, 30 µl of well-mixed agarose beads with IgG was added, and samples were shaken at room temperature for 2 hours. Samples were then spun down in a table top centrifuge (10,000 rpm, 10 min., 4°C), the supernatant removed, and 1 ml immunoprecipitation buffer (150 mM HEPES, pH 7.5, 200 mM NaCl, 1 mM EDTA) added; great care was taken to not disturb the pellet. The sample was re-suspended, and rinsing process repeated 6 times.

For western detection of the immunoprecipitated P19, the agarose bead pellet was re-suspended in 35 µl cracking buffer (50 mM Tris, pH 6.8, 100 mM Dithiothreitol, 0.1% bromophenol blue, 10% glycerol, 2% SDS), boiled 3 min., and loaded onto a 5% acrylamide gel for SDS-PAGE. For 17% acrylamide gel with 8M urea, to detect siRNAs bound to the immunoprecipitated P19, the pellet was re-suspended in siRNA loading dye, boiled 3 min., and set on ice immediately before loading on gel.

Results

The experiments highlighted in this chapter were done in collaboration with Dr. Rustem Omarov.

Biochemical characterization of TBSV Δ19 infected plant tissue with Sephacryl S200 or anion exchange chromatography

To determine if any ribonuclease activity could be detected from virus-infected plants, TBSV-infected plant tissue was first subjected to Sephacryl S200 gel filtration column chromatography to separate out macromolecules. For this purpose, *N.*

benthamiana plants were infected with the P19 deficient mutant, TBSV Δ19, and the infection was allowed to progress for one week. Following establishment of infection, plants were homogenized, and the crude extract was applied to a S200 gel filtration chromatography column. The resultant fractions were then tested for ribonuclease activity with the addition of TBSV transcripts generated in vitro, and the results verified by northern blotting (Fig. 2.1A) The results show that TBSV RNA transcripts were degraded predominately in fractions 6-9. Based on size markers for this column, the complex would be approximately 500 kDa. This same experiment was performed for plants infected with wtTBSV, and no ribonuclease activity was detected in those same fractions (data not shown, see Chapter V), which is consistent with the effect of a silencing suppressor protein on the RNAi pathway; P19 binds to siRNAs to prevent their loading onto RISCs, and subsequently, no RNA targeting occurs.

Fractions exhibiting ribonuclease activity were combined. Because RISC contains a divalent metal ion as part of Piwi domain catalytic site (Tomari and Zamore, 2005), the fractions were tested with the addition of two types of divalent metal cations, Mg^{2+} and Mn^{2+}, as well as a metal chelator, EDTA, to examine the effects these would have on the ribonuclease present in fractions active against RNA (active fractions) (Fig 2.1B). Results showed that with the addition of EDTA, activity is inhibited (Fig. 2.1B, lane 'E') Moreover, both Mn^{2+} and Mg^{2+} seemed to increase the ribonuclease activity (Fig 2.1B, lanes Mn and Mg, compared to lane A), though Mn^{2+} had a greater effect. Since the DNA template for transcription was present in high quantities in Fig. 2.1B, this verified that the nuclease was RNA-specific.

Using S200 column chromatography, there were still many proteins present in these gel filtration fractions which would make it very hard to correlate any proteins with the measured activity. For better separation of the proteins present, TBSV Δ19 infected plant tissue was also applied to a DEAE anion exchange chromatography column for separation by charge. These fractions were silver stained to visualize the proteins present that might contribute to the ribonuclease activity (Fig. 2.2A). Fractions with RNase

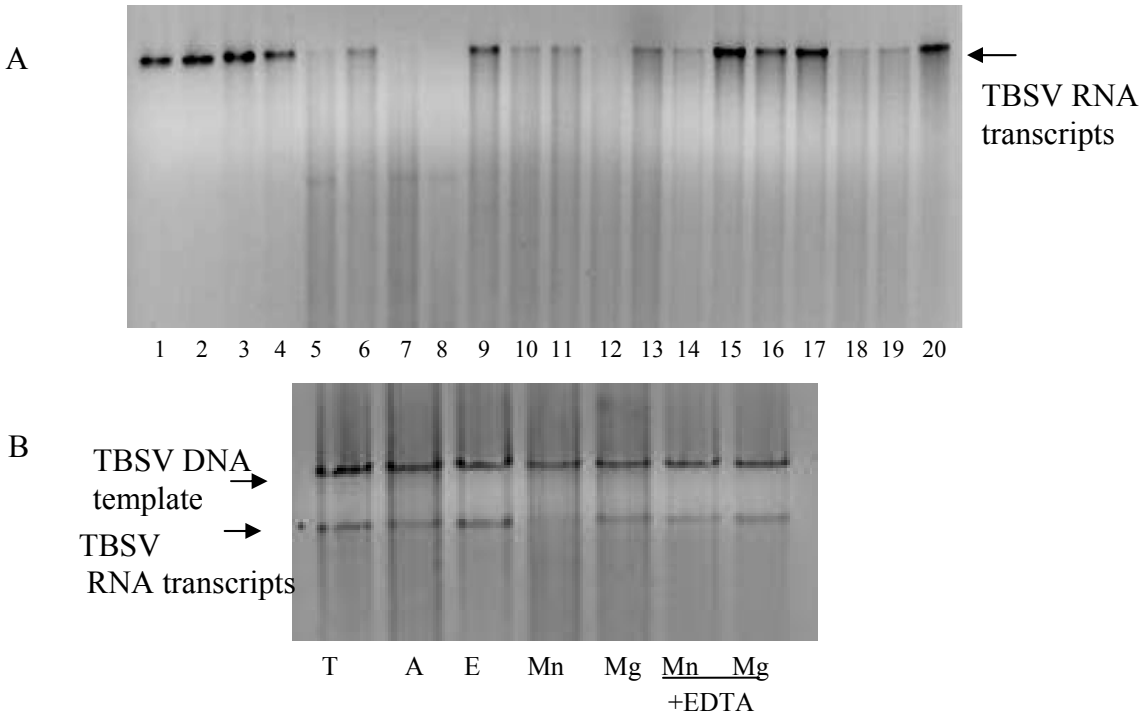

Fig 2.1 Sephacryl S200 gel filtration column chromatography of TBSV Δ19-infected plants. A.) Fractions were analyzed for ribonuclease activity against added TBSV RNA transcripts, as indicated by the arrow. Fractions 5-8 show degradation of virus transcripts. B.) Due to the capacity to degrade TBSV transcripts, fraction 7 was further tested for ribonuclease activity with the addition of EDTA and divalent metal cations, in addition to these in combination. T = only transcripts, A is transcripts plus the active fraction and H20, E is the fractions and with the addition of EDTA. The next two lanes each have the reaction mixture of fractions and transcripts, plus the addition Mg^{2+} and Mn^{2+}, respectively. The last two reactions have Mg^{2+} and Mn^{2+} in combination with EDTA.

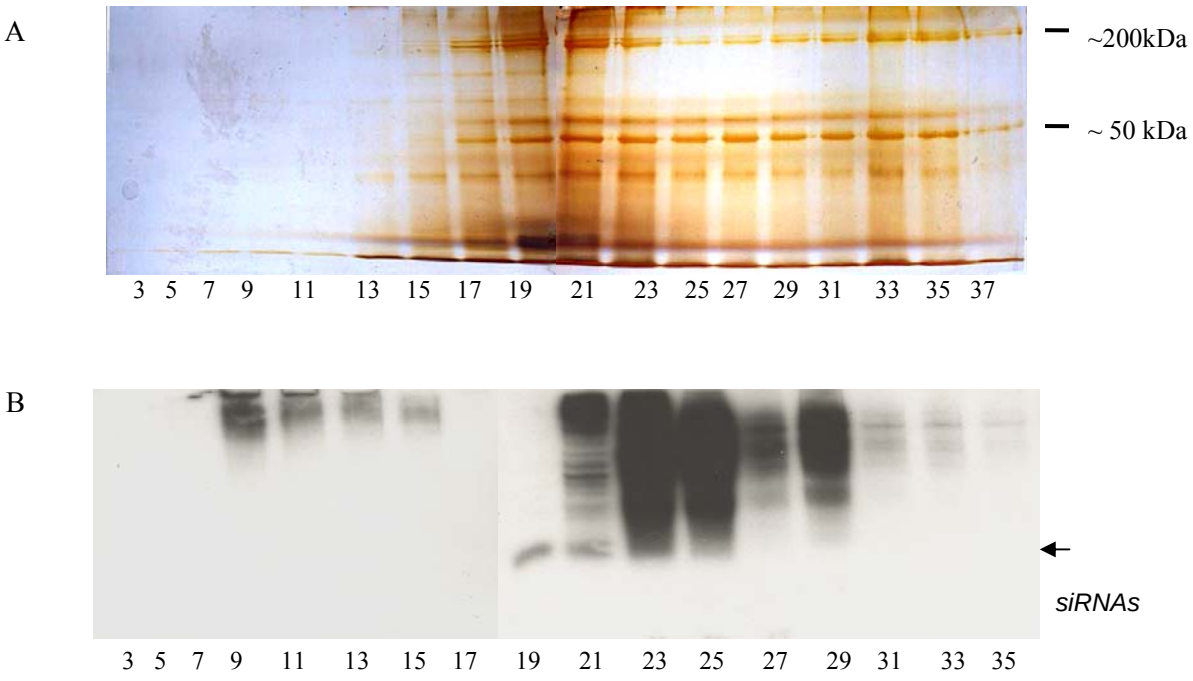

Fig 2.2 Sephacryl S200 fractions following anion exchange chromatography. Fractions were assayed for A.) proteins present in fractions visualized by silver staining, and B.) siRNAs extracted from the anion exchange chromatography fractions, then visualized after northern hybridization for TBSV. Fractions displaying ribonuclease activity also had detectible levels of siRNAs (19-21). The size of siRNAs is approximately between 20-25 nts based on similar analyses that incorporated size markers.

activity had a range of proteins present, and fractions 17-19 have a band at about 200-100 kDa (indicated in Fig. 2.2A) not present in other fractions which might correspond to an Ago protein. The siRNAs were extracted from all DEAE anion exchange chromatography fractions, and northern blotted on a 17% acrylamide gel with 8M urea. Fraction 19 and those following it contained small RNAs of about 20-25 nt (Fig. 2.2b) and had RNase activity (not shown). Because of the multitude of proteins present in these fractions, further protein purification was performed by combining fractions containing ribonuclease activity after DEAE anion exchange chromatography, and subsequent separation with S200 gel filtration. The fractions containing activity after this additional step were then denatured on an SDS-PAGE gel, and silver-stained to reveal the protein content (Fig 2.3). These fractions all contain similarly sized proteins, from about 200 kDa to about 75 kDa, as best seen for the silver stained fraction from gel filtration after anion exchange chromatography (Fig. 2.2a-b). The densest of these bands were sent in for analysis by mass spectrometry (Yale University's Keck Center), though no proteins are known to be involved in the RNAi pathway (i.e, Dicer, Ago, heatshock, loading proteins, etc.) were represented. Instead, the proteins were found to share identity with Phosphoenolpyruvate or Rubisco.

Hydroxyapatite chromatography

Because the proteins analyzed failed to yield a protein that was a signature for the RNAi pathway, such as Ago, additional separation techniques were needed. Fractions from TBSV Δ19-infected tissue were collected using hydroxyapatite column chromatography, and again first tested for ribonuclease activity against TBSV RNA transcripts (Fig 2.4). Fraction 7 and those following displayed ribonuclease activity. Then, 300 µl of these fractions were also assayed for siRNAs. Fraction 7 and, even more so later fractions, were shown to contain siRNAs (Fig 2.5A). Because of the mixed-affinity aspect of hydroxyapatite chromatography, a silver stain was also done for these fractions to examine protein (Fig 2.5B). Again, this single type of chromatography yielded multiple proteins present. To further separate fractions containing RISC-like proteins, these active hydroxyapatite fractions were loaded onto a DEAE anion exchange

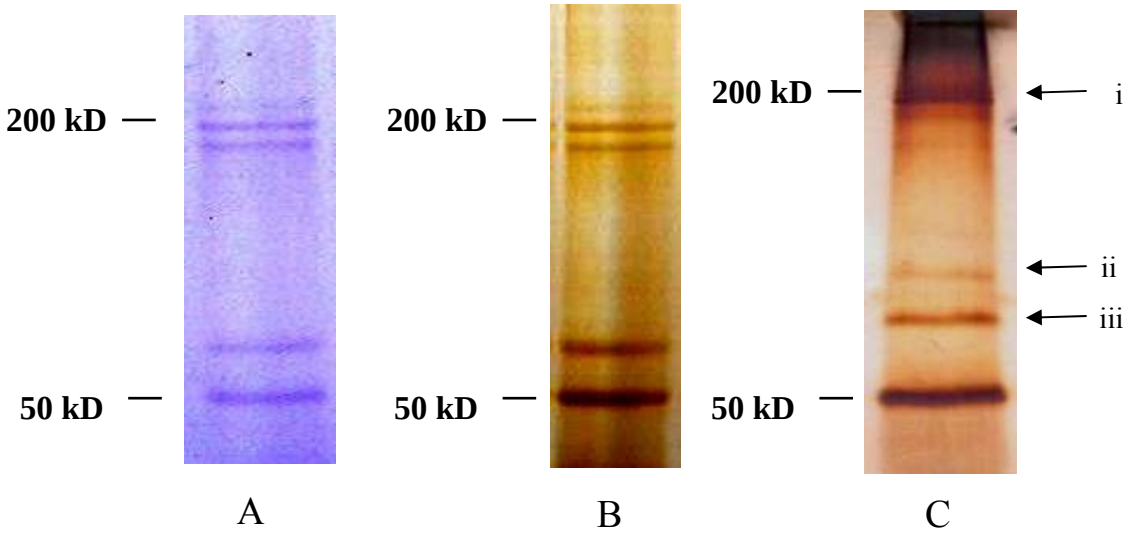

Fig 2.3 Proteins present in anion exchange fractions containing ribonuclease activity. A.) Proteins in active fractions following anion exchange chromatography of TBSV Δ19 infected tissue, stained with coomassie blue. B.) Proteins detected by silver staining of an anion exchange chromatography fraction containing ribonuclease activity C.) Concentrated fraction with ribonuclease activity following Sephacryl S200 gel filtration after anion exchange column chromatography, silver stained to display potential RISC proteins. Upon sequencing, however, the heaviest bands were not those usually attributed to RISC; i was determined to share identity with Rubisco, ii was phosphoenolpyruvate, and iii was found to also share identity with Rubisco.

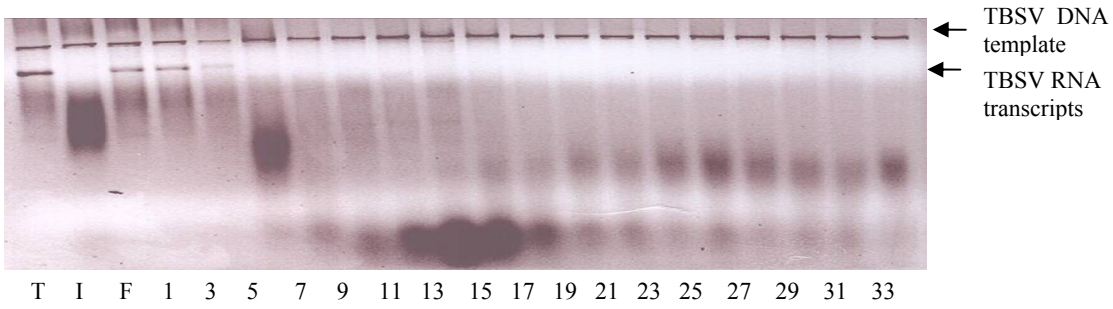

Fig 2.4 Ribonuclease activity test of TBSV Δ19 fractions. TBSV Δ19 infected plant tissue applied to a hydroxyapatite chromatography column and eluted with a 10 mM to 400 mM sodium phosphate gradient: 5 µl of the resultant combined fractions were tested for ribonuclease activity with the addition of 2 µl full length TBSV transcripts. The samples were incubated for 20 min., and viewed with a UV light after gel electrophoresis on a 1% agarose gel and staining with EtBr. Fractions with ribonuclease activity begin around fraction 5. T is transcripts without addition of fractions (volume equilibrated with sterile ddH2) I is column crude input, F is column flowthrough.

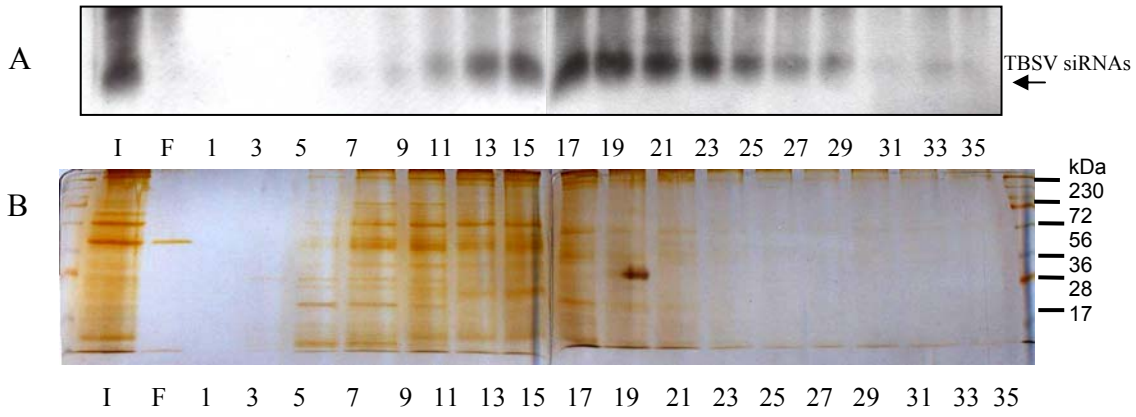

Fig 2.5 siRNAs and proteins detection in hydroxyapatite fractions from TBSV Δ P19. A.) siRNAs were extracted following hydroxyapatite column chromatography of TBSV Δ19–infected plants. These siRNAs were separated on a 17% acrylamide gel with 8 M urea, and blotted to a nylon membrane for northern blotting. The hybridization probe was specific for TBSV, and siRNAs are present starting around fraction 7. B.) Fractions were run on 15% acrylamide SDS-PAGE, and silver stained. I is column crude input, F is column flowthrough.

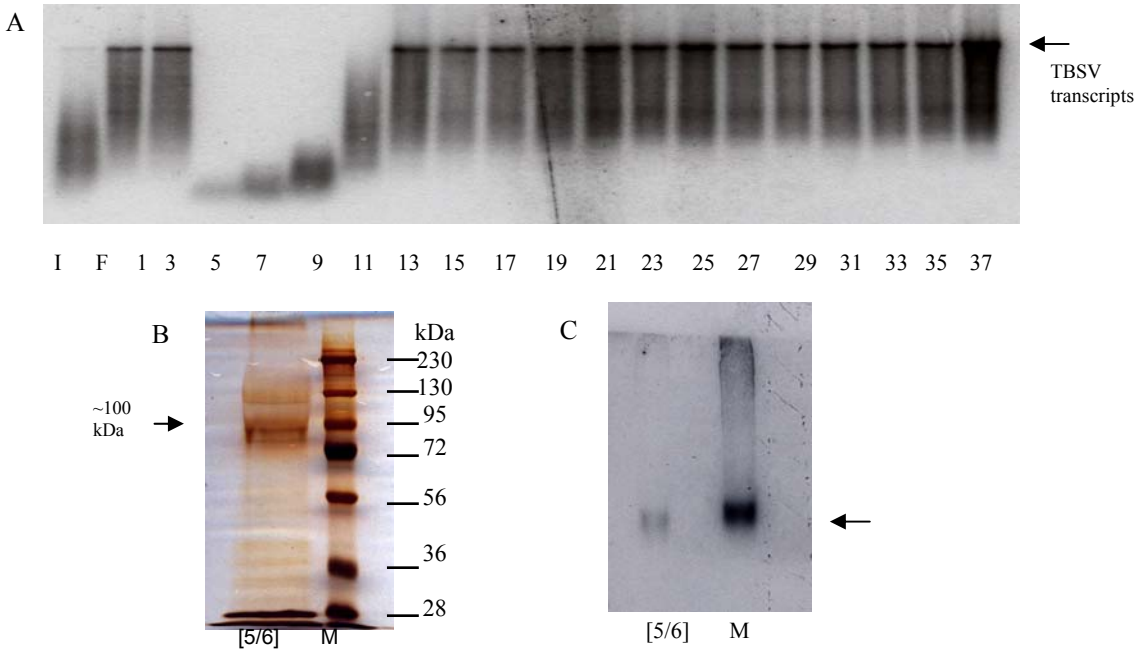

Fig. 2.6 DEAE chromatography after hydroxyapatite chromatography of TBSV Δ19-infected plant tissue. Following hydroxyapatite chromatography of TBSV Δ19-infected plant tissue, fractions with ribonuclease activity were pooled and subjected to DEAE anion exchange chromatography. These fractions then were tested for ribonuclease activity with the addition of TBSV RNA transcripts, and the resultant blot was probed with a TBSV-specific hybridization probe. Fraction 5/6 demonstrates the best activity. B.) This fraction was concentrated by spin-filtration in a centrifuge, and the resultant sample was loaded onto a 7.5% acrylamide SDS-PAGE gel, which was silver stained to detect proteins. Bands are apparent at about 100 kDa, appropriately the expected size for Ago. C.) siRNAs were also extracted from the concentrated fraction, and run on a 17% acrylamide gel with 8 M urea alongside a ~21 nt marker, indicated by an arrow. This is indicative of siRNAs, and that the complex has the hallmarks of a potential RISC. I is column crude input, F is column flowthrough.

chromatography column. When tested for ribonuclease activity against TBSV RNA transcripts, fractions 3-11 degraded transcripts (Fig 2.6A). Fractions 5 and 6 were then concentrated for analysis of proteins present via silver staining (Fig. 2.6B). There was a 100 kDa protein present, which is approximately the size for Ago. Moreover, when this concentrated sample was assayed for siRNAs (Fig. 2.6C) alongside a known 21 nt RNA marker, it shows a fairly clean, readily detectable 21 nt siRNA signal.

Biochemical characterization of TBSV-wt infected plant tissue

The hypothesis was that if the complex that is under investigation represents RISC, it should not become programmed against TBSV in the presence of P19. Therefore, to further characterize the RNAi response as seen in a natural virus infection, wt TBSV (containing p19) -infected plant tissue extract was fractionated with hydroxyapatite chromatography. Resultant fractions were tested for ribonuclease activity (Fig 2.7) against TBSV RNA transcripts, as done in previous experiments. While some activity was observed (fractions 5-23), it was to a much lower intensity that that seen for the TBSV Δ19, with a minor band of transcripts remaining instead of the typical 'wash' of RNA and complete degradation of the TBSV RNA transcripts; the arrow indicates partial RNA transcript bands that remained. Additionally, for hydroxyapatite fractions collected from TBSV Δ19-infected tissue, the input lane usually shows degradation of transcripts (Fig 2.4, lane 'I'), though this was not the case for the wt TBSV-infected tissue hydroxyapatite fractions – the transcripts added to the input lane remained intact (Fig 2.7A, lane 'I').

Western blotting with antibodies against TBSV P19 and CP was performed for the wt TBSV-infected tissue hydroxyapatite fractions (Fig 2.7B, C, respectively). P19 proteins accumulate in fractions that show inhibited ribonuclease activity. For assurance that P19 is present in these fractions and binds siRNAs, IP for P19 was performed on the input, flowthrough, and fraction 9, which showed both activity and an intense siRNA signal, and fraction 33, which had unspecific activity and low siRNAs signal (included as a (-) control). The IP successfully precipitated P19, as shown by western blot. However, when these same IP samples were assayed for siRNAs, only the denser band from the

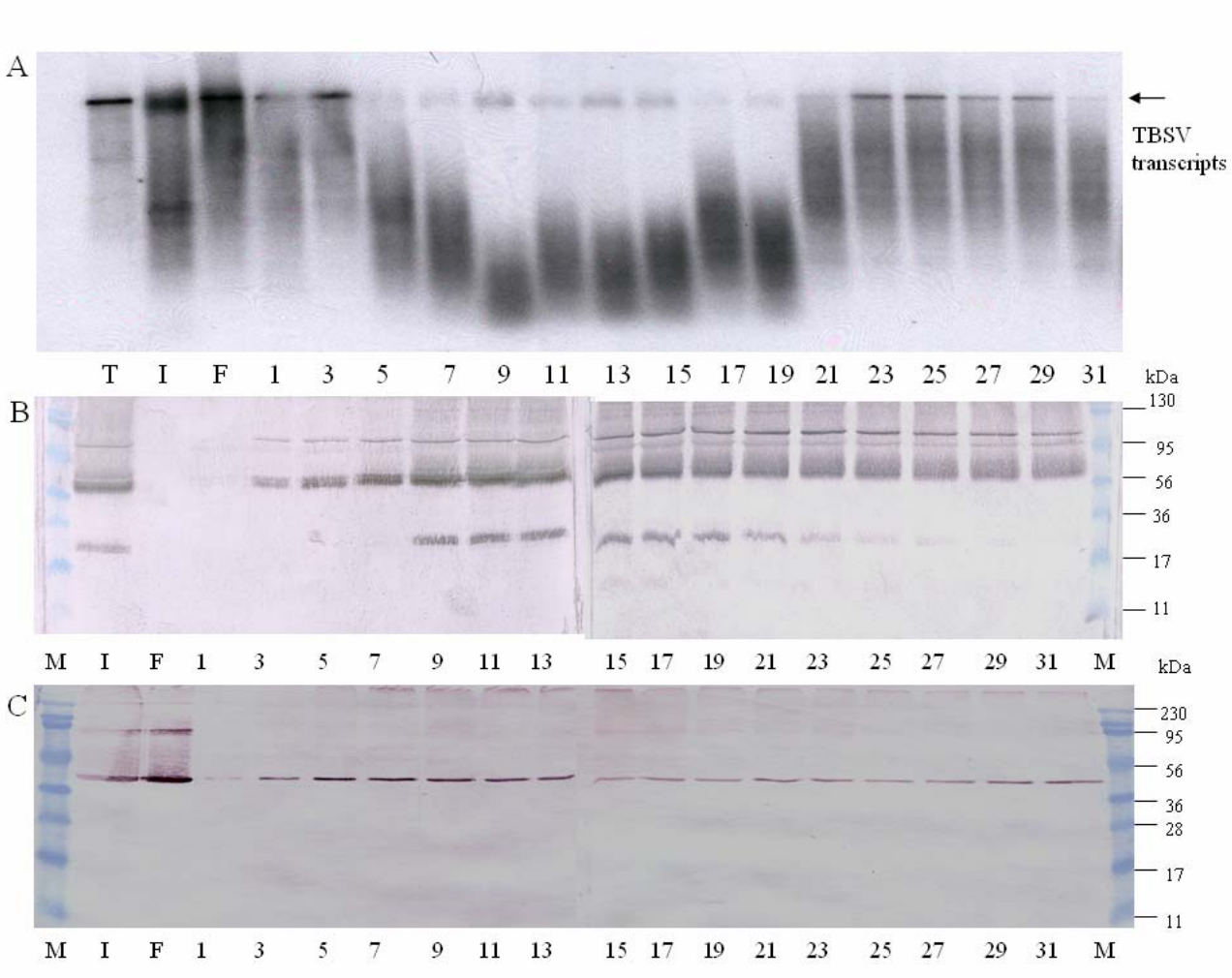

Fig 2.7 Fractions from the hydroxyapatite chromatography of wt TBSV-infected *N. benthamiana.* These were tested for A.) ribonuclease activity with the addition of TBSV full length transcripts, then blotted to a nylon membrane for hybridization with a TBSV-specific probe. Fractions were assayed for B.) TBSV P19 and C.) CP proteins after running on a 15% acrylamide gel, and transfer to nitrocellulose membrane for protein detection by western blotting with appropriate antibodies.

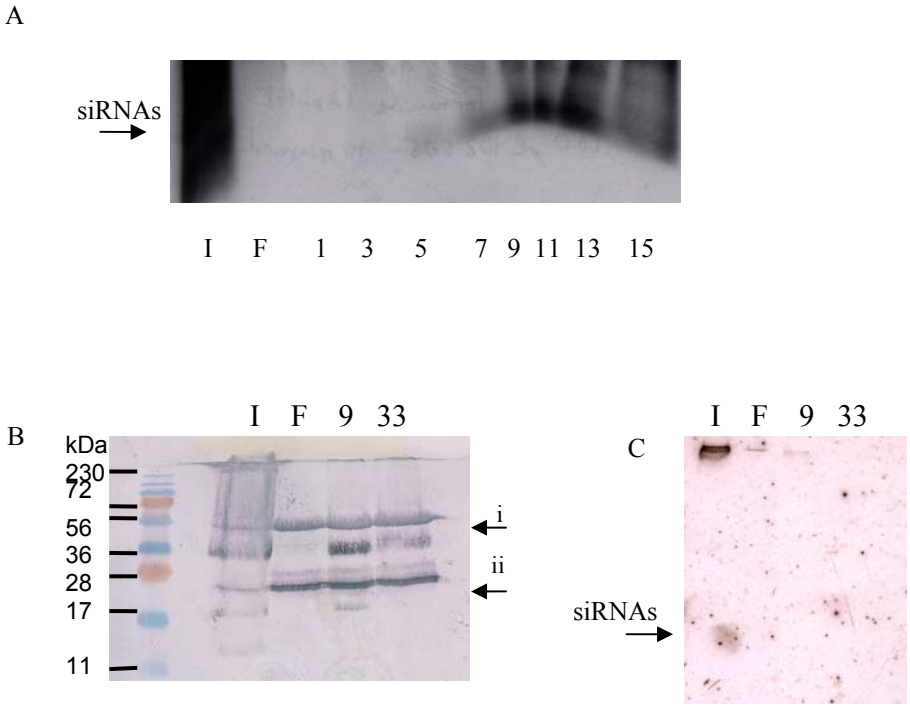

Fig 2.8 Detection of siRNA from wtTBSV-infected tissue following hydroxyapatite column chromatography. A.) Northern blotting of fractions with a hybridization probe for TBSV. These siRNAs appear in about fraction 5, and angle of the bands is due to the increasing amount of sodium phosphate present following chromatography. B.) Fraction 9, which shows a very strong siRNA signal, and 33, which shows a much weaker signal were subjected to immunoprecipitation (IP) with P19 antibodies to correlate presence of P19 and siRNAs with inhibited ribonuclease activity (fraction 33 was included as a control) and subjected to a western blot for P19 following IP. Input and fraction 9 show the presence of P19. (i indicates the dimerized P19, ii indicates P19 monomer C.) siRNAs are evident in the input, but undetectable following IP. At this time, it is hypothesized that reduced amounts of P19 in fraction 9 is the reason these levels are undetectable.

column input showed a band on the western blot. Nevertheless, the results indicate that even though siRNAs are abundantly present in the plant, the presence of P19 has diminished the programming of the anti-TBSV RNA ribonuclease activity.

Discussion

RISC-like anti-viral ribonuclease activity

As described in the Introduction, there is a lot of evidence for RNAi in plants. At this time, however, much of this has been determined using forward or reverse genetics, like knocking out or mutating DCLs and Ago genes to determine effects on the RNAi pathway, both for the endogenous regulatory pathway, as well as for a defensive, anti-viral pathway (for example, Jones et al, 2006) The majority of this research focuses on the model plant *Arabidopsis thaliana* (as illustrated by Baumberger and Baulcombe, 2005). However, little work has concentrated on the direct biochemical isolation of RNAi pathway proteins in plants toward determining which proteins contribute to an anti-viral defense. To be brief, it is expected that the anti-viral response in plants, specifically *N. benthamiana* here, will be comprised of a Dicer or DCL protein (Xie et al., 2004), which cleaves specifically viral RNA into about 21 nt duplexes (Baulcombe, 2004). These duplexed siRNAs will associate with a protein complex, RISC, possibly through the use of some Dicer-type loading protein for association with a protein complex. The complex itself would contain an Ago-family protein, which are hallmarks of RNAi (Song and Joshua-Tor, 2006). Silencing has implicated Ago1 and Ago4 for this in *N. benthaminana* (Jones et al., 2006), though other studies indicate that Ago1 is involved in anti-viral RISCs for *Arabidopsis* (Baumberger and Baulcombe, 2005). Therefore, to biochemically determine if these virus-infected plants launch a RNAi anti-viral response, siRNAs and Ago proteins should be present in these plants, 'programmed' against viral RNAs.

To examine the antiviral plant defense following a viral infection of plants, 2 week old *N. benthamiana* plants were inoculated with a plant virus, TBSV, which has been shown to produce a large amount of dsRNA in the plant (serving as a substrate for Dicer), and encodes a known silencing suppressor, P19 that was shown to bind siRNAs (Omarov et al., 2006). The plants were first infected with mutants of TBSV that do not produce functional P19 (TBSVΔP19), to ensure that an optimal RNAi response is

stimulated without the hindrance of a silencing suppressor. Infected plants were then harvested upon display of obvious viral infection symptoms, and the first experiments used Sephacryl S200 gel filtration to separate out proteins present that would contribute to the plant defense. To test for fractions that might contain RNAi associated ribonuclease activity, TBSV RNA transcripts, generated in vitro from cDNA with a T7 polymerase promoter, was added to each of the fractions. Fractions containing ribonuclease activity demonstrated this activity in vitro against the TBSV RNA transcripts, resulting in degradation (Fig. 2.1A). This fits with the current literature; plants infected with a virus should result in the generation of siRNAs which are then loaded onto a RISC, to further target viral RNA (Baulcombe, 2004). These anti-viral ribonucleases are separated out by column chromatography, and target TBSV transcripts in vitro.

In addition, these results suggested that upon gel filtration, at approximately 500 kDa anti-viral RISC-like complex could be isolated. To confirm that this was a real complex and that results were not due to the co-incidental co-fractionation of elements, other separation techniques were incorporated. Other types of column chromatography were also used to improve protein separation, with the intent to isolate protein complexes associated with activity. Towards this, TBSV plants infected with TBSVΔP19 were subjected to anion exchange chromatography. After ribonuclease activity was determined, divalent metal cations were added to the active fractions to determine the effects. Current literature states that Piwi and PAZ domains contain divalent metal cations; the Piwi domain uses these for catalytic activity (Song et al., 2004), and the PAZ domain is thought to hold a Mg^{2+} to anchor the RNA molecule in a conserved hydrophobic pocket by interacting with the phosphates present on the RNA (Parker et al., 2005). Therefore, the addition of divalent metal ions might stimulate activity following column chromatography, or prevent activity loss due to ion dissociation. As a metal chelator, EDTA would bind to the metal ion present and prevents ribonuclease activity, if indeed the metal ion is contributing to it. This is precisely what was observed in the present study, EDTA inhibited ribonuclease activity. When surplus divalent metal ions were added to active fractions in which activity was inhibited by EDTA, the degradative activity was partially rescued. This supports data that the divalent metal ions contribute to

RISC activity, most likely to the catalysis mechanism of RISC; if the addition of divalent metal ions in this experiment affected the binding of siRNAs, it is unlikely that activity could be stimulated. When the divalent metal cations were added at the same time as EDTA, RNA was still degraded, though not to the same extent as that of Mn^{2+} and Mg^{2+} alone.

siRNA and protein components of RISC

Following DEAE anion exchange chromatography, siRNAs were extracted from all fractions to further confirm the presence of active, genuine RISC; a true RISC carries a ss-siRNA molecule to use as a template for target mRNA (Baulcombe, 2004). The siRNAs were extracted from all DEAE anion exchange chromatography fractions; fractions found to have ribonuclease activity also were shown to contain siRNAs, indicated by the arrow in Fig. 1.3B. Again, this is strongly indicative of a RISC. After checking potential protein content of the fractions by silver staining (Fig. 2.2A), a multitude of proteins were shown. Again, the Ago protein family is widely conserved across many species, though the actual Ago proteins themselves vary in size and precise function (Song and Joshua-Tor, 2006). The Ago that contributes to RISC in *Drosophila* (Ago2) was predicted to be ~130 kDa in size, based on the coding sequence (Hammond et al., 2001), though that same paper cites smaller bands visualized by SDS-PAGE corresponding to the same *ago* gene, predicted to be products of protein proteolysis. Other papers place the *Drosophila* Ago2 at about 235-500 kDa (Nykanen et al., 2001), and the human RISC proteins at 90-160 kDa after isolation by affinity purification (Martinez et al., 2002).

There are several proteins present in Fig 1.3A that might match the expected size. However, because of the multitude of proteins present in these fractions, further protein purification was performed by combining fractions containing ribonuclease activity after DEAE anion exchange chromatography, then additional purification with S200 gel filtration. When these fractions were stained for protein content (Fig 1.4), several prospective bands remained, and these were sent for protein identification by MS/MS. These did not turn up any matches to known RISC proteins; they were found to be proteins found in energy synthesis of the plant. Because these proteins are among the

most abundant in plant tissue, this result is not illogical, though this does not reveal anything about the anti-viral RNAi response, such as Ago, Dicer, or perhaps an additional protein. However, it was decided at this point that a different method of column chromatography might allow for differential separation, without co-elution of these proteins.

The next type of column chromatography used was hydroxyapatite, which was selected as the media interacts with both ionic and anionic groups. This would give a very different protein elution profile than those previously seen. Additionally, it has been seen that hydroxyapatite chromatography does not inhibit ribonuclease activity in other systems (Hammond et al., 2001). When TBSV Δ19 infected plant tissue was separated by this method and tested for ribonuclease activity as well as the presence of siRNAs, again, these were found to co-elute. Following hydroxyapatite fractionation, the fractions were tested for ribonuclease activity with the addition of EDTA and divalent metal cations (data not shown). The effect was found to be similar to that seen upon gel filtration in Fig. 2.1B. Additionally, these fractions displayed activity against genomic RNA, though the activity was limited to only TBSV RNA. When studies were done with the addition of viral transcripts for another virus (PMV), fractions did not target and degrade the PMV RNA (unpublished data). This indicates that the ribonuclease activity is specific for TBSV RNA, which is consistent for real RISC; only viral RNA for which the RISC has been programmed is targeted for degradation (Baulcombe, 2004). This further validates the presence of a complex that is in agreement with RISC; siRNAs (Fig 2.7A) and fractions that target RNA transcripts for degradation (Fig. 2.4A) are the same for three different types of chromatography.

After an additional step of DEAE chromatography, fractions demonstrating activity (Fig. 2.6A) were concentrated, checked for siRNAs (Fig. 2.6C) alongside a 21 nt marker, as well as tested for protein content by silver-staining. When the proteins in this concentrated sample were visualized, a reasonably clear set of bands were detected around 100 kDa, roughly the size of Ago determined for other organisms. Ago alone displays minimal RISC activity for some systems (Baumberger and Baulcombe, 2005), so it is possible that this protein is the anti-viral protein present in plants, although other data, like the gel filtration experiments, where fractions with ribonuclease activity eluted

from the column in fractions corresponding to about 500 kDa, suggest that this protein might act in combination with other proteins. At this time, a reverse approach was undertaken by generating Ago-specific antibodies. These did detect bands in the fractions containing activity. This assay was done for this project by Dr. R. Omarov. I will incorporate this technique into Chapter III.

Effect of P19 on RISC-like activity

The work described above was performed with TBSV Δ19 to examine RNAi silencing without inhibition by the viral suppressor. However, most natural viral infections of plants occur for viruses that encode silencing suppressors. Earlier work had been performed with Sephacryl S200 that suggested for plant tissue infected with wt TBSV, the RNAi response is inhibited (Omarov et al., 2007). The presented study showed that following hydroxyapatite column chromatography of wt-TBSV-infected plants, fractions still contained activity in a manner similar to that seem for TBSV Δ19, though to a much lower extent; partial RNA bands remained intact, and the input lane did not seem to degrade transcripts at all. This helps to illustrate the protective function of a silencing suppressor for the virus in the RNAi pathway. P19 has been shown to bind duplexed siRNAs for sequestration before they are loaded onto a RISC (Voinnet et al., 1999; Qiu et al., 2002; Park et al., 2004; Omarov et al., 2006; Scholthof, 2006). Degradation of transcripts in crude extract from TBSV Δ19 –infected tissue, and lack thereof in the crude extract of wt-TBSV infected tissue can be interpreted to mean that due to the presence of the silencing suppressor P19, presumably isolating siRNAs, RISCs are inefficiently loaded with viral siRNAs in wt-TBSV infected tissue and do not target transcripts. Likewise, this interpretation can be extended to the fractions themselves. Because of the much lower amount of anti-viral programmed RISCs in wt-TBSV fractions, TBSV RNA transcripts remain. The minor amount of ribonuclease activity present can be attributed to the concentrating effect of a chromatography column; fractions contain much more of the same anti-viral protein than does an equal amount of the crude plant extract.

To determine if the P19 shown to accumulate in the same fractions (Fig 2.7B) as those containing ribonuclease activity bind siRNAs as predicted (Qiu et al., 2002; Ye et

al., 2003), immunoprecipitation was preformed with P19 antibodies. When siRNAs were extracted from the immunoprecipitated P19, the fraction with input showed a very minor band, though this was not detected for a fraction with slight ribonucleic activity. This might be related to the amount of P19 that was pulled down; a western for the IP shows a reduced amount of P19 for that fraction than for the input (Fig. 2.8C). Additionally, this also might be related to the amount of ribonuclease activity present; the input fraction contained more P19 with bound siRNAs than did the fraction with slight ribonuclease activity; more siRNAs bound to P19 indicate less siRNAs that can be bound to RISC. Fraction 9 shows slight activity; the amount of siRNAs bound to RISC would imply less siRNAs bound to P19, and less to be detected by immunoprecipitation. Regardless, this further substantiates the claim that the ribonuclease activity seen in these fractions can be attributed to RNAi, as it is inhibited, at least partially, by a silencing suppressor.

In conclusion, the data indicate that fractions from TBSV-infected plants contain a TBSV-specific ribonuclease complex with characteristics shared by RISC seen in the RNAi pathway. The complex can be isolated with three independent separation techniques indicating that the residual activity and siRNAs are associated with the same complex. This ribonuclease activity is enhanced by the addition of divalent metal cations, inhibited by EDTA, is specific for TBSV, and affected by a silencing suppressor. This work documents one of the first successful attempts for any virus-host system towards isolation of a high molecular-weight protein complex that is programmed against a specific virus, and displays properties consistent with RISC.

CHAPTER III
DETERMINATION OF AN ANTI-VIRAL RESPONSE FOLLOWING INFECTION OF PLANTS WITH TRV, PMV AND SPMV

Introduction

RNAi has been shown to be strongly conserved across multiple species, as a method to regulate gene function in everything from plants (Baulcombe, 2004) to fungi (Romano and Macino, 1992), insects (Hammond et al., 2001) and mammals (Liu et al., 2004). Chapter II and recent papers (Omarov et al., 2007; Pantaleo et al., 2007) demonstrated RISC-like antiviral ribonuclease activity specific for *Tombusviruses*. There is evidence that other viruses trigger a virus-specific ribonuclease that is attributed to an RNAi response, specifically illustrated by those used to trigger virus induced gene silencing (VIGS) (Ratcliff et al., 2001; Batten et al., 2003; Burch-Smith et al., 2006). Furthermore, many viruses encode silencing suppressors (Voinnet, 2005; Li and Ding, 2006); viruses favor the smallest functional genome size, and it is reasonable to assume that the silencing suppressors would not be encoded without purpose. To strengthen the model for a conserved anti-viral silencing pathway, and to determine if it corresponds to the postulated models currently based on other systems like *Drosophila*, it is necessary to biochemically analyze the defensive response of plants to viruses other than TBSV.

This work attempted to determine how similar these plant responses are for *Tobacco rattle virus* (TRV), which is not related to TBSV, and identify possible common elements that delineate a conserved RNAi pathway in plants by in vitro examination of subcellular elements. Furthermore, an antiviral defense was studied for a monocot plant model system, versus the dicot system outlined above. *Panicum mosaic virus* (PMV) and satellite panicum mosaic virus (SPMV) were used to study antiviral elements induced in the monocot *Panicum miliaceum* (proso millet) plants upon infection, for comparison to those seen in *N. benthamiana*.

Tobacco rattle virus (TRV) is a viral vector commonly used to silence genes (VIGS) in a wide range of plants (Ratcliff et al., 2001; Burch-Smith et al., 2006). The form of TRV used in this study is a TRV virus vector, constructed for infiltration into the host plant using *Agrobacterium*, based on a construct originally generated by Ratcliff and

colleagues (Fig. 3.1) (Ratcliff et al., 2001). Our T-DNA constructs consist of cDNAs of the TRV strain Ppk20 as constructed by by Liu and colleagues; viral cDNAs were inserted behind CaMV 35-S promoters, with a self-cleaving ribozyme from the satellite viroid of *Subterranean clover mottle virus* at the 3' end (Liu et al., 2002b). RNA1 remains pretty much intact as described above for the wild type virus, with only minor alterations before insertion into the pBIN19 binary vector T-DNA plasmid (Liu et al., 2002b). The RNA2 CP gene remains intact, followed by a multiple cloning site (MCS). The MCS carries a 369-nt segment of a conserved region of the plant phytoene desaturase (*pds*) gene (Fig. 3.1A). This gene is a precursor of the plant carotenoid pathway, and when targeted for silencing by VIGS, the plant tissues turn white.

SPMV is not required for systemic infection of PMV in a host, though a tandem infection has a synergistic effect on host symptom severity (Scholthof, 1999). PMV alone will give a mild mottled phenotype, with slight stunting in millet. Co-infection with SPMV results in much more severe symptoms, including streaked, chlorotic leaves with occasionally necrotic regions (Qiu and Scholthof, 2004). This virus system was chosen for study because it infects monocots. RNAi silencing suppressors have been discovered for viruses that infect monocots (Hemmes et al., 2007), leading to the possibility that RNAi occurs in monocots in a manner similar to that of dicots, though studies have yet to determine whether this occurs. Part of this objective aims to determine if RNAi elements similar to those seen for virus-infected dicots are present in virus-infected monocots. As PMV is classified within the *Tombusviridae*, a virus family with a known RNAi response (Omarov et al., 2007; Pantaleo et al., 2007), PMV stands as a good choice for this work.

The system used to study the RNAi defensive response is essentially the same as that used in Chapter II for the characterization of an RNAi response against TBSV. Plants were inoculated with viruses, and tissue was harvested once the infection was established. Column chromatography was used to separate proteins present, and these fractions were tested for virus-specific ribonuclease activity. Fractions containing ribonuclease activity

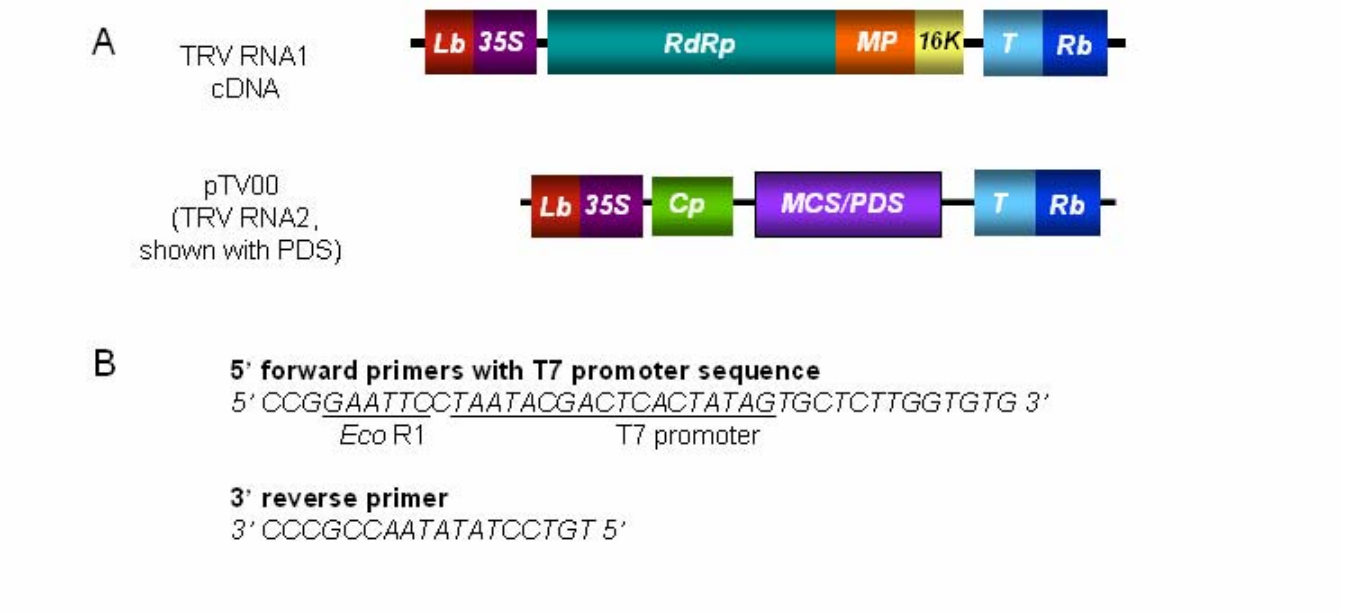

Fig. 3.1 *Tobacco rattle virus* (TRV) agro-infiltration construct and primers. A.) TRV is commonly used as a virus vector, as TRV RNA2 is not required for a systemic infection. This particular construct is used for *Agrobacterium* infiltration, and has cDNA for TRV RNA1 between the left border (Lb) and right border (Rb) of the *Agrobacterium* Ti plasmid, behind a CaMV 35S promoter (35S) and upstream of a ribozyme (Rb) and nopaline synthase terminator (poly A) signal (T) for expression *in planta*. TRV RNA2 has a similar design, but with a multiple cloning site (MCS) replacing the nematode transmission factors. For this project, a portion of the *N. benthamiana* PDS gene, with high sequence homology to other plant PDS genes, has been inserted (PDS). C.) Primers used to generate TRV-RNA2.PDS transcripts used later in this chapter. These primers encompass part of the TRV RNA2.PDS *cp* and *pds*. The forward primer has a sequence for the T7 polymerase promoter to allow synthesis of RNA directly from PCR products.

were tested for the presence of small RNAs, specifically those corresponding to the virus used to infect the plant, as the presence of siRNAs is a hallmark of RNAi. These fractions were then assayed for the presence of potential Ago proteins with western blotting with antibodies against the conserved region of the Piwi domain. Fractions containing both siRNAs and proteins with a Piwi domain were then tested to determine if the ribonuclease activity was inhibited by the addition of EDTA, which is a metal chelator, and high concentrations of NaCl. The hypothesis was that if the plant defensive response is RNAi-based, EDTA would act as an inhibitor because the Ago protein of RISC uses metal ions for catalysis of the ribonuclease activity (Tomari and Zamore, 2005).

NaCl has been shown to have an impact of RISC activity (Rand et al., 2004), though it might inhibit it in a different way; siRNAs are shown to be associated with the PAZ domain using ionic interactions (Song and Joshua-Tor, 2006). It might be that an increase of salt would remove siRNAs from RISC, though this has not been observed for other systems; treatment with high concentrations of salt has been used to as part of the Ago purification process (Hammond et al., 2001). Additionally, NaCl would prohibit unspecific binding of siRNAs by causing the associated guide siRNAs to bind more tightly to the target long ssRNA. Because RISC has been shown to use divalent metal ions in catalysis, as mentioned above, Mg^{2+} and Mn^{2+} were also used for stimulation of RISC activity in ribonuclease-containing fractions. The coincidence of these factors would indicate with high likelihood the presence of a genuine RISC-type protein.

The results show that TRV and PMV/SPMV -induced RNAi responses share key features with those observed for TBSV Chapter II, but some unique features were observed as well.

Materials and Methods

Infection of plants with TRV and PMV/SPMV

Agrobacterium-mediated infection of plants using T-DNA plasmids that express TRV RNA1 and the RNA2 vector with a PDS gene (Burch-Smith et al., 2004) were used to examine a potential RNAi plant response. Overnight cultures of *Agrobacterium* were added to 50 ml of Luria broth with 1 ml 10 mM 2-(4-Morpholino)-ethanesulfonic Acid (MES) and $MgCl_2$, 50 µl kanamycin, 50 µl tetracyline, 25 µl rifampicin and 20 mM

acetosyringone for 12 hours. These cultures were centrifuged for 30 min. at 4000 rpm with a Beckman S4180 rotor, the bacterial pellet re-suspended in 10 ml of 10 mM MES and 10 mM $MgCl^{2+}$, plus 150 µl 150 mM acetosyringone, and incubated at room temperature following a 20 min. agitation period. Equal amounts of these cultures for TRV RNA1 and TRV RNA2 were combined, and 3 leaves of 3 wk old *N. benthamiana* plants were infiltrated with 1 ml per plant using a needle-less syringe. These plants were grown at 25° C until infection was established, after which tissue was harvested.

As the project progressed, plants infiltrated with the TRV constructs were harvested at different timepoints. The earliest experiments used obviously silenced (whitened) tissue harvested about 8 weeks post inoculation. As the project progressed, it became obvious that fractions from this older tissue gave a very unspecific ribonuclease response, and it was thought that tissue collected from TRV-infiltrated plants earlier in the infection (2 weeks, 1 week) would give a more virus-specific defense response. Thus, TRV-infected plant tissue was harvested at these times.

Three-week old proso millet (*Panicum miliaceum* L.) plants were rub-inoculated with infected tissue. This tissue was obtained from millet that had been inoculated with infectious PMV and SPMV in vitro-generated infectious transcripts, made via a T7 RNA polymerase system (Turina et al., 1998), as done with TBSV RNA transcripts in Chapter II. These transcripts were then used to rub-inoculate three week-old proso millet plants using RNA-inoculation buffer (50 mM KH_2PO_4, 50 mM Glycine, pH 9.0, 1% celite, 1% bentonite).

Infected tissue was processed by grinding in a chilled mortar and pestle with 10 mM sodium phosphate buffer, with sea sand as added abrasive. This crude extract was then further homogenized with a blender, and clarified using centrifugation, as described in Chapter II. The plant extract was filtered through cheesecloth into falcon tubes, and placed on ice until it was applied to the hydroxyapatite chromatographic column. For column packing, please refer to Chapter II and the appendix. Again, fractions from hydroxyapatite chromatography were combined for easier manipulation, mixing equal amounts of the fractions, 2 at a time (for instance, fractions 1 and 2, 3 and 4, 5 and 6, etc.), before storing at - 20° C.

Extraction of siRNAs from chromatographic fractions

This was done as described in the Material and Methods section of Chapter II.

SDS-PAGE and Western analysis of samples for Piwi-containing proteins.

The peptide "kivegqryskrlnerq" was used for production of the antibody as BLAST analysis of plant Ago proteins show this to be a conserved plant-Ago specific domain, specifically for the Piwi-domain of Ago1 and 2 from *N. benthamiana.* The antibodies were raised in rabbits (SigmaAldrich, St. Louis, MO). SDS-PAGE was performed as described in the Chapter II Materials and Methods section.

Upon protein gel electrophoresis with very small amounts of protein/samples, these proteins were detected using antibodies and chemiluminesence. After rinsing the blot following addition of primary antibodies, the horseradish-peroxidase anti-rabbit secondary antibody (Pierce) was added to 10 ml of 7.5% milk solution. This was then incubated at least 2 hours, then the blot was rinsed extensively with TBS-Tween (20 ml for 15 min., 4-6 times). The blot was then developed with the chemiluminesence western detection kit (Pierce), immediately exposed to Kodak BioMax X-ray film (Bio-rad) for 1 min., then the film was developed.

Assays to further characterize ribonuclease activity.

Total RNA extraction from infected tissue

For TRV, many assays were carried out using total RNA extracted 1 week post inoculation from TRV-RNA1 and RNA2-PDS infected plants. About 1 gram of infected tissue was ground with 1 ml 2X STE+1% SDS (2 mM Tris, 20 mM NaCl, 0.002 mM EDTA, and 1% SDS) with chilled mortars and pestles. Then, 1 ml 1:1 phenol/chloroform was added, and tissue was reground to mix. This was centrifuged at 10,000 rpm, at 4° C using a Beckman F2402 rotor for 20 min. The upper aqueous phase was removed to a separate 1.5 ml microfuge tube, 1 ml of 1:1 phenol:chloroform was added, the sample vortexed, then centrifuged at 10,000 rpm again for 20 min. at 4°C. The upper aqueous phase (~400 µl) was again placed in a new microfuge tube, and 40 µl 8M lithium chloride was added to precipitate RNA while the sample was placed on ice for 15 min. The RNA

was then pelleted by centrifugation at 10,000 rpm in a Beckman F2402 for 20 min. at 4°C, and rinsed with ice cold 70% ethanol, centrifuging again at 10,000 rpm for 10 min. at 4°C. The 70% ethanol was discarded, and the pellet dried very briefly by vacuum centrifugation (no more than 5 min. to completely remove the ethanol). The RNA was re-suspended in a/c ddH2O plus RNasin and DTT [100 µl sterile ddH20, 1 µl Ribolock RNase inhibitor, and 2 µl 0.1 mM DTT (Fermentas, Glen Burnie, MD)], depending upon the final concentration as detected by nanodrop. The assays typically used ~250 ng/ µl RNA/fraction sample, unless otherwise noted.

TRV RNA2.PDS PCR and RNA transcripts

Additionally, ribonuclease activity was assayed using RNA transcripts generated in vitro from linearized cDNA. For TRV, a PCR reaction to amplify a 2 kb segment TRV-RNA2.PDS was made using primers that overlap the PDS-region of the TRV-RNA2 vector carrying a segment of the *N. benthamiana pds* gene (TRV-RNA2.PDS) (Fig. 3.1B), designed to add a T7 polymerase promoter sequence for in vitro transcription. For PCR, TRV-RNA2.PDS was amplified in overnight cultures consisting of 2 mls LB and Kan^{50}. DNA was extracted using Qiagen Mini-prep kits (Valencia, CA), and stored at - 20°C until needed. For PCR, primers were diluted to about 50 ρm; 1 µl of the DNA was mixed with 1 µl each primer, 1 µl 12.5 mM dNTP mix, 1 µl $MgSO_4$, 5 µl Thermopol buffer, 40 µl a/c ddH20, and 1 µl Vent DNA polymerase (2000 U/ml) (New England Biolabs) in bubble-topped tubes. PCR settings used were 3 min. pre-denature at 93° C, 1 min. denature at 93° C, 1 min. re-annealing at 55 ° C, and 2 min. 15 seconds extension at 72 ° C, for 35 cycles. The resultant DNA was checked by ethidium bromide staining after electrophoresis on a 1% agarose gel, and purified with phenol-cholorform as described above. RNA transcripts were then made from this PCR template as described above. PMV transcripts were generated as outlined in a previous section.

<u>Assays for the presence and characterization of ribonuclease activity</u>

Fractions from column chromatography were mixed with either total RNA extracted from virus-infected plants, or with transcripts generated in vitro from linearized viral cDNA as outlined above. For the 5 dpi TRV and PMV experiments, the

concentration of RNA was determined using a nanodrop, and standardized to ~250 ng/µl to ensure uniformity of ribonuclease substrate. In other experiments, RNA was assayed by electrophorsis with a 1% agarose gel, stained with ethidium bromide, and checked for quality using a UV light.

To test for activity of ribonucleases, 5 µl of each combined fraction was incubated at room temperature (about 25°C) with 1.5-2 µl RNA for 20 min. with 1.5 µl RNasin-treated ddH2O [100 µl sterile ddH2O, 2 µl DTT, 1 µl Ribolock RNase inhibitor (Fermentas, Glen Burnie, MD)]. Then, 2 µl DNA loading dye was added, and samples were run on a 1% agarose gel, 120 volts, in 1X TBE until the lower dye band was about ¾ of the way from the front of the gel. These gels were then stained with ethidium bromide for 15 min., and viewed with a UV light box. To test for inhibition by EDTA or NaCl, the indicated amount of 50 mM or 100 mM EDTA or 5 M NaCl stock solution was added to each fraction before the addition of RNA. To stop a reaction, EDTA was added at the time detailed in the assay, or after 20 min.. Determination of the effect of divalent metal cations on ribonuclease activity present in the fractions, 50 mM $MgCl_2$ and 50 mM $MnSO_4$ were used in the amount specified by the assay.

Northern blotting and hybridization with radioactive DNA probes

Northern hybridizations were performed essentially as described in Chapter II.

Results

Determination of an anti-viral plant defense response against TRV.

N. benthamiana plants infected with TRV RNA1 plus RNA2.PDS displayed a 'silenced' phenotype of whitened tissue. This photo-bleached phenotype was readily visible after about 5-7 days post-infiltration for *N. benthamiana* (Fig. 3.2A). The region of the inserted gene is conserved not only in *N. benthamiana*, but shares homology to the tomato *pds* gene (Liu et al., 2002b), and also triggers a white phenotype in pepper plants (Fig. 3.2.B). Interestingly, manifestation of the photo-bleached phenotype took much longer in pepper, up to 3 weeks post-infiltration (Fig 3.2B), versus 5-7 days in *N. benthamiana.*

The first experiments for characterization of a TRV RNAi-associated ribonuclease used 8 week post infiltrated *N. benthamiana* plants, particularly the upper, whitened tissue. This tissue was applied to both DEAE anion exchange chromatography columns (Fig. 3.3), and later, hydroxyapatite chromatography (not shown). The resultant fractions were tested for degradation of TRV RNA2.PDS RNA transcripts. The northern blot from the 1% agarose gel shows degradation of RNA transcripts beginning in fraction 5, showing complete degradation in fractions 7 as well as later fractions (Fig. 3.3A). This activity was inhibited with the addition of EDTA (Fig. 3.3B), and a kinetics study for ribonuclease activity showed that RNA was nearly totally degraded at about 5 and a half min. (data not shown). However, fractions also displayed activity against TBSV RNA transcripts. No siRNAs were detected upon extraction from the fractions, and with an additional chromatography step of S200 gel filtration, no ribonuclease activity against TRV RNA2.PDS RNA transcripts was observed (data not shown).

With the idea that perhaps the infection was established too long, more *N. benthamiana* plants infiltrated with TRV RNA1 and RNA2.PDS were harvested for hydroxyapatite chromatography at 14 dpi. These fractions displayed ribonuclease activity, against TRV RAN2.PDS RNA transcripts (Fig. 3.4A), which appeared to begin in fraction 11. Fractions were also tested for the specificity of this degradation with the addition of TBSV wt RNA transcripts, alongside degradation of TRV RNA2.PDS RNA transcripts (Fig. 3.4B). Activity corresponds in fraction 11, again, for both sets of transcripts, indicating unspecificity. This activity was inhibited by the addition of 1.5M NaCl as well as EDTA (data not shown). A small Sephacryl S200 gel column was used to separate out fractions 7-13. RNA from the fractions was electrophoresed on a 17% acrylamide gel with 8M urea, blotted to a nylon membrane, and probed with a TRV RNA2.PDS hybridization probe. After the membrane had been exposed to film for over 2 weeks, the film was developed. A small RNA signal can be seen in active hydroxyapatite fractions collected from both 2 mts and (very faint for) 2 wks –pi plant tissue, but none was seen for the fractions collected after hydroxyapatite plus gel filtration (Fig. 3.5).

A  B 

Fig. 3.2 TRV-infected plants. A.) *N. benthamiana* and B.) *C. annuum* (pepper) were agro-infiltrated with the TRV RNA1 and RNA2.PDS constructs. Picture was taken 2 weeks post infiltration for *N. benthamiana*, and about 4 weeks post infiltration for pepper. Visible silencing of the plant PDS gene is illustrated by the white tissue of the upper leaves.

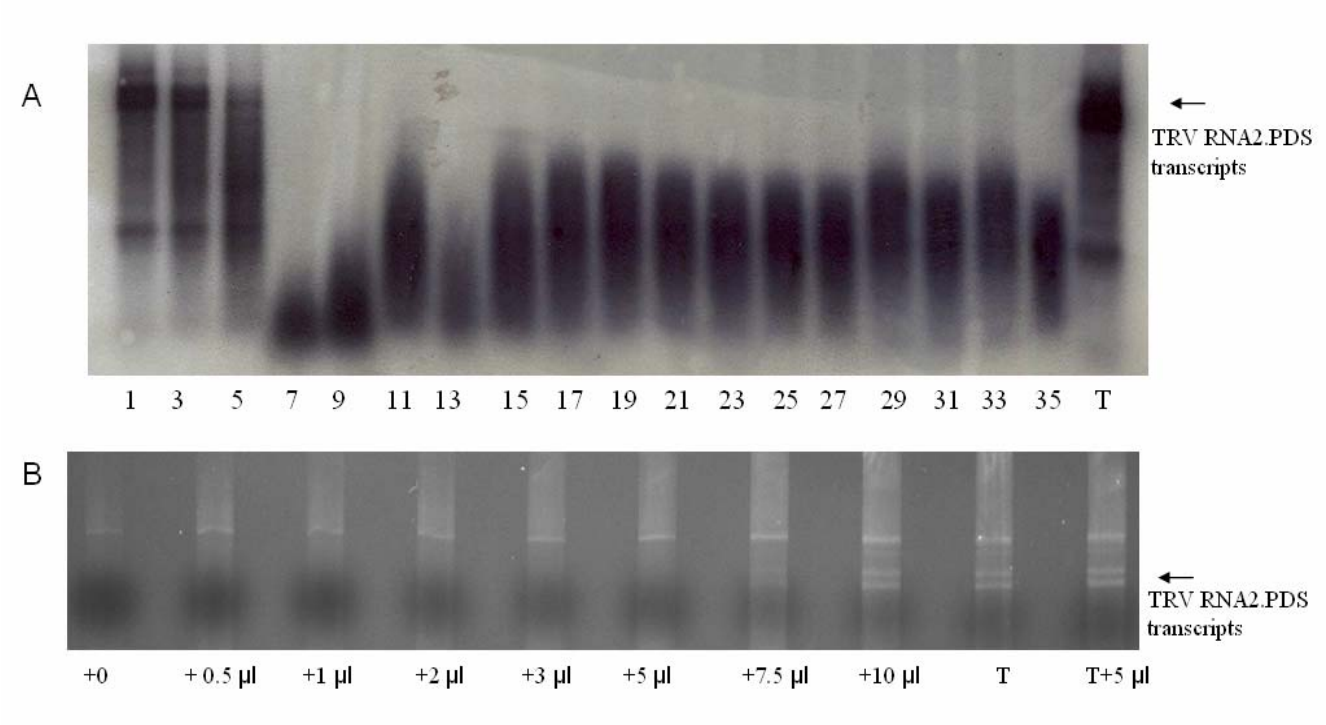

Fig. 3.3 DEAE ion exchange chromatography was performed on *N. benthamiana* 8 weeks post infiltration. A.) Transcripts generated i*n vitro for* TRV-RNA2.PDS were added to fractions, incubated for 20 min., and electrophoresed on a 1% agarose gel, then followed by northern hybridization against TRV-RNA2. (T= 2 µl transcript only, plus 5 µl a/c ddH2O; 2 µl transcripts were added to 5 µl combined fractions). These fractions show ribonuclease activity, starting in fraction 7. B.) hydroxyapatite fraction 7 was assayed for inhibition of ribonuclease activity with the addition of increasing amounts of 100 mM EDTA. For each sample, 5µl fraction 7 (H2O for T) + 2 µl transcript were combined and incubated for the amount of EDTA indicated, then samples were analyzed by ethidium bromide staining after gel electrophoresis. (i:TBSV DNA, ii: TBSV RNA transcripts, iii: TRV RNA2.PDS transcripts)

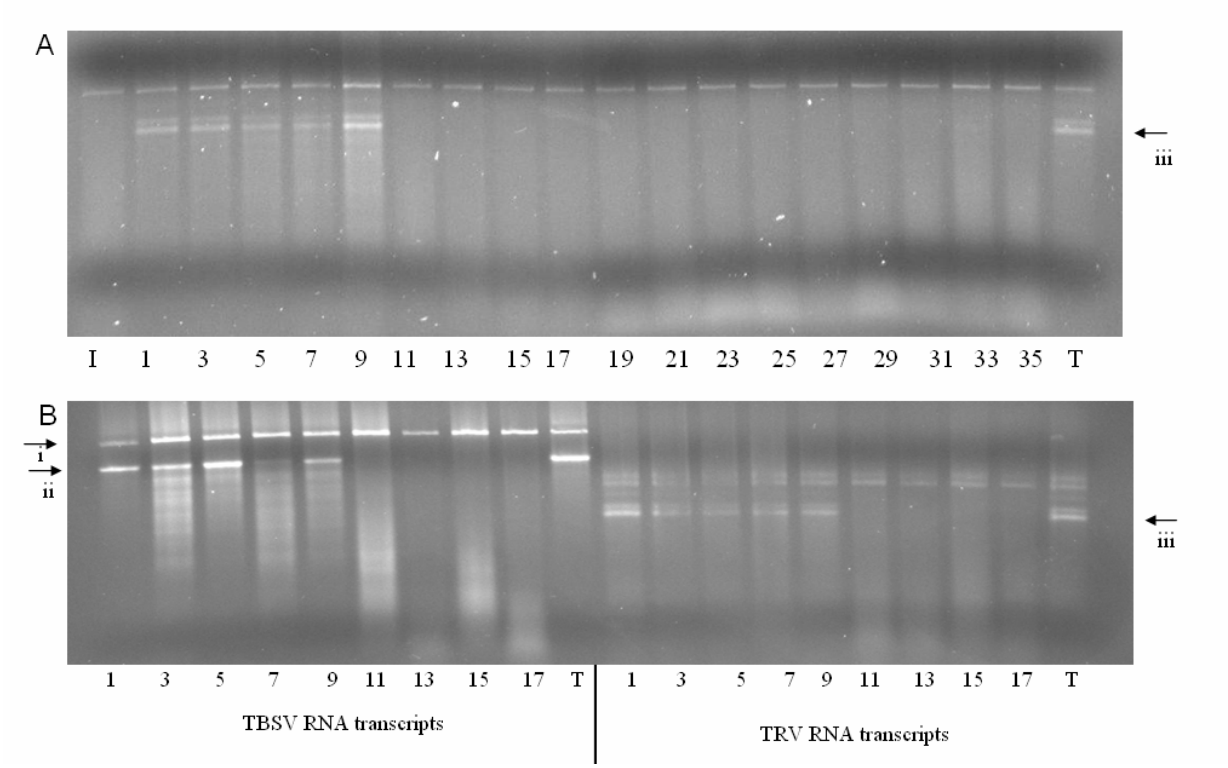

Fig 3.4 Hydroxyapatite fractions collected from 14 dpi TRV-infected *N. benthamiana* plants were characterized. A.) Fractions were tested for ribonuclease activity against A.) TRV-RNA2.PDS transcripts; 5 µl of each combined fraction (T with a/c ddH20) was combined RNA. B.) Test for specificity of RNA degradation, as indicated. 5 µl of each combined fraction (T with a/c ddH20) was combined with either 2 µl TBSV or TRV RNA2 transcripts, prepared in vitro. These fractions and transcripts were then subjected to gel electrophoresis, and stained with ethidium bromide.

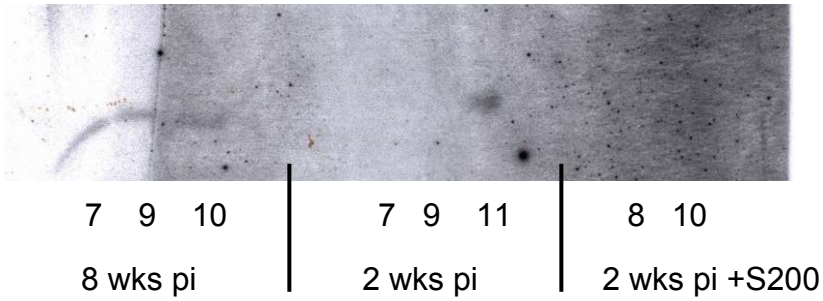

Fig 3.5 siRNA assay for TRV-infected plant tissue extract chromatography fractions. Combined fractions indicated, taken from hydroxyapatite chromatography fractions 8 weeks post infiltration, 2 weeks post infiltration, and the 2 week post infiltration hydroxyapatite chromatography fractions 7-13 following Sephacryl S200 column chromatography fractions were collected and used for siRNA extraction. Resultant samples were then separated by 17% acrylamide, 8 M urea gel electrophoresis, and blotted to a nylon membrane for northern detection of TRV-RNA2.PDS. Visible potential siRNAs are apparent for fractions containing activity 8 weeks and 2 weeks post inoculation following hydroxyapatite fractionation steps, but unapparent following an additional gel filtration step.

Despite numerous tests, the above summarizes results showing that fractions did not display TRV-specific ribonuclease activity, nor were siRNAs detected reliably. It was suggested that plants be harvested even earlier in the course of infection. For this purpose, tissue from TRV RNA1/RNA2.PDS infected plants was harvested 5-7 dpi, and applied to a hydroxyapatite chromatography column. Fractions were tested for degradation of RNA this time using total RNA extracted from TRV-infected plants, instead of using TRV RNA2.PDS transcripts. Unspecific ribonuclease activity was seen beginning in fraction 3 (data not shown). From this fraction to fraction 15, siRNAs were extracted, run on a 17% acrylamide SDS-PAGE with 8 M urea, and blotted to a membrane to probe with a hybridization probe using a TRV RNA2 vector without a gene insert in the MCS. The resultant northern blot showed a clear signal for siRNAs in fraction 9 and later fractions (Fig 3.6A), though it is possible that siRNAs are present in undetectable levels in earlier fractions.

These siRNA-containing fractions were then subjected to western blotting with antibodies generated against a conserved region of the Ago Piwi domain, which is a hallmark of RNAi pathway. Fractions showed several bands (about 130 kDa, 95 kDa, 60 kDa, 50 kDa, and faint others), with those of an appropriate size (around 100 kDa or larger) (Hammond et al., 2001). Beginning around fraction 9, corresponding to the first siRNAs detected by northern analysis, the presence of a much smaller band was detected (about 17 kDa) (Fig 3.6B).

To possibly increase specificity, these fractions with detectable siRNAs and potential Ago proteins were concentrated and further separated using a Sephacryl S200 gel column. Fractions were again analyzed with total RNA extracted from TRV-infected plants, and northerns probed with TRV RNA2 showed ribonuclease activity in fractions 8 – 10 (Fig 3.7A), though these same fractions did not degrade TBSV RNA transcripts (Fig 3.7B). This result verifies that the ribonuclease activity displayed in these fractions is virus-specific. The experiment was repeated for another set of TRV- infected plants, these were harvested 5 dpi and subjected to hydroxyapatite and gel chromatography. The second set of fractions also displays ribonuclease activity for TRV total RNA as illustrated by northern blotting, but not for TBSV RNA transcripts, also detected by northern blotting (Fig 3.7 C, D). The exact fraction with activity varies between these two

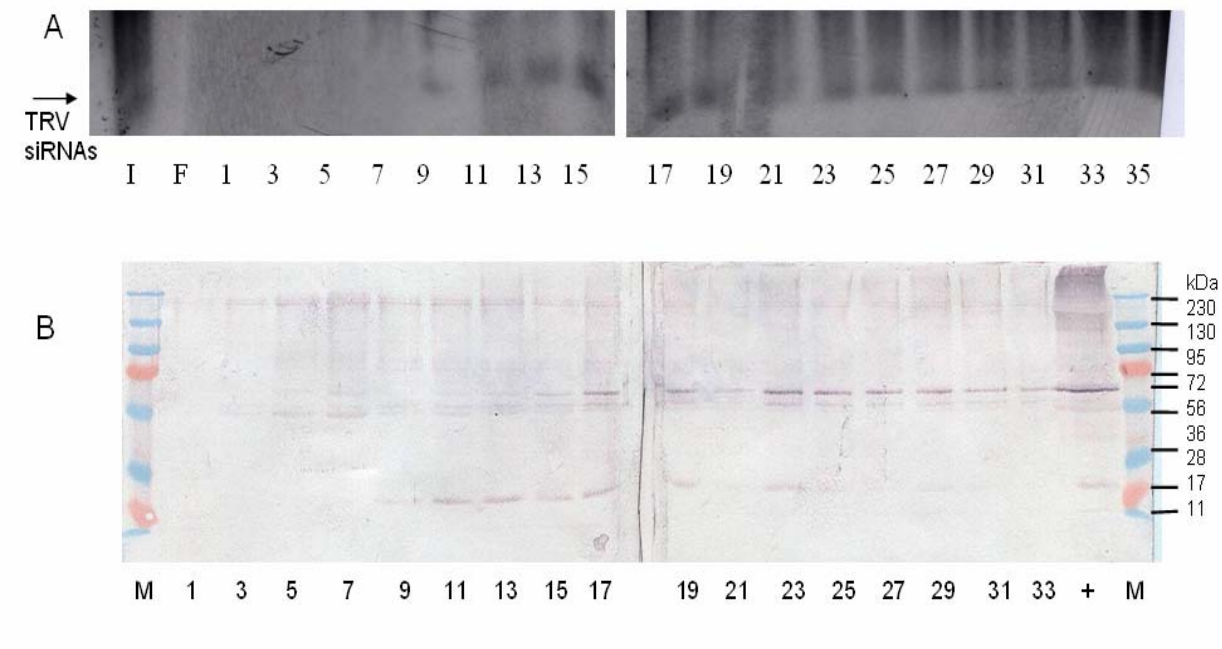

Fig. 3.6 Analysis of siRNAs and Ago-associated proteins present in fractions collected from hydroxyapatite fractionation of TRV-infected *N. benthamiana* plants, 5 dpi. A.) siRNAs extracted from hydroxyapatite fractions visualized by northern hybridization for TRV-RNA2. Arrow indicates siRNAs. B.) Western blot for Piwi domain of Ago protein in hydroxyapatite fractions of TRV-infected plant extract. Fractions 9-17, which show ribonuclease activity, show a smaller band that might possibly be associated with RISC activity. The + lane is a positive control consisting of TBSV crude extract, previously demonstrated to have a positive response with the Piwi antibody, which also has the smaller band.

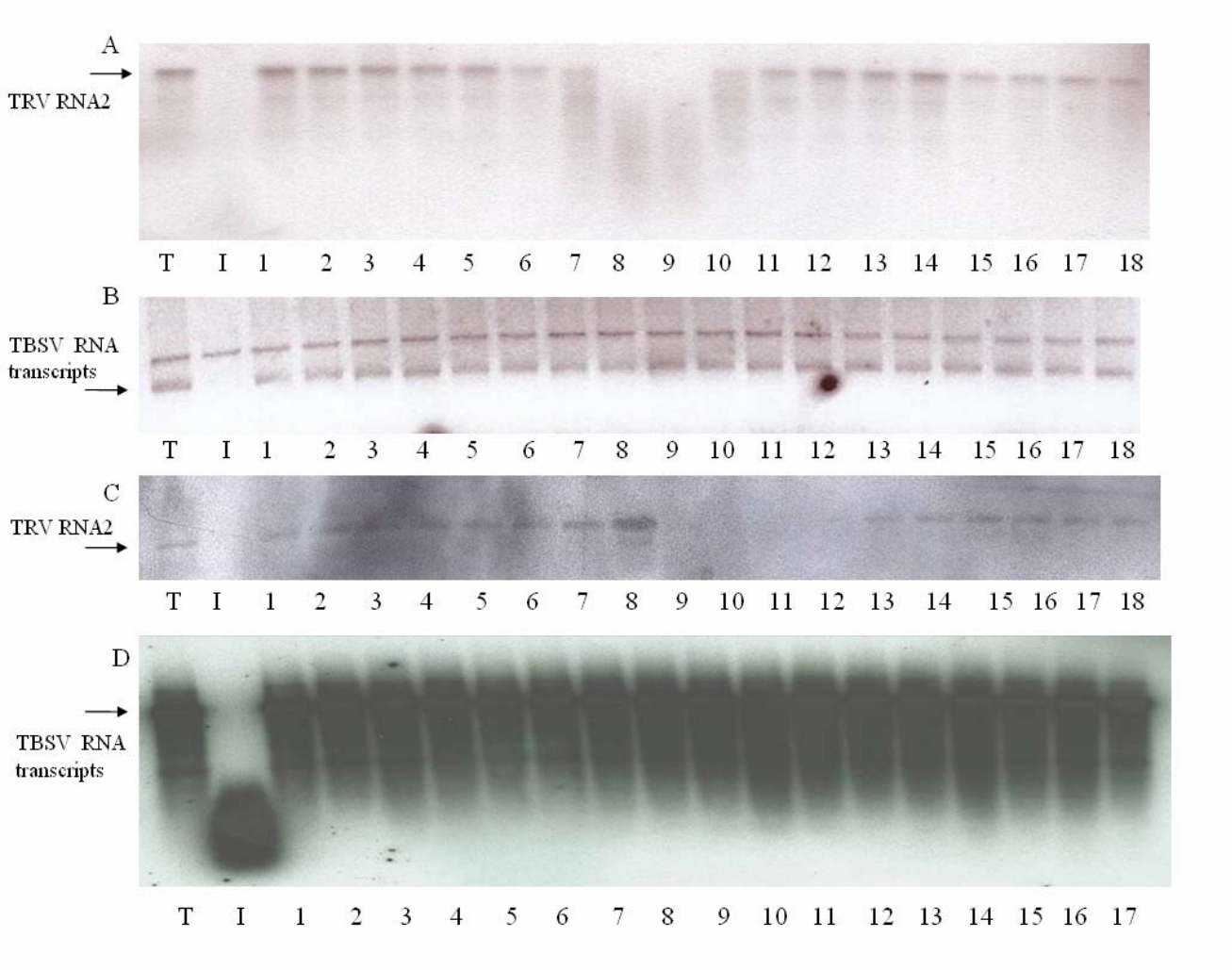

Fig 3.7 Sephacryl S200 chromatography of TRV hydroxyapatite fractions. Following hydroxyapatite chromatography, fractions containing ribonuclease activity and potential Ago proteins were subjected to Sephacryl S200 gel filtration to test for activity (A and B are from same fractionation, C and D are from corresponding fractions). A.) and C.) Fractions were mixed with total RNA from TRV-infected followed by northern hybridization with TRV-RNA2. B.) and D.) Ribonuclease activity with TBSV RNA full length transcripts, generated in vitro. C.) Ethidium bromide stained agarose gel, and D.) Northern blot probed with TBSV hybridization probe. (Lane T is RNA without addition of fractions, lane I (input) consists of hydroxyapatite fractions showing activity and presence of siRNAs before S200 chromatography, plus addition of TRV RNA. M is a DNA ladder. Lanes 1-18 are S200 fractions with the addition of RNA. Activity against TRV seen in different lanes for different fractionations, due to variability in collecting fractions following elution. This variability does not affect activity; it only changes the fraction number.

iterations; this is due to normal column variability and the collection of eluted fractions. Protein elution is detected by spectroscopy as fractions are collected, and minor variances in the timing lead to differences in fraction number, though not elution profile of proteins.

These results indicate that at early timepoints following infection, a true anti-TRV ribonuclease was programmed in virus-infected plants. To obtain additional evidence that this ribonuclease acts similarly to that seen in the previous chapter for TBSV, as well as to determine how it fits the model RNAi pathway, the fractions containing activity were then subjected to a battery of biochemical analyses.

Characterization of TRV-specific ribonuclease activity

Fractions from gel filtration after hydroxyapatite were tested with differing amounts of 100 mM EDTA, to establish the amount of EDTA required for inhibition following another chromatography separation step (Fig 3.8A); 10 mM EDTA was determined adequate for inhibition of activity. Active fractions were also assayed with increasing amounts of total RNA from TRV-infected tissue, to determine how the ribonuclease activity would be affected with the addition of more substrate (Fig. 3.8B). For this purpose, the standard amount of RNA (1.5 µl RNA) was compared to fractions that had 2, 3, and 4 µl of RNA added (a/c ddH2O was added to all reactions to bring the total volume to 16 µl). Fractions demonstrating ribonuclease activity continued to target TRV RNA2, though to a level proportionate to the amount of RNA added. TRV RNA2.PDS transcripts were also added to the fractions alongside total RNA extracted from TRV-infected plant tissue. Fraction 9 displayed ribonuclease activity against the in vitro generated transcripts, and increased activity against plant-extracted TRV RNA, though fraction 8 also degraded plant-extracted TRV RNA, to a lesser extent than fraction 9 (Fig 3.8C). TRV RNA I was also degraded, as determined by northern blotting (data not shown).

Collectively, this and other tests showing that the anti-TRV RISC-like complex is active against in vitro and in planta generated TRV RNA in an EDTA and substrate dosage dependent manner.

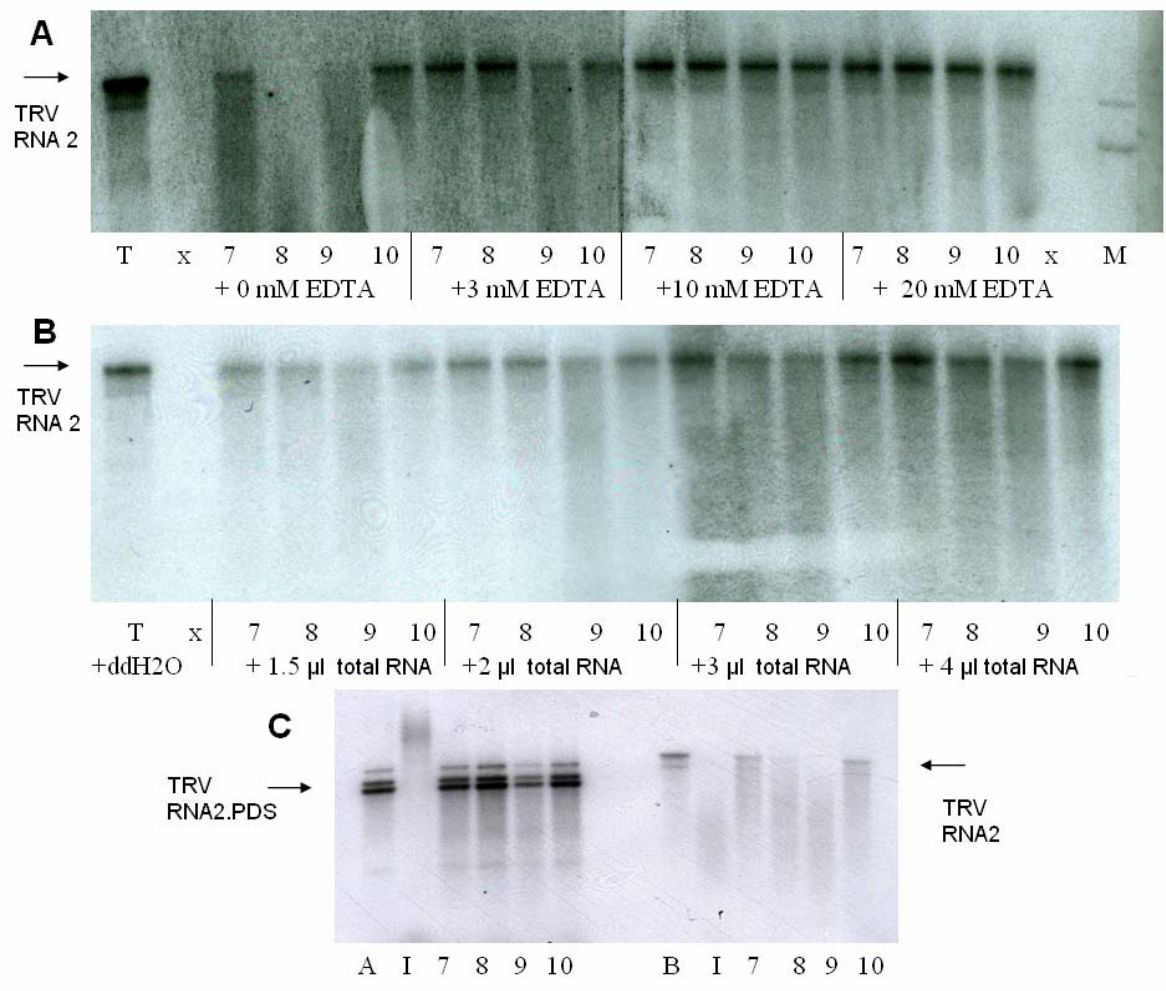

Fig. 3.8 Further characterization of ribonuclease activity following S200 and hydroxyapatite chromatography of 5 dpi TRV-infected plant tissue. Active fractions (7-10) were mixed with RNA extracted from plants infected with TRV (all volumes standardized with the addition of a/c ddH2O), incubated for 20 min., and visualized by northern blotting of the resultant 1% agarose gel. A.) 5 µl of the active fractions were tested for inhibition of ribonuclease activity for 1.5 µl RNA with increasing concentrations of EDTA, as indicated. Ribonuclease activity is inhibited by addition of 10 mM EDTA. B.) Five µl of each active fraction was mixed with amount of RNA indicated. Ribonuclease activity still functions with the addition of ~1000 ng/ µl RNA, though proportionately decreased. C.) Five µl fractions were mix with 1.5 µl RNA from TRV-RNA2.PDS transcripts (left), or total RNA extracted from TRV-infected plants (right). It is not known what is the significance of the RNA II duplex band.

Effects of NaCl on ribonuclease activity for hydroxyapatite fractions with S200 gel filtration

To determine the influence of NaCl on (possibly inhibiting) ribonuclease activity, hydroxyapatite fractions with ribonuclease activity were also applied to a Sephacryl S200 gel filtration column that had been equilibrated with 250 mM NaCl (as added to the 50 mM Tris buffer, pH 7, used for gel filtration). Fractions were then assayed as described above. For detection of ribonucleic activity, fractions were assayed with total RNA extracted from TRV-infected plants (Fig 3.9A). Fractions 11 and 12 displayed definite activity, though to a lesser extent than fractions collected following gel filtration without NaCl, which suggests siRNA dissociation. Intriguingly, when these fractions were assayed with total RNA collected from plants infected with TBSV ΔP19 (see Chapter II), fractions did demonstrate activity against the TBSV genomic RNA though not against subgenomic RNA, a finding that is in agreement with the ribonuclease activity seen for Sephacryl S200 fractions after hydroxyapatite chromatography of TBSV-infected plant extracts (unpublished data). Moreover, based on the northern blot hybridization data from this experiment, it appears that this activity against TBSV gRNA is even more vigorous than that observed with the addition of TRV-infected plant total RNA (Fig. 3.9B). Fractions, following gel filtration with salt, do not target TBSV RNA full length transcripts generated in vitro (data not shown), suggesting that the total RNA extracted from infected plant tissue carries with it some element that re-programs the ribonuclease activity. These are very exciting observations, and will be addressed in the discussion.

Considering the strong ribonuclease activity displayed by the NaCl-gel filtration fractions 10-12, these were tested for the presence of potential Ago proteins by western blotting with antibodies against the Ago Piwi-domain (Fig 3.10A). It was nearly impossible to detect any proteins at all in fractions using colorimetric detection with alkaline phosphatase, as has been done in previous westerns, though the gel column input positive control showed a positive signal. Therefore, a more sensitive assay was preformed with secondary antibody conjugated to horseradish peroxidase to detect Piwi-containing proteins. Positive signals were observed for fractions 10 and 11, estimated to represent approximately 90 and 60-80 kDa proteins, when compared to the low weight molecular markers by film overlay on the membrane.

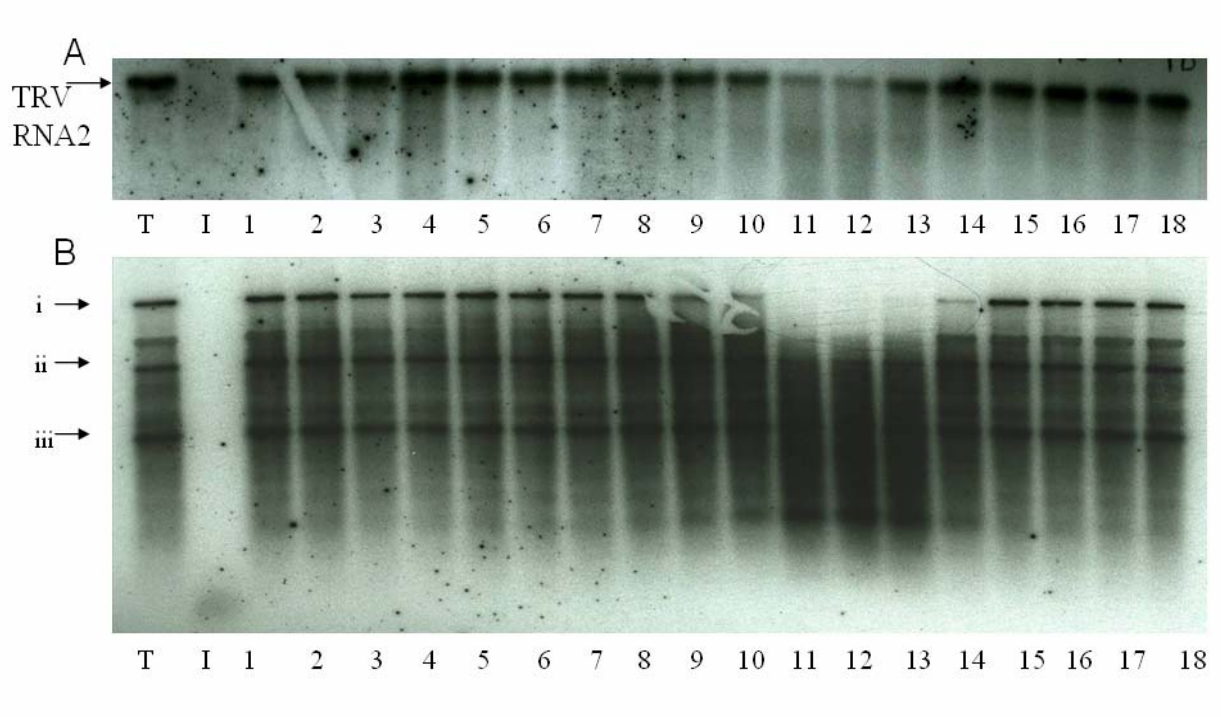

Fig. 3.9 Ribonuclease test for NaCl gel filtration of TRV hydroxyapatite fractions. Fractions containing ribonuclease activity following hydroxyapatite column chromatography were fractionated on a Sephacryl S200 gel chromatography column equilibrated with 250 mM NaCl, to test for increased specificity of ribonuclease activity and potential dissociation of siRNAs. Two µl (~250 ng/µl) total RNA was added to 5 µl fractions in the presence of an RNase inhibitor, and incubated for 20 min., then separated on a 1% agarose gel, and blotted to a nylon membrane for northern blotting.
A.) Fractions were assayed for TRV ribonuclease activity with the addition of total RNA extracted from TRV-infected plants. The resultant northern blot was probed with a TRV-RNA2 hybridization probe. Fractions 11 and 12 display residual ribonuclease activity.
B.) Same fractions plus the addition of total RNA extracted from a TBSV P19 deficient-infected plant. Northern hybridization using the TSBV P19-deficient cDNA probe. The arrows indicate i.) TBSV gRNA; ii.) TBSV sgRNA1; iii.) TBSV sgRNA 2.

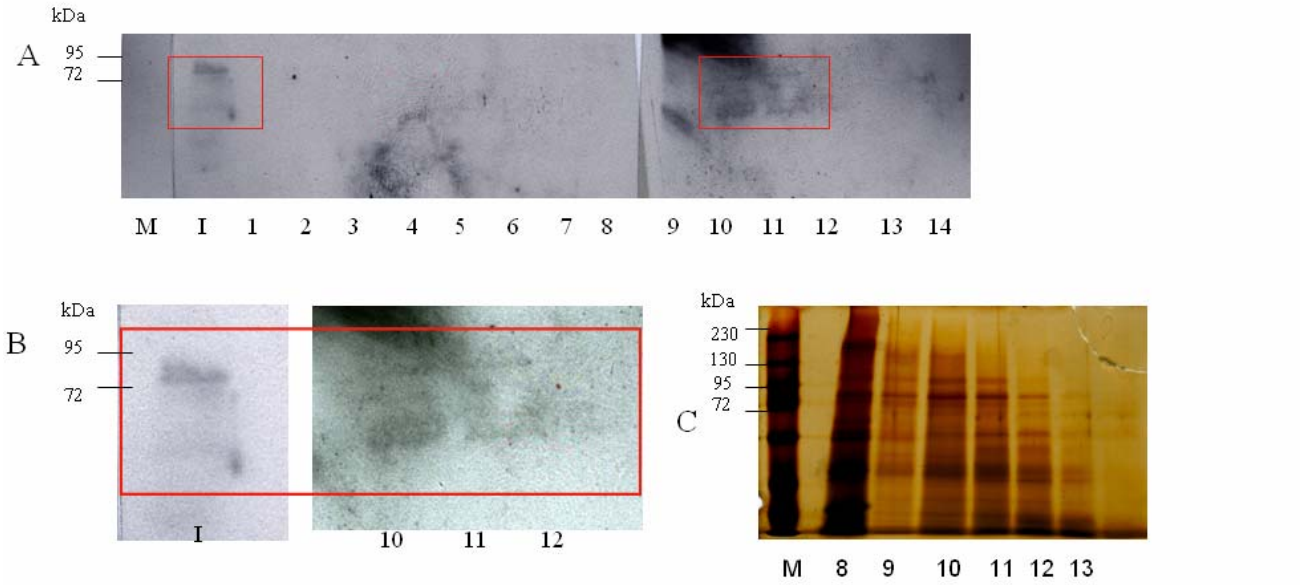

Fig 3.10 Westerns for NaCl gel filtration of TRV hydroxyapatite fractions. Following hydroxyapatite column chromatography fractionation and further protein purification by gel filtration with a Sephacryl S200 column with 250 mM NaCl, fractions were analyzed by western blotting with antibodies generated against a conserved region of the Piwi domain from Ago. A.) Thirty µl of each fraction (I = input) were boiled with cracking buffer and loaded onto 7.5% acrylamide SDS-PAGE gels, then blotted to a nitrocellulose membrane for detection of proteins present by western analysis using chemiluminescence. Fractions displaying activity (namely, 10, 11 and 12) displayed bands, red box indicated region highlighted for B. B.) Bands present for input, and Fractions 10 and 11 were enlarged for illustration. C.) Fractions 8-13 were visualized on a 5% SDS-PAGE gel with silver staining.

To better visualize this, the bands were compared to that seen in the column input lane in Fig. 3.10B. These fractions were separated by 5% SDS-PAGE followed by silver staining (Fig. 3.10C), showing several likely bands present in the silver stained gel. As expected following S200 chromatography, later fractions do not contain larger proteins in large quantities (judged by band density), through these do contain ribonuclease activity. There are 2-3 bands present in the size (Fig. 3.10C) range corresponding to the bands seen with western blotting for a Piwi-domain containing protein (Fig. 3.10B), but most likely do not represent this protein as a positive signal required chemiluminescense to detect. It is possible that these are proteolyic products of RISC, as was observed for *Drosophila RISC* purifications (Hammond et al., 2001), or components of RISC. It is also possible that the ribonuclease proteins are present in quantities undetectable by silver staining.

These fractions displaying activity after hydroxyapatite plus gel filtration with NaCl were then tested with the addition of divalent metal cations and 50 mM EDTA (Fig 3.11). Because TBSV fractions showed an increase in activity following addition of very minute amounts of metal ions, these were added to NaCl-gel filtration fractions with 1.5 mM and 3 mM concentrations of Mg^{2+} and Mn^{2+}, and then with the addition of these two concentrations plus varying concentrations of EDTA to test for re-stimulation of activity. Mn^{2+} appears to enhance ribonuclease activity better than Mg^{2+}, though both enhance activity in 3 mM concentrations. Where EDTA, when added to ribonuclease-containing fractions in 12.5 mM and 25 mM concentrations, interferes with this RNA degradation, the addition of metals seems to refresh activity. Despite the notable ribonuclease activity, the presence of potential Ago proteins, and predicted response to the exogenous addition of EDTA and divalent metal cations, numerous attempts to detect siRNAs from these fractions have failed. This is likely due to a dilution factor imposed by additional steps of column chromatography, and will be addressed in the discussion.

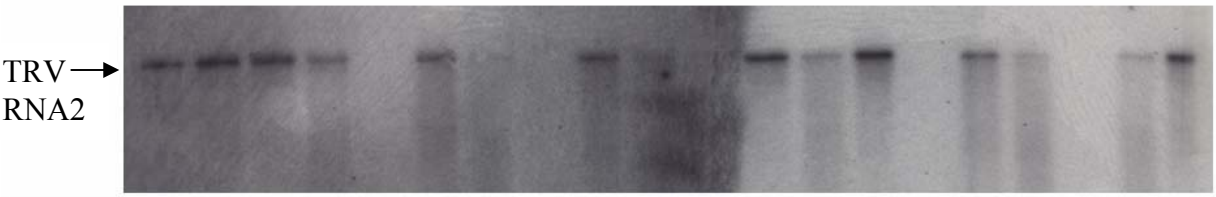

Fracts.				5		5	5		5	5			5	5		5	5		5	5
Mg^{2+}		2				1			2							2			2	
Mn^{2+}			2				1			2							2			2
EDTA												4	2	4		2	2		4	4

Fig 3.11 Further characterization of NaCl gel filtration of TRV hydroxyapatite fractions. Characterization assays of ribonuclease activity following hydroxyapatite and Sephacryl S200 column chromatography (with 250 mM NaCl). For this, 1.5 µl RNA extracted from TRV-infected plants was analyzed in the presence of RNasin and fractions containing activity. Fractions 9, 10, 11 and 12 (Fig. 3.9) were combined, and tested with the addition of 1.5 mM (1 µl) and 3 mM (2 µl), and for inhibition with 12.5 mM (2 µl) and 25 mM (4 µl) EDTA. These were also done in combination, to determine if activity could be re-stimulated following treatment with EDTA. All were equilibrated to 16 µl with sterile ddH2O.

Preliminary determination of an anti-viral plant defense response against PMV and SPMV

To test for RNAi-like ribonuclease activity in a monocot-virus system, 2 week old Proso millet plants were infected with PMV and SPMV. The infection was allowed to establish for about two and half weeks, until systemic chlorotic symptoms were very obvious. Extracts from these plants were then applied to a hydroxyapatite chromatography column, and fractions were collected following elution via a gradient of 10 mM to 400 mM, in a manner similar to that done for TBSV- and TRV- infected plants.

For characterization of PMV/SPMV infected tissues, CP for both viruses was detected using western blotting (data not shown), showing plants were infected. When PMV transcripts, generated in vitro, were added to the fractions, degradation was observed (Fig. 3.12) for fractions 11 and beyond. siRNAs were also extracted from these fractions, and small PMV/SPMV RNAs seem to be present for fraction 7 and thereafter (data not shown). Likewise, when Piwi-containing proteins were detected in fractions 7-19 with western blotting, these blots displayed a very interesting, very prominent band at aboutut 100 kDa, as well as the usual bands around 60 kDa and one at 11 kDa (Fig. 3.13). These preliminary tests indicate that in this monocot virus-host model system, an antiviral RISC is present potentially with features similar to those described for the dicot system.

Discussion

Based on current literature and work described in the previous chapter for TBSV, it was expected that a similar RISC-like anti-viral plant defense response could be isolated from TRV and PMV/SPMV -infected plant tissue using column chromatography. Properties would include ribonuclease activity against viral RNA, presence of siRNAs, inhibition with EDTA and high concentrations of salt, and possibly proteins that correlate to those expected for Ago.

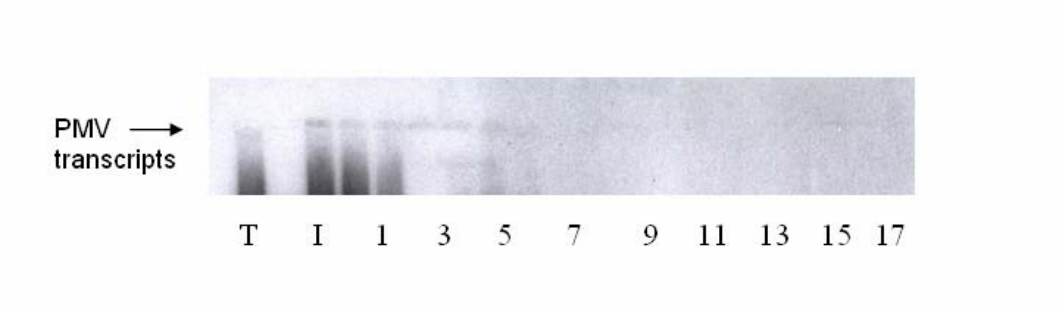

Fig 3.12 Hydroxyapatite fractions from PMV/SPMV infected plants, tested for ribonuclease activity. Five µl fractions were mixed with 2 µl PMV RNA full length RNA transcripts generated in vitro, with 1.5 µl a/c ddH20 treated with RNasin. These samples were incubated for 20 min., and visualized after electrophoresis on 1% agarose and staining with ethidium bromide, and blotting to a nylon membrane for hybridization probing with PMV cDNA.

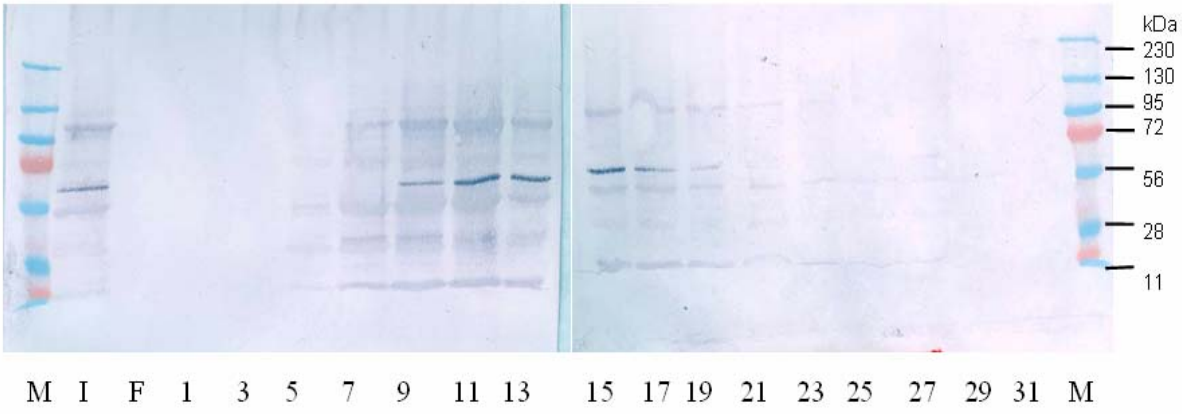

Fig. 3.13 Preliminary characterization of hydroxyapatite fractions from PMV/SPMV-infected millet plants. Fractions were boiled with cracking buffer, and loaded on 15% acrylamide SDS-PAGE gels. These were blotted to a nitrocellulose membrane for western detection of a Piwi-containing protein. The blot looks very similar to those seen for TRV and TBSV.

Early experiments to characterize the RNAi-associated anti-viral response in TRV-infected tissue was done using 2 mt. post infiltrated plant tissue, with the thought that this tissue, being obviously silenced, would give the best RNAi- associated characterization. This was performed using both DEAE as well as hydroxyapatite column chromatography; hydroxyapatite chromatography was chosen for use in later experiments based on results from results determined in Chapter II. With both types of chromatography, fractions contained very intense activity against TRV RNA2.PDS transcripts, though these fractions also targeted TBSV RNA transcripts, indicating unspecific activity. Also, I was unable to detect siRNAs from these fractions. When these results were compared to those seen for TBSV-infected tissue fractions undergoing the same chromatography methods (Fig. 2.5B, 2.7A, and 2.9, and (Omarov et al., 2007)), the fractions derived from TRV-infected plant extracts contained much more intense ribonuclease activity.

Several conclusions were reached at that point. The ribonuclease activity was unspecific, leading to the thought that potentially other anti-viral pathways might be triggered in these plants, as RNAi should be specific for the RNA used to program RISC (Fire et al., 1998; Baulcombe, 2004). For example, current literature describes a link between the plant defense salicylic acid pathway, usually involved in hypersensitive responses, and the RNAi pathway via the *Tobacco mosaic viru*s RNA-dependent RNA polymerase. This suggests the possibility that other plant defense response pathways may be triggered following a long infection, to degrade viral RNA indiscriminately (Singh et al., 2004). In hydroxyapatite fractions from infected plants collected after a prolonged infection, it is possible that other plant defense responses are mounted. Plants infected with a P19-deficient mutant of TBSV have been shown to eventually 'clear' the viral infection (Omarov et al., 2006); the infection is much shorter lived, so the RNAi response is adequate. Because TRV is introduced into the host plant with agro-infiltration, this means that TRV is inserted into the host genome and as such, would be constitutively expressed. While typically *Agrobacterium*-mediated infections are silenced, as these obviously are (exhibited by the whitening phenotype), TRV RNA is still produced.

Additionally, other recent literature reports that for yeast and *Drosophila* RISCs induce the formation of P-bodies, discrete foci within the cell. These are not static in size,

and contain enzymes involved in RNA degradation (Sheth and Parker, 2003; Rossi, 2005; Eulalio et al., 2007). It is logical that these P-bodies grow to accommodate the amount of RNA being degraded; not only are RISC elements present, but other RNA degradation enzymes also accumulate to process RISC targets. Components of these P-bodies might co-elute in true RISC-containing fractions following chromatography and demonstrate unspecific degradation. It has also been shown that the addition of a high concentration of siRNAs leads to unspecific activity (data not shown), but that idea is at odds with the lack of siRNA detection.

Further experiments were designed to take plant material at an earlier time post infiltration, before potential stimulation of unspecific ribonucleases or P-body formation (Eulalio et al., 2007), and to test for ribonuclease activity with a different TRV RNA substrate. Detached leaf assays show that the silencing signal (possibly siRNAs) is transmitted into the rest of the plant by 3 dpi (data not shown). Considering this, it was hypothesized that RISC was programmed at this time, and these fractions were collected at 5 dpi. An additional modification was that ribonuclease activity was tested with TRV RNA present in total RNA isolated from infected plants. This was done to address the concern that while RISCs loaded with siRNAs targeting PDS, comprising a major part of the in vitro transcripts, might be present in infected tissues, it is more likely that a greater amount ribonuclease activity will be demonstrated against a larger substrate, the TRV RNA itself. Moreover, for TRV, it has recently been shown that siRNAs are produced heterogeneously along the full length RNA instead of a particular region of RNA (Donaire et al., 2008), and the silencing signal is thought to involve ds-siRNAs (Lecellier and Voinnet, 2004). To take advantage of this theory, a hybridization probe against TRV RNA2, as a whole, might detect a larger amount of siRNAs (generated against TRV at random instead of specifically at the PDS insert). This was tested and performed successfully. While fractions tested for activity against total RNA from TRV infected plants demonstrated degradation of not only TRV but also ribosomal RNAs (it has been shown that RISC is loaded with siRNAs against ribosomal RNA), fractions demonstrated the presence of TRV-specific siRNAs. As seen for a TBSV-specific, high molecular weight ribonuclease (Omarov et al., 2007), ribonuclease activity co-eluted with siRNAs, indicative of a RISC (Baulcombe, 2004).

Another hallmark of RISC is the presence of Ago proteins (Hammond et al., 2001; Song et al., 2004). To determine if these were present, antibodies against a conserved region of the Ago-protein Piwi domain were used. Hydroxyapatite fractions, collected at 5 dpi, were western blotted to a nitrocellulose membrane and analyzed with these antibodies. Bands corresponding to potential Ago proteins were observed. Fractions containing both TRV-specific siRNAs and potential Ago proteins were combined, concentrated from about 5 ml to 1 ml, and applied to Sephacryl S200 gel filtration columns, equilibrated with and without a high concentration of salt. Again, these fractions were assayed for TRV-specific ribonuclease activity (Fig 3.7). Specific fractions demonstrated ribonuclease activity against total RNA extracted from TRV-infected plants, but not TBSV transcripts, indicating the presence of an Ago-protein containing high molecular weight TRV-specific RISC-like ribonuclease.

For fractions applied to a Sephacryl S200 gel filtration column equilibrated with 250 mM NaCl, total RNA from TRV-infected plants was added to the fractions. These fractions exhibited RNase activity in fractions 10, 11, and 12, though to a much decreased extent than activity observed against fractions applied to a S200 gel column without salt. When TRV RNA2.PDS transcripts were added to these fractions, the amount of ribonuclease activity was even lower than that seen for total RNA from TRV-infected plants, a result that is in agreement with gel-filtration studies done without NaCl (Fig. 3.9C). While this might be related to the concentration of the actual TRV RNA added, it is also very likely that total RNA extracted from TRV-infected plants brings with it several species of RNAs, including siRNAs, while TRV RNA2.PDS transcripts are only TRV RNA. To further explore this possibility, total RNA extracted from TBSV-infected plants was added to these fractions. Ribonuclease activity, apparently directed against genomic RNA as determined by Northern blot hybridization, was observed to be even more intense than the RNase activity seen for total RNA from TRV-infected tissue. When TBSV RNA transcripts were added to these fractions, no ribonuclease activity was observed.

This has several interesting implications. An early working hypothesis to explain this result was that possibly high concentrations of NaCl (250 mM) dissociate the siRNAs from RISCs, which were then ‘re-programmed’ by the siRNAs that are

presumably brought in by the total RNA extracted from virus-infected plant tissue, due to reports that siRNAs associate to the PAZ domain of Ago using base-stacking and ionic interactions (Toila and Joshua-Tor, 2007). However, further delving into the literature disagrees with this model of siRNA dissociation; other systems report that RISCs containing siRNAs can be purified using affinity chromatography and then washing with high concentrations of salt (Hammond et al., 2001). Additional reports exist of high salt concentrations affecting RISC activity itself as well as the loading of siRNAs onto holoRISCs, but having no effect on programmed RISCs once the salt is removed (Rand et al., 2004). At this time, it is unclear why exogenous addition of viral RNA present in total RNA from virus-infected plants, used at the same concentration as full length RNA transcripts generated in vitro, are targeted for degradation whereas the exogenously added transcripts remain intact.

It is possible that because of the early time point post-infiltration that the samples were taken that some tissue was included to which the virus had not yet located, nor the postulated RNAi systemic signal had spread (Hannon, 2002). This raises the likelihood that the fractions containing loaded RISCs also contain holoRISCs, which can then be loaded in vitro with the addition of total RNA from infected plants to result in ribonuclease activity against that virus RNA. This might contribute to the effect seen with the addition of RNA taken from TBSV-infected plants (Fig. 3.10B).

Upon viral infection and subsequent generation of anti-viral siRNAs, it is possible that these anti-viral siRNAs out-compete endogenous small RNAs to load RISCs, eventually saturating the RNAi system. This leads to not only targeting of viral ssRNA for degradation, but also unspecific activity against host mRNA, plus perturbation of normal host functions usually controlled via miRNA pathways (as all RISCs are loaded with siRNAs and not host miRNAs). This is supported by the unspecific activity of fractions collect from infected plant tissue following prolonged infection, as well as the interesting phenotypes seen in virus-infected younger plants, like severe deformation of leaves. It is also possible that there is a timeframe for the amount of RISCs present in cells – younger plants have many more RISCs to help regulate cell development, whereas older plant cells might have down regulated RISC production - less RISCs mean more virus accumulation, and greater infection.

The data presented for monocots infected with PMV and SPMV is still a work in progress. It is interesting to note that while fractions demonstrate ribonuclease activity for PMV transcripts, activity seems to begin in later fractions than those displaying ribonuclease activity for the earliest experiments with TRV. Preliminary data suggests that siRNAs are present in fraction 7 and later fractions, also agreeing with data observed for TBSV and TRV- originating siRNAs following hydroxyapatite chromatography; this suggests that the anti-viral RISC-like plant defense is present across plant species. This supports the current theory that RNAi is conserved across kingdoms (Hannon, 2002; Baulcombe, 2004). The western blot for Piwi-containing proteins seems to be the most promising piece of data for this particular experiment. A distinct band at a little over 100 kDa is present (Fig 3.13B), which is what would be expected for a plant RISC-associated Ago protein (Martinez et al., 2002; Baumberger and Baulcombe, 2005).

In summary, it was demonstrated that TRV-infected *N. benthamiana* plants mount an anti-viral RISC-like response, as indicated by: the presence of virus-specific ribonuclease activity following hydroxyapatite and Sephacryl S200 gel filtration column chromatography; inhibition with EDTA and high concentrations of NaCl; the presence of Piwi-containing proteins suggestive of the signature RISC Ago protein; and siRNAs in hydroxyapatite fractions with activity. Likewise, hydroxyapatite column chromatography of fractions from PMV and SPMV yield fractions containing siRNAs, ribonuclease activity, and Piwi-containing proteins.

Based on the observations reported above, it seems very likely that the ribonuclease activity demonstrated can indeed be attributed to a genuine RNAi RISC response. These observations also agree with those shown for corresponding fractions taken from TBSV-infected *N. benthamiana* tissue after column chromatography (Chapter II). Therefore, the RISC-like complex shows similar characteristics for different virus-host combinations. This lends support to a common anti-viral RNAi defense in plants irrespective of the particular virus or host, signifying a conserved RNAi pathway as denoted by the current model (Baulcombe, 2004).

.

CHAPTER IV
USE OF SILENCING SUPPRESSORS TO EXTEND AND ENHANCE THE LENGTH OF TIME A FOREIGN PROTEIN IS PRODUCED VIA *AGROBACTERIUM TUMAFACIENS* AND A VIRAL VECTOR

Introduction

Silencing suppressors

Viruses have evolved mechanisms to overcome or impede the RNAi pathway by encoding silencing suppressor proteins (Voinnet et al., 1999), though these proteins often have other functions in addition to their roles in silencing suppression, including acting in viral movement, as transcriptional activators or replication enhancers (Voinnet, 2005). Furthermore, many proteins that are now known as silencing suppressors were previously determined to be pathogenicity or virulence factors, as their presence enhance symptom severity in viral infections (Brigneti et al., 1998). Suppression of RNAi is a widely used manner of host defense evasion, and there are myriad suppressors and modes of action (Silhavy and Burgyan, 2004; Voinnet, 2005).

The veritable arms-race between the host defense proteins and viruses is well established with silencing suppressor proteins encoded not only from plant viruses, but also animal and insect viruses (Li and Ding, 2006; Hemmes et al., 2007). These silencing suppressors have been shown to act at nearly every step of the RNAi model pathway, a brief example of suppressors known to act at each step is outlined here (Fig. 4.1). Following viral replication, the *Flock house virus* protein B2 has been shown to bind to dsRNA and prevent cleavage by Dicer into 21-nt duplexed siRNAs (Chao et al., 2005) (Fig. 4.1B), Other proteins have been shown to target Dicer directly, as seen with HIV Tat protein (Bennasser and Jeang, 2006). HcPro is a silencing suppressor encoded by potyviruses, and possibly modifies the function of plant Dicer-like enzymes that generate duplexed siRNAs (Mlotshwa et al., 2005), as illustrated by the observed accumulation of

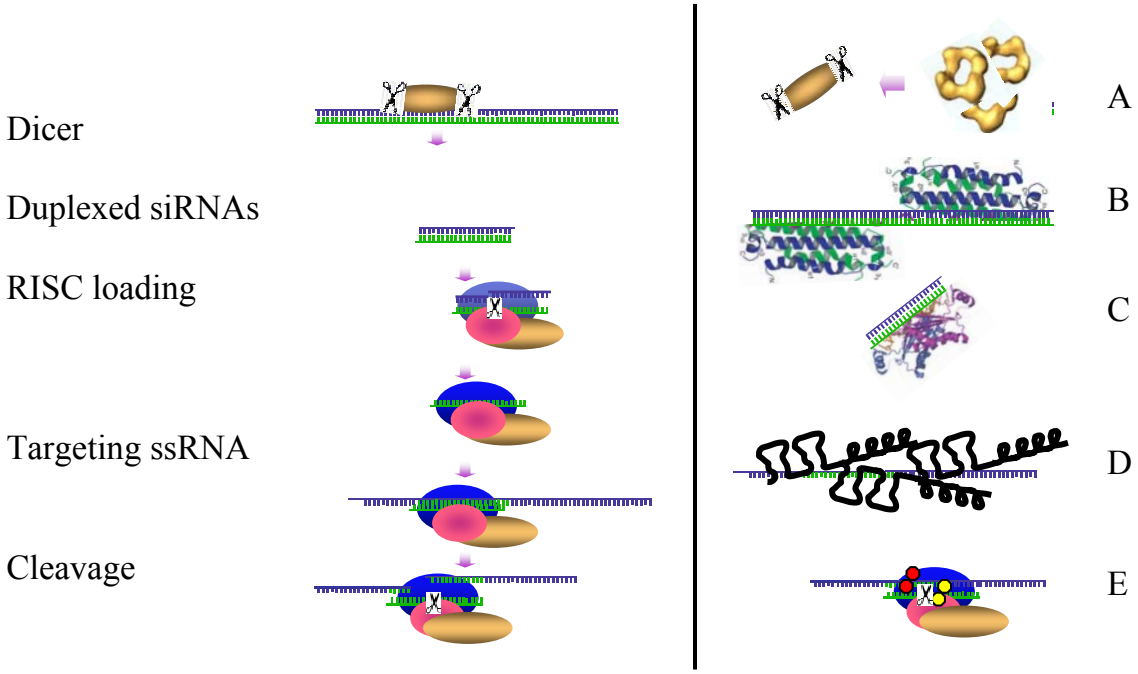

Fig. 4.1 RNAi silencing suppressors. Suppressors act to inhibit different stages of the RNAi pathway. This is illustrated to the right of the figure. A.) The HIV tat protein and potyvirus protein HcPro might act to modify Dicer. B.) *Flock house virus* 2B binds dsRNAs, so Dicer is unable to generate siRNAs. C.) Many silencing suppressors bind to siRNAs (the tombusvirus protein P19 is pictured), to prevent the loading and activation of RISCs. D.) The hordeivirus *Barley stripe mosaic virus* protein γb binds to ssRNA, which might prevent RISC targeting. E.) Proteins like the *Cucumber mosaic virus* protein 2b and the P0 protein from poleroviruses inhibit RISC from cleaving by binding to the PAZ or Piwi domains. (Original figure provided by Dr. Rustem Omarov; 2b from Chao et al, 2005, HcPro from http://www.cib.csic.es/es/ detalle_linea_investigacion.php?idlinea_ investigacion=43 ; P19 from Ye et al, 2003; and γb based on structure in Rakitina et al, 2006.)

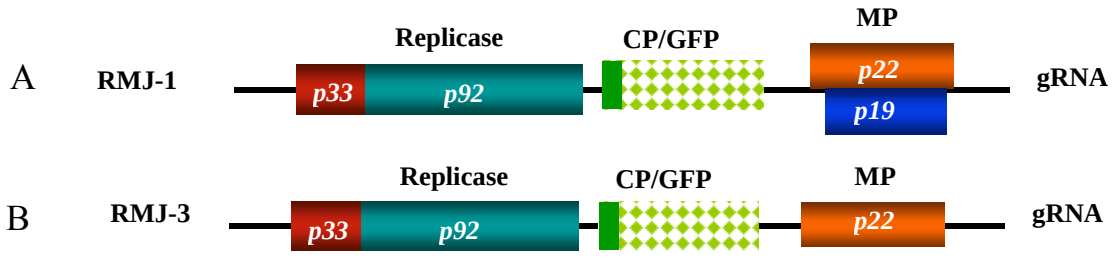

Fig. 4.2 TBSV vectors expressing GFP. A.) RMJ-1, TBSV with only about 75 nt of the CP fused with GFP. B.) RMJ-3 is identical to RMJ-1, except modified so that the P19 protein is not expressed. (RMJ-1 and RMJ-3 constructed by M. Shamekova)

long dsRNAs in the plant (Fig. 4.1A). However, HcPro has also been shown to associate with duplexed siRNAs (Lakatos et al., 2006), indicating that it might also function at that step in the RNAi pathway. Multiple silencing suppressors act by binding dsRNA, including those shown to work across species (Lakatos et al., 2006). These silencing suppressors interact with the siRNAs following generation by Dicer, before the duplex is incorporated into the RISC. This method is used by the P19 protein from Tombusviruses, where dimers interact with the sugar-phosphate backbone on the siRNAs in a sequence unspecific manner to sequester the siRNAs away from RISCs (Fig. 4.1C).

The *Barley stripe mosaic virus* γb protein, from displays a cysteine-rich motif at the C-terminal region, to which RNA binding (Donald and Jackson, 1996) and anti-silencing actions are attributed (Yelina et al., 2002; Bragg and Jackson, 2004). The γb protein likely binds in a sequence unspecific manner to ssRNA via a coiled-coiled domain with zinc binding sites, to prevent it's degradation by RISC (Donald and Jackson, 1996; Rakitina et al., 2006) (Fig. 4.1D). Other silencing suppressors act on Ago proteins, like the *Cucumber mosaic virus* 2b protein, which has been shown to bind to the interface of the Piwi and PAZ domains of Ago to inhibit slicing (Voinnet et al., 2003; Zhang et al., 2006; Ruiz-Ferrer and Voinnet, 2007) (Fig. 4.1E). Another silencing suppressor that acts at this step is the F-box protein P0 from polerovirus, which adds polyubiquitins to proteins. This stimulates their degradation by proteosomes, though P0 also seems to act in another manner when functioning as a silencing suppressor, targeting the Piwi domain of Ago1 and preventing ribonuclease activity (Baumberger et al., 2007; Bortolamiol et al., 2007).

Virus vectors

Traditionally-produced transgenic plants employ genetics to clone in a gene for production of a protein. However, this requires a large amount of time and resources. The use of *Agrobacterium tumafaciens* also provides a transient method (as opposed to transgenic) for expression of foreign proteins in plants, but limitations for this system include the host range for *Agrobacterium*, public concerns about genetically modified organisms (GMOs) localization of protein expression to only the tissue treated with

Agrobacterium, plus occasional loss of expression due to random insertion of the gene into the host genome as well as stimulation of RNAi, which promptly silences expression of the protein of interest (Ratcliff et al., 2001).

Viruses provide an extremely efficient manner of expressing foreign proteins in plants (Scholthof et al., 2002). Plant virus gene vectors offer a very high level of expression potentially for a broad host range, ease of transmission to a large amount of plants, quick genetic manipulation, and systemic infections for high levels of protein expression. However, limitations involve vector instability and induction of RNAi (Scholthof, 2007). This chapter offers a perspective on how to overcome the induction of RNAi by viral vectors with the use of viral silencing suppressors, in this case using TBSV derived vectors carrying a *gfp* gene (Fig. 4.2).

There are several types of strategies to use viral vectors available, pending desired result (Scholthof et al., 2002). These can include the simple insertion of a gene of interest into the virus genome, as done best with rod-shaped viruses, as there are space constraints associated with icosahedral viruses. To address space constraints, it is sometimes possible to delete a viral gene that is dispensable for replication or systemic infection in a host, and insert the gene of interest in its place. Epitope display involves engineering fusions of gene segments into the *cp* gene so that the protein(s) of interest are displayed to the exterior of the particle (Scholthof et al., 1996). Complementation is used for multi-partite viral genomes or helper-virus systems; one genome segment can be used for genes required for replication, while another genome segment can carry gene(s) for production of the protein(s) of interest. These methods can be used in combination with others, like gene replacement and complementation. In all viral vectors, the gene of interest is placed behind promoter elements for expression or are expressed as read-through proteins, with suitable processing elements in place (Scholthof et al., 1996; Qiu and Scholthof, 2007).

It has been shown in several instances that viral vectors stimulate the RNAi pathway; indeed, this response is used in many instances to transiently silence host genes in plants, as referred to above in the previous chapter on TRV (Liu et al., 2002a; Liu et al., 2002b; Burch-Smith et al., 2004). However, viral vectors in plants also provide an elegant system for amplification or over-expression of native proteins to discern their

effect on the host. Virus vectors also can be used to generate non-native proteins, usually for pharmaceutical purposes, recently shown with antibodies, human cytokines, and allergens (McCormick et al., 2003; Wagner et al., 2004; Matsuo et al., 2007). These therapeutic proteins can be used for oral delivery of the therapeutic proteins, or proteins can be recovered from plant tissue for further purification and processing (Matsuo et al., 2007). Unfortunately, plants do not distinguish between genes to be silenced and proteins to be expressed; RNAi is activated in both cases. This often limits the optimal use of virus vectors.

To avoid the negative effects of silencing, suppressors obviously present a set of useful tools. However, they are not without limitation either. As addressed in recent studies (Siddiqui et al., 2008), silencing suppressors seem to have different efficiencies in inhibiting RNAi. Additionally, certain silencing suppressors affect plant tissue development by interfering with miRNA steps (Chapman et al., 2004), particularly those suppressors which act by binding small RNAs. To explore the effects that these silencing suppressors have on developing plant tissues, experiments were conducted where 6 suppressors from different virus genera were expressed in different species of N*icotiana* transgenic plants and the phenotypes were observed. Results indicated that the severity of deformation induced by the silencing suppressor varied with the strain of virus from which that particular suppressor was isolated, as well as which species of *Nicotiana* served as the host (Siddiqui et al., 2008). This might be due to the expression strategy of the virus normally encoding the suppressor, as hypothesized for TRV, that encodes as weak suppressor for infection in meristematic tissue, where a stronger suppressor would affect tissue development and subsequent virus dissemination (Martin-Hernandez and Baulcombe, 2008). Other explanations include at which step of the RNAi pathway that the suppressors act; for instance, if the suppressor binds small RNAs, then miRNA and plant developmental pathways would be affected. Furthermore, viruses adapt to different hosts in numerous ways, which might also have an impact on involvement in the miRNA pathway.

This has bearing on this work in that the choice of silencing suppressors can have a large influence on the host-virus vector model system. By expressing different

suppressors transiently instead of transgenically, and separate from the viral genome, undesired secondary effects may be minimized.

To explore the inhibition of RNAi by suppressors for potential use for biotechnology, part of this work sought to extend non-native protein production in plants. The use of silencing suppressors to extend the length of time that proteins of interest, vectored by *Agrobacterium tumafaciens,* has been the subject of several recent papers (Voinnet et al., 1999; Voinnet et al., 2003; Chiba et al., 2005; Scholthof, 2007; Shams-Bakhsh et al., 2007). Based on this, I hypothesize that by using silencing suppressors vectored in by *Agrobacterium*, proteins of interest carried by viral vectors will also have an extended time of expression. The present study includes the examination of the effect of silencing suppressors singly and in combination, on the expression of a co-introduced green fluorescent protein (GFP) cDNA. I have used the well-characterized silencing suppressors P19 from TBSV, HcPro from the potyvirus *Tobacco etch virus* (TEV), and the γb protein from *Barley stripe mosaic virus* (BSMV), with the goal of maximizing the length of time that GFP is produced either from a co-inoculated T-DNA, or expressed by a virus vector. It is hypothesized that as the silencing suppressors act at different steps in the RNAi pathway, their use in combination will provide expression of GFP for a longer length of time than inoculation with a single silencing suppressor or with GFP alone.

Agrobacterium infiltration

Agrobacterium tumafaciens (*Agrobacterium*) is a gram-negative plant bacterium that naturally causes uncontrolled proliferation of infected cells in many plants, usually resulting in tumors for natural infections. It has been shown to transform many types of cells, including fungal and human cell lines (Tzfira and Citovsky, 2006). It acts by transferring its DNA (T-DNA, or transfer DNA) into the host genome where it is integrated at a random location, and expressed along with host genes using host cell machinery. This system can be used to insert any DNA for expression into a plant cell, and the result varies depending upon the contents of the T-DNA (Grimsley et al., 1986; Tzfira and Citovsky, 2002; Lacroix et al., 2006) T-DNA plasmids have *vir* genes, some of which are known to induce opines, to enhance the cellular environment for proliferation of *Agrobacterium*, and enzymes for the control of tissue proliferation. These

are carried by Ti (tumor-inducing) plasmids. Phenolic compounds and sugars produced by wounded cell walls stimulate the Ti plasmid with VirA/VirG 2 component regulatory system. T-DNA is excised from the plasmid using a VirD2/VirD1 endonuclease complex, generating a ss-T-DNA defined by two borders of 25-bp repeats (Tzfira and Citovsky, 2002). The T-DNA is then injected into the plant cell using a type IV secretion system originating from the bacterium along with other *Agrobacterium*-related virulence proteins. Once the T-DNA is inside the cell, it forms a complex with other *Agrobacterium* virulence proteins that is then imported into the nucleus. On gaining entry into the nucleus, the associated virulence proteins are removed from the T-DNA, which is then converted to a ds-DNA molecule, and is integrated into the host genome (Lacroix et al., 2006; Tzfira and Citovsky, 2006). Because it is the T-DNA 25-nt borders that specify integration into the host genome, and not the DNA between them, the DNA that is integrated into the host genome can be replaced with DNA for genes of interest very successfully (Hooykaas and Schilperoort, 1992). This system can be used to great effect for stimulation of RNAi as well as a vector for proteins (Grimsley et al., 1986; Ryu et al., 2004). *Agrobacterium* carrying the gene of interest can be injected into plants using a needle-less syringe (agroinfiltration), integrate into the host genome, and the protein of interest will be expressed very quickly, usually within a week.

The work described in this chapter means to establish if agroinfiltration of silencing suppressors can be used singly and in combination to enhance and extend the length of time that a foreign gene is transiently expressed, particularly from a viral vector.

Materials and Methods

Agroinfiltration of *N. benthamiana* with silencing suppressors and GFP

The plasmids carrying the silencing suppressors Hc-Pro and γb are pGD binary vectors, specifically created to be used with *Agrobacterium*, modified from the binary vector pCAMBIA-1303, with a multiple cloning site downstream of a CaMV 35S promoter, and upstream of a nopaline synthase polyA terminal (Goodin et al., 2002; Bragg and Jackson, 2004). P19 is expressed from the binary vector pCass4N (provided by S. Gowda), a derivative of a PBin19 binary vector. The plasmid carrying the *gfp* gene is 35S-*gfp* (provided by D. Baulcombe) (Voinnet and Baulcombe, 1997). All of the

silencing suppressors are infiltrated into *N. benthamiana* using the *Agrobacterium* strain EHA, for consistency (Hood et al., 1986). This strain has a less virulent host response than C58C1, the strain that was used in the earliest experiments and caused necrosis of infiltrated tissue (data not shown).

To insert the plasmids into *Agrobacterium*, cell electroporation was used. For this, 1 µl (about 400 ng/µl) of each plasmid was mixed with 50 µl of *Agrobacterium* strain EHA, thawed on ice. This mixture was inserted between the metal hubs of a chilled GIBCO-BRL electroporation cuvette (Cat. No. 11608-031), and subjected to electroporation with a GIBCO-BRL Cell-porator system (LCT) as follows: the chamber of the cell-porator system was packed with ice and water, and the loaded cuvette set in the tray. The cover was fastened, and settings adjusted to a capacitance of 330 µF, Low Ω DC volts, Fast Charge rate, and the voltage booster set at 4KΩ . Once the machine charged up to 400, the cell-porator was armed and cells were electroporated for about 2 seconds. The cells were then transferred into a 1.5 ml microfuge tube with 1 ml of a tryptone/yeast extract containing (LB) broth, and shaken at 28° C for about 2 hours. This culture was then centrifuged at 10,000 rpm for one minute, and the supernatant discarded. The pellet was plated out onto a kanamycin-containing LB plate, and incubated at 28° overnight, or until colonies were established.

A single colony was added to 3 ml of Kanamycin-containing LB broth, and grown to turbidity in a 28° C shaker overnight. Then, 500 µl of this culture were added to 50 ml of LB broth containing kanamycin (Kan^{50}), 1 ml of 10 mM MES buffer [2-(4-Morpholino)-ethanesulfonic acid] and 6.5 µl of wound-inducing 150 mM acetosyringone (gallacetophenone 3'-4'-dimethyl ether in DMSO), and incubated at 28° C for at least 12 hours. The culture was pelleted by centrifugation at 4000 rpm with a Beckman S4180 rotor, and the supernatant discarded. To re-suspend the pellet, 10 ml of 10 mM MES plus 10 mM $MgCl_2$ and 150 µl 150 mM acetosyringone were used, and the re-suspension was shaken for 20 min. then allowed to incubate at room temperature for at least 8 hours.

In order to establish that the system was functioning, preliminary experiments were arranged so that the silencing suppressors were co-infiltrated with *Agrobacterium* carrying a *gfp* gene as originally described (Voinnet et al., 2003). This system worked very well; once the infection was established and GFP was visible, gene expression was

monitored visually. Later experiments refined this system; bacterium concentrations were determined by finding the optical density (OD) with spectrophotometry. ODs of the *Agrobacterium* cultures were found using a 1/10, 1/100, and 1/1000 dilutions of each *Agrobacterium*/silencing suppressor*, Agrobacterium*/GFP and *Agrobacterium* strain EHA with a Spectronic20 spectrophotometer (Molton Roy). The spectrophotometer was calibrated ('blanked') with 10 mM MES/$MgCl_2$ at 425 nm, the wavelength appropriate for cultures in clear medium, and between each set of samples. Each dilution was then plated out on LB plates (Kan^{50}) to establish colony forming units. Once the optical densities were known, the cultures were adjusted to the specified OD (0.6 or 0.8) by dilution, and these were verified again by spectrophotometry.

The cultures were then mixed (Table 4.2), and infiltrated into 3 week-old *N. benthamiana* plants. *Agrobacterium* EHA was added to standardize the amount of bacteria infiltrated into a plant; each leaf was infiltrated with 1 ml total of a combination of either *Agrobacterium* with GFP, one of the silencing suppressors, and/or the silencing suppressors in combination and the remainder was brought up to volume with the untransformed strain EHA. This was to ensure that expression did not vary due to amount of bacteria infiltrated into the leaf, which might alter the resultant amount of protein expression. Infiltration occurred by filling a needle-less syringe with the mixed cultures and carefully injecting 1 ml of the cultures into the underside of the leaf (once on each side of the leaf mid-rib). This was typically sufficient to infiltrate an entire leaf.

Verification of protein expression by western blotting

Expression of the silencing suppressors and GFP was verified with western blots following extraction of proteins on days 3 and 12 following infiltration. For this, areas infiltrated with GFP/silencing suppressor *Agrobacterium* (1-cm^2) sections were removed with a razor blade. These sections were homogenized in 300 µl 2X STE+1% SDS (2 mM Tris, 20 mM NaCl, 2 nM EDTA, and 1% SDS) with chilled mortars and pestles. Then, 200 µl of the crude extract was then added to 1.5 microfuge tubes containing 60 µl 5X cracking buffer, and boiled for 3 min. These samples were centrifuged for 1 min. at 10K rpm to pellet cellular debris, and 30 µl of each sample was loaded onto a 15 % SDS-poly acrylamide gel (gel consisting of 5ml 30% acrylamide stock, 2 ml water, 3.8 ml 1.5 Tris

pH 8.8, 100 µl 10% ammonium persulfate, 100 µl 10% SDS and 30 µl Temed; stacking gel with 600 µl 30% acrylamide, 500 µl Tris pH 6.8, 2.7 ml water, 100 µl 10% ammonium persulfate, 40 µl 10% SDS, and 3.2 µl Temed), and electrophoreised at 90 and 120 volts for 2 hours in 1X running buffer (24.8 mM Tris, 192 mM glycine, 3.5 mM SDS). The SDS-PAGE gel was then transferred to nitrocellulose membrane (300 mA, 1 hour), and the membrane was then blocked with 7.5% milk solution (7.5 grams skim milk power, 1X TBS/Tween-20; 50 mM Tris, 200 mM NaCl, 500 µl Tween-20) for an hour. This was then rinsed 3 times for 15 min. apiece with about 20 ml TBS-Tween-20, and the primary antibody added (GFP B2 monoclonal antibodies generated in mice, Santa Cruz Biotechnology; HcPro generated in rabbits, a gift from M. Goodin; γb generated in mice, kindly provided by A. Jackson; and anti-rabbit P19, Scholthof lab) in 1:2,000 dilutions for at least 2 hours. The secondary antibody in 7.5% milk solution was added to each blot following 3 15-min. 20 ml TBS-Tween washes, and the blots were developed with BCIP (66 µl) and NBT (33 µl) in alkaline phosphatate buffer.

Visualization of GFP

The agro-infiltrated plants were inspected under a UV light for visualization of GFP expression, to track the length of time that GFP protein was produced before silencing. Pictures were taken of these plants under 488 nm-emitting UV light with a 4 second exposure, no flash, over a time period of 3 weeks, beginning 3 dpi and occurring every second day or until silencing/tissue necrosis occurred.

Infection of *N. benthamiana* with silencing suppressors and GFP expressed from a virus vector.

Later experiments involved the use of TBSV-based virus vectors carrying *gfp* instead of the *Agrobacterium*-vectored *gfp*. The virus vector used is a TBSV-GFP modified vector, which fuses the 5' 75 nt of the CP in frame to GFP (Fig. 4.2). This vector was modified into two versions, one producing the TBSV silencing suppressor P19 (TBSV-RMJ-1, Fig. 4.2A) and the other deficient of P19.

Half-leaf assays to examine the effects of the silencing suppressors on the virus vector

Half-leaf assays were used to compare the TBSV-P19 expressing- and deficient-virus vectors. Because it has been shown that agroinfiltrated proteins reach maximum expression 3 days post inoculation (Shamekova, unpublished data), 2 leaves (the 2nd and 3rd true leaves) of 3 wk-old *N. benthamiana* were inoculated with 1 ml of the silencing suppressor/*Agrobacterium* culture, and allowed to recover for 24 hours before rub-inoculation of each leaf with TBSV-RMJ1 RNA transcripts on the left half of the leaf, and TBSV-RMJ-3 RNA transcripts on the right half of the leaf, with great caution taken to not cross the boundary formed by the mid-vein. RNA transcripts were generated in vitro using a Fermentas T7 transcription kit as described in Chapter II. These transcripts were then mixed in a 1:4 dilution with cold RNA inoculation buffer (50 mM KH_2PO_4, 50 mM Glycine, pH 9.0, 1% celite, 1% bentonite), and each leaf mechanically inoculated with 10 µl of each transcript. The recovery time between agro-infiltration and rub-inoculation was designed to allow for maximum expression of the viral-vector proteins and agro-infiltrated silencing suppressors coincidentally.

About an hour prior to first assaying plants by UV light, the inoculated leaves were very carefully rinsed with 5 ml A/C ddH2O (from a squirt bottle), each leaf half separately, as celite and bentonite fluoresce as white under UV, and interfere with the GFP signal visibility. Leaves were allowed to dry, the plants were assayed visually for virus expression by GFP signal under a 488 nm UV-light, and pictures were taken with 4 second exposures, no flash. Again, initial silencing suppressor protein expression was verified by western blotting of extracted proteins with silencing suppressor-specific antibodies.

Results

System set-up

The earliest experiments were performed for the purpose of determining the best experimental design for later experiment iterations. Three week-old *N. benthamiana plants* were infiltrated with *Agrobacterium* carrying the silencing suppressors and with those expressing GFP. Three days were allowed for protein expression to become established, and then plants were viewed under a 488 nm black light (data not shown).

Later experiments involved the infiltration of the silencing suppressors in combination (Table 4.2), along with GFP (Figs. 4.3, 4.4, 4.5). This was repeated twice, though the optical density of infiltrated *Agrobacterium* cultures was adjusted to avoid tissue necrosis. The first incarnation was performed with an OD of 1.2. Plants infiltrated with multiple silencing suppressors and GFP displayed heavy yellowing and some tissue necrosis (Fig. 4.3b). The second set of plants were infiltrated with *Agrobacterium* cultures at ODs of 0.8, and avoided the previous issue in all but the very last days of the timecourse (Fig. 4.5). Then, the lower OD was preferred in subsequent experiments.

Table 4.1 Additions of GFP and silencing suppressors, following standardization of optical density.

	GFP*	HcPro	γb	P19	Untransformed *Agrobacterium* Strain EHA
GFP only	0.5 ml				1.5ml
Single suppressors	0.5 ml	0.5 ml			1 ml
	0.5 ml		0.5 ml		1 ml
	0.5 ml			0.5 ml	1 ml
Double suppressors	0.5 ml	0.5 ml	0.5 ml		0.5 ml
	0.5 ml	0.5 ml		0.5 ml	0.5 ml
	0.5 ml		0.5 ml	0.5 ml	0.5 ml
All	0.5 ml	0.5 ml	0.5 ml	0.5 ml	

* for the experiments involving the RMJ virus vectors, *Agrobacterium*-GFP is omitted.

Additionally, proteins were extracted from these plants co-infiltrated with silencing suppressors and *Agrobacterium-gfp* for western blot analysis, to ensure that proteins were being expressed (Fig. 4.4A). This was done an additional time at 12 dpi, to see if protein expression might persist (Fig 4.4B). For the proteins tested both times, both GFP and P19 seem to be expressed in greater amounts in Fig 4.4B that that seen on the

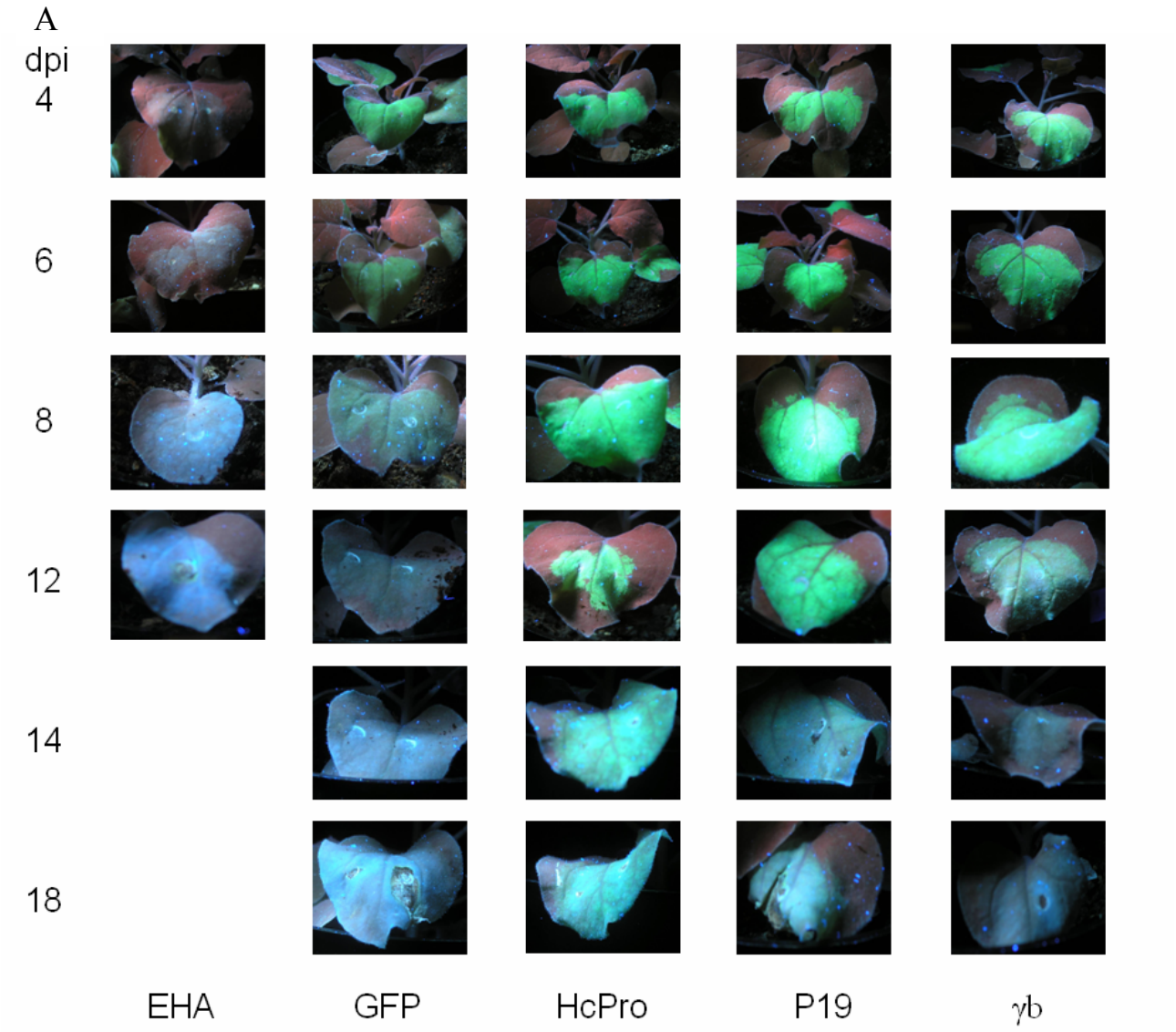

Fig. 4.3 Silencing suppressors infiltrated with high optical density *Agrobacterium* cultures. Three week-old *N. benthamiana* plants were infiltrated with *Agrobacterium*-mediated GFP and silencing suppressors at an optical density of 1.2, mixed as indicated. The plants were then photographed at each time point indicated under a 488nm wavelength UV light with a 4 second exposure, no flash, to monitor levels of visible GFP expressed.

A.)The plants in the first column, labeled EHA, are those infiltrated with untransformed *Agrobacterium*, as a negative control. The plants in the second column are those infiltrated with 0.125 ml *Agrobacterium-gfp* per leaf, plus *Agrobacterium EHA* to ensure each leaf was inoculated with 0.5 mls of the culture. The plants in later lanes were infiltrated with 0.15 ml *Agrobacterium-gfp* plus 0.125 ml of one of the silencing suppressor cultures.

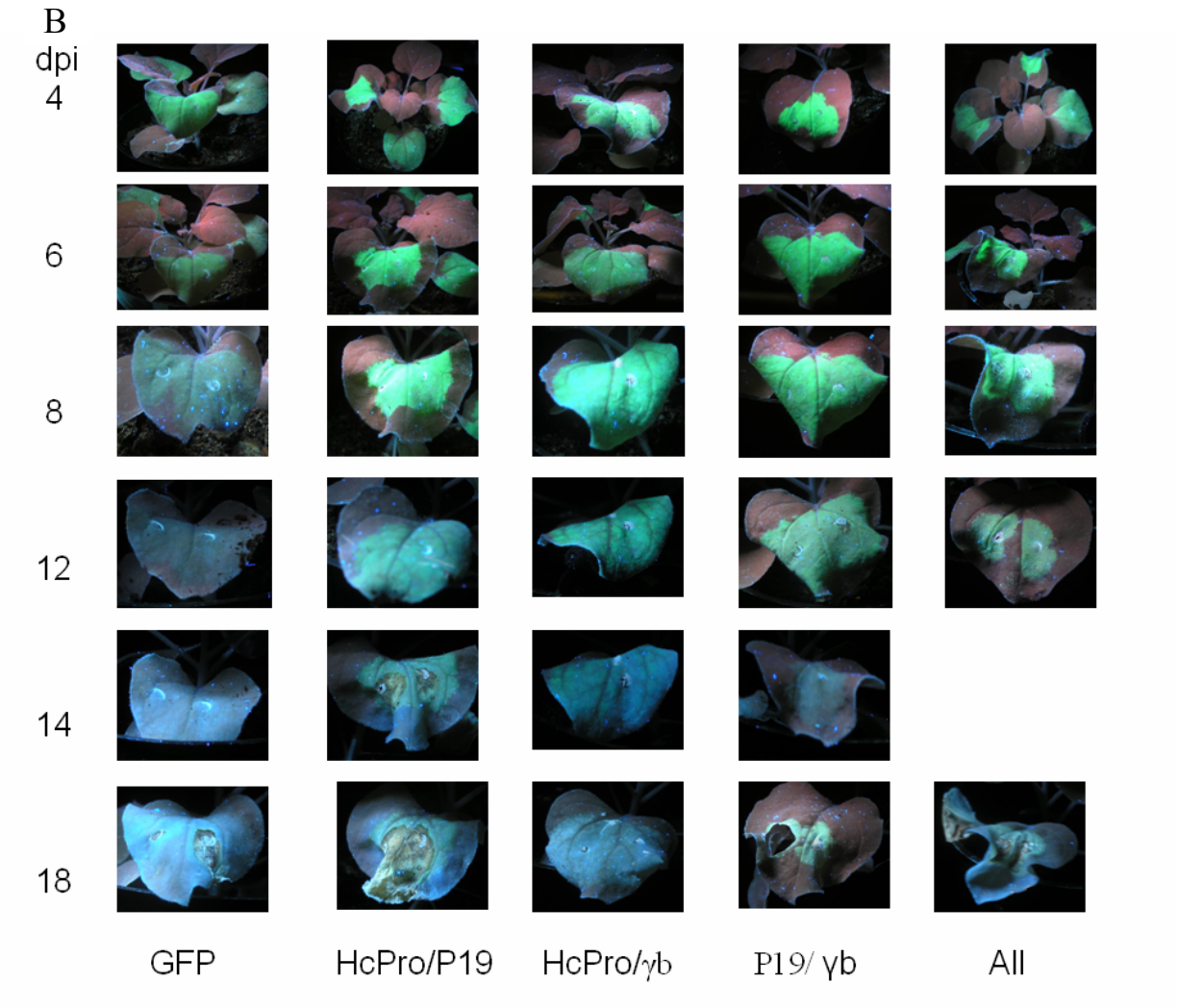

Fig. 4.3 Continued
B.) The plants in the first column, again, are infiltrated with 0.125 ml *Agrobacterium-gfp* per leaf, plus *Agrobacterium EHA* to ensure each leaf was inoculated with 0.5 ml of the culture. The plants in columns 2-4 are infiltrated with 0.125 ml *Agrobacterium-gfp,* 0.125 ml each of the other silencing suppressors, and 0.125 *Agrobacterium EHA*. The plants in the 5th column are infiltrated with 0.125 ml *Agrobacterium-gfp,* and 0.125 ml each of *Agrobacterium-hcpro, Agrobacterium-p19,* and *Agrobacterium-γb*. These combinations were mixed in this manner to ensure each leaf was infiltrated with 0.5 ml *Agrobacterium.*

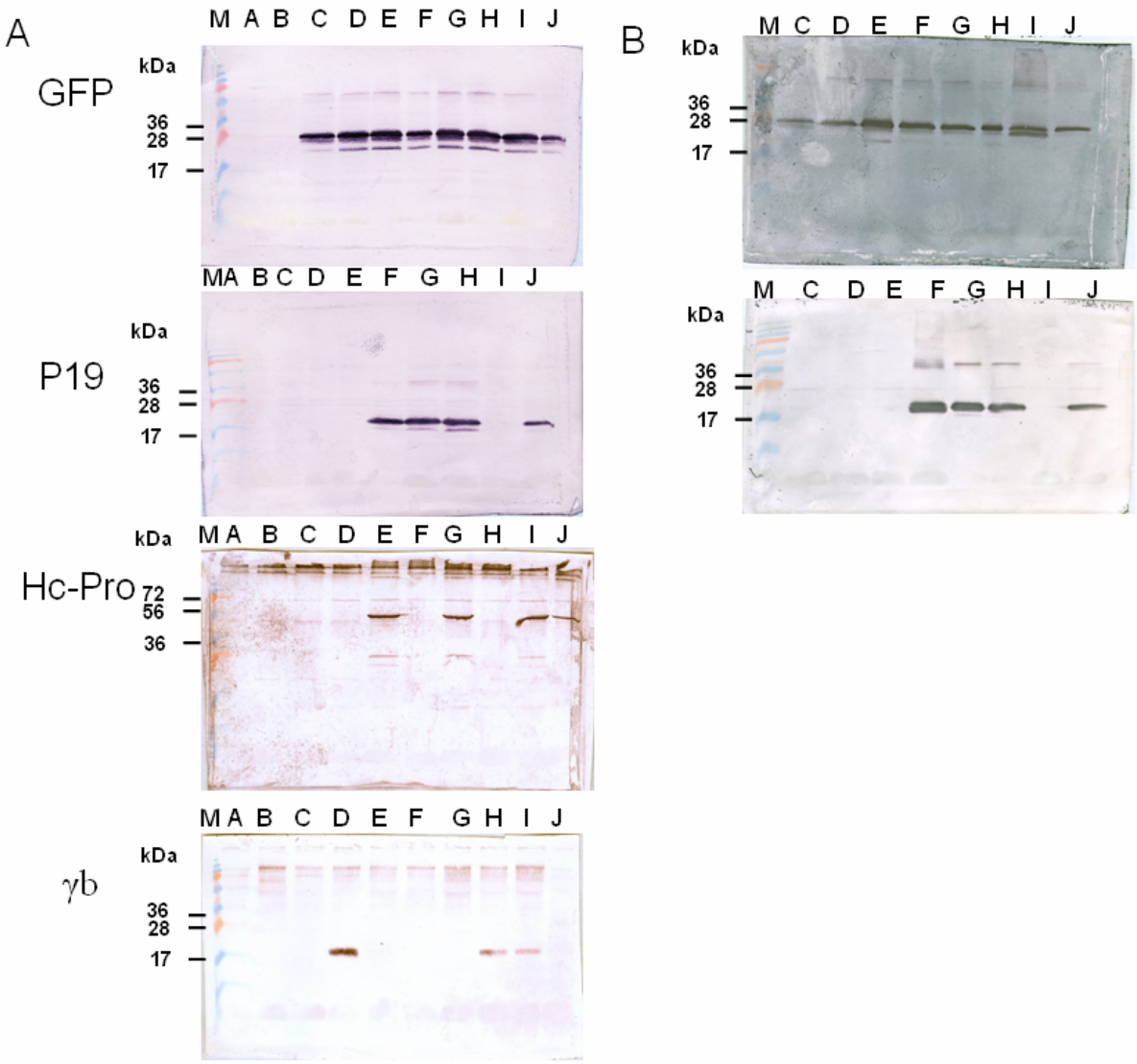

Fig 4.4 Western blots from protein extractions of plants infiltrated with high OD cultures of *Agrobacterium.* These were probed with antibodies against the silencing suppressors indicated. Centimeter-square sections were taken from 1.2 starting OD infiltrated plant tissue, and the proteins extracted by homogenization, boiled with cracking buffer, and 30 µl of each sample was loaded, along with 3 µl of the low weight protein ladder. These westerns were then probed with antibodies against the proteins indication, and visualized with alkaline phosphatase reactions. Lanes are marked as follows: M- low molecular weight protein marker, A – healthy, B – A*grobacterium EHA*, C – *Agrobacterium-gfp*, D - *Agrobacterium-gfp and -γb,* E – *Agrobacterium-gfp and -hcpro,* F – *Agrobacterium-gfp and - p19,* G – *Agrobacterium- gfp, - p19, -hcpro,* H – *Agrobacterium-gfp, -p19 and - hcpro*, I – *Agrobacterium-gfp, -γb, and –hcp*, and J – *Agrobacterium-gfp, -hcpro, -p19, and γb.* For unknown reasons, γb was not detected in the indicated blot. (lane 6)
A.) These samples were taken from infiltrated plants at 3 dpi.
B.) These samples were taken 12 dpi, to check for continued protein expression.

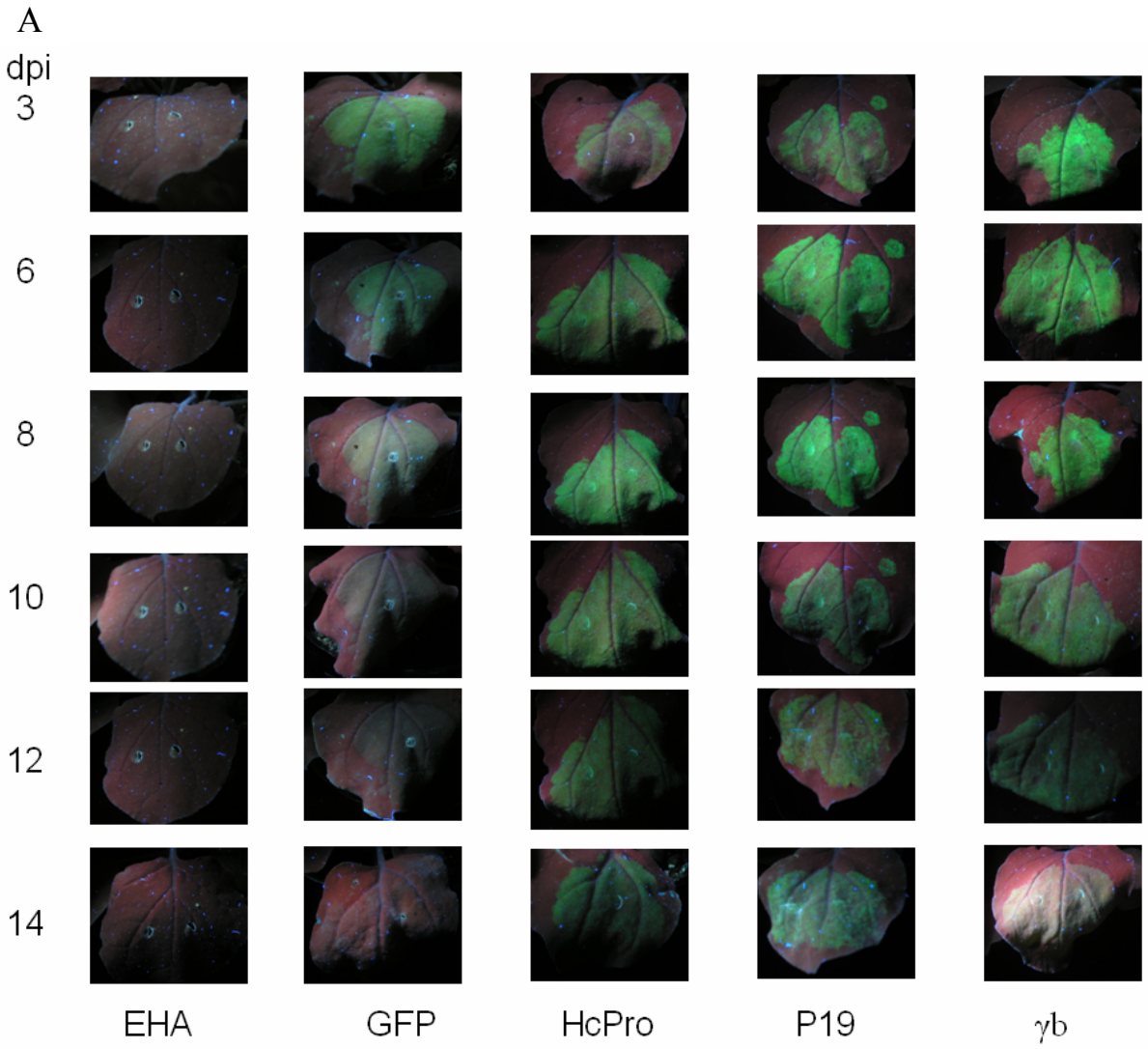

Fig. 4.5 Silencing suppressors infiltrated with low OD *Agrobacterium* cultures. Three week-old *N. benthamiana* plants were infiltrated with *Agrobacterium*- mediated GFP and silencing suppressors at an optical density of 0.8, mixed as indicated. The plants were then photographed at each time point indicated under a 488 nm wavelength UV light with a 4 second exposure, no flash, to monitor levels of visible GFP expressed.

A.) The plants in the first column, labeled EHA, are those infiltrated with untransformed *Agrobacterium*, as a negative control. The plants in the second column are those infiltrated with 0.125 ml *Agrobacterium-gfp* per leaf, plus *Agrobacterium EHA* to ensure each leaf was inoculated with 0.5 ml of the culture. The plants in the later lanes were infiltrated with 0.15 ml *Agrobacterium-gfp* plus 0.125 ml of one of the silencing suppressors.

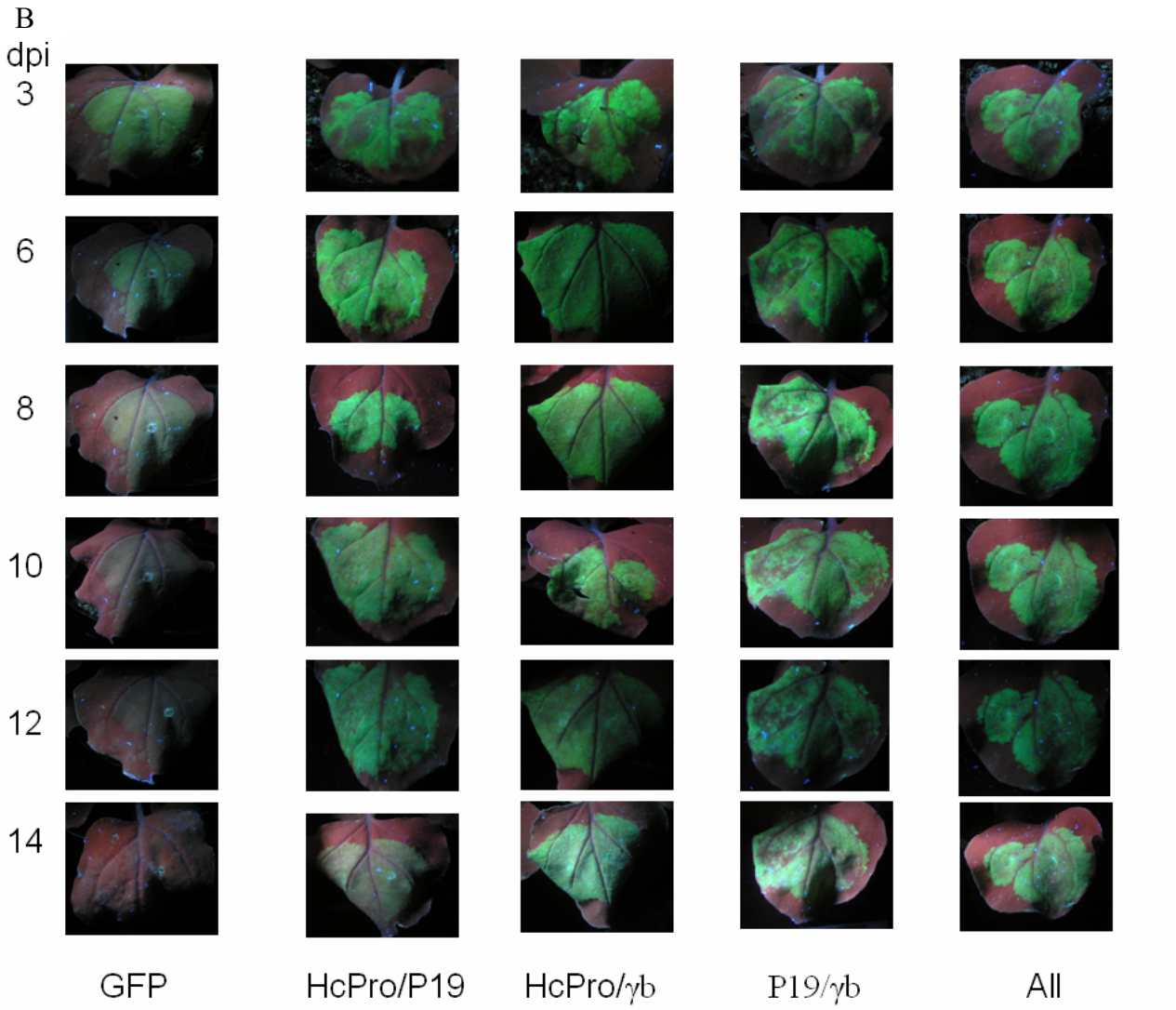

Fig. 4.5 Continued
B.) The plants in the first column, again, are infiltrated with 0.125 ml *Agrobacterium-gfp* per leaf, plus *Agrobacterium EHA* to ensure each leaf was inoculated with 0.5 ml of the culture. The plants in columns 2-4 are infiltrated with 0.125 ml *Agrobacterium-gfp,* 0.125 mls each of the other silencing suppressors, and 0.125 *Agrobacterium EHA*. The plants in the 5th column are infiltrated with 0.125 ml *Agrobacterium-gfp,* and 0.125 ml each of *Agrobacterium-hcpro, Agrobacterium-p19,* and *Agrobacterium-γb*. These combinations were mixed in this manner to ensure each leaf was infiltrated with 0.5 ml *Agrobacterium.*

prior blot in Fig. 4.4A. This might indicate that as the infection progressed, proteins accumulated, which supports the aims of this chapter. For the plant tissue initially infiltrated with *Agrobacterium* with the low OD of 0.8, proteins were extracted at 3 dpi to ensure proteins were expressed (Fig. 4.7).

Effect of silencing suppressors on GFP expression as vectored by *Agrobacterium.*

For plants infiltrated with *Agrobacterium* strain EHA alone, slight non-green (grayish) fluorescence was seen as the *Agrobacterium* established a very mild infection, usually seen as a slight chlorosis of the infiltrated tissue that progressively becomes more yellowed over time. *Agrobacterium* carrying the *gfp* gene behind a CaMV 35S promoter showed a definite green signal peaking around day 6, and declining thereafter to a level nearly indistinguishable from the *Agrobacterium* strain EHA- infiltrated tissue around 12 days post inoculation. This was consistent in all repetitions of the experiments, following both infiltrations with ODs of 1.2, and 0.8. For each of the silencing suppressors infiltrated singly with GFP, the GFP signal was not only enhanced on the 3rd day following infiltration, but the length of time that GFP was detected visually was increased (Fig. 4.3A), the GFP signal itself enhanced, and the density of the band yielded by western blotting with GFP antibodies was more prominent with tissue taken at 12 dpi than at 3 dpi (Fig. 4.4).

The silencing suppressors themselves varied in extension and enhancement of the GFP signal (Fig. 4.3A). In general, HcPro and P19 extended the length of time that GFP was visible more so than γb, for which extension seemed to peak around 8 days post inoculation and then decline. P19 and HcPro took a longer length of time for maximum expression of the GFP visual signal, as seen with the timecourse data from plants infiltrated with a starting ODs of 0.8 (Fig. 4.5). *Agrobacterium-gfp* by itself, the maximum level of visible GFP expression, did not reach the level of visible signal comparable to that oberserved with the co-infiltrated silencing suppressors/GFPs at their peak GFP expression. While P19 enhanced the GFP signal to the level of HcPro, it did not lengthen the expression of the signal for as long (12 dpi for P19 versus 14 dpi for HcPro, Fig. 4.5A).

GFP visual expression was monitored for the silencing suppressors infiltrated in dual combinations and then all together. Expression was certainly enhanced when compared to tissue infiltrated with only *Agrobacterium-gfp,* as well as certain instances with combined suppressors when compared to the suppressors alone. Visual levels of GFP expression were comparable at 3, 6, and 8 dpi time points for the silencing suppressors expressed in singly, in tandem, and in triplicate, though HcPro- and P19- mixtures co-infiltrated with γb gave an enhanced signal at these points when compared to HcPro- and P19- infiltrated with *Agrobacterium-gfp* alone (Fig 4.3, 4.5). Between 8 and 12 dpi, the silencing suppressors expressed dually and in triplicate enhanced signals when compared to the singly- infiltrated silencing suppressors. For plants infiltrated with a higher starting OD (1.2), however, this extended time of protein expression is offset by necrosis in the infiltrated tissue (Fig 4.3B, lower rows). What tissue remained intact still gave a vivid GFP signal, particularly for the HcPro/P19 combination as well as with all of the suppressors co-infiltrated (Fig. 4.3B). For tissue infiltrated with a lower OD (0.8), this necrosis was circumvented, as expected (Fig. 4.5B). At 12 dpi, constructs containing HcPro seem to exhibit the most obvious GFP signal, though this was diminished by 14 dpi, when all three silencing suppressors co-infiltrated with *Agrobacterium-gfp* was the most vivid (Fig. 4.5A). This agrees with the hypothesis, and will be addressed in the discussion section.

Effect of silencing suppressors on GFP expressed from a virus vector.

Due to necrosis observed at later time-points when plants were infiltrated with a culture OD of 1.2, the starting OD was diluted to 0.8 for plants to be infiltrated with *Agrobacterium*-silencing suppressor constructs followed by inoculation with the virus vectors (RMJ-1 and RMJ-3). Plants infected with only the RMJ-1 and RMJ-3 virus vectors displayed differing phenotypes on each of the comparable ½ leaf assays. RMJ-1 displayed vivid, broad GFP lesions, with the lesions growing in size over time to nearly confluence (Fig. 4.6). RMJ-3 yielded very weak GFP-expression lesions under UV light, and these lesions decreased in size and intensity until no longer displaying a visible GFP signal at 10 dpi, similar to the loss of signal seen with *Agrobacterium-gfp* (Fig 4.6). The resultant phenotypes for *Agrobacterium*-mediated silencing suppressors inoculated with

either form of the viral construct was in agreement. RMJ-1, expressing P19 itself, gives a nearly overwhelming GFP signal when inoculated with the silencing suppressors. For RMJ-1 half leaf assays, the GFP lesions were larger overall, and the *Agrobacterium*-silencing suppressors had generally the same effect on GFP expression as that demonstrated with RMJ-3. There was a slight increase in the amount of necrotic tissue present in RMJ-1 assays (compared to RMJ-3).

Because RMJ-3 lacks P19 expression, the resultant phenotypes had greater variance than those for RMJ-1, and so will be described here in greater detail. RMJ-3 lesions had a much stronger GFP signal when co-expressed with silencing suppressors (Fig. 4.6). While GFP was visible at 3 dpi for the tissues expressing a single silencing suppressor, it increased with progression of the time-course. At 3 dpi, the visible GFP signal was strongest for plants infiltrated with *Agrobacterium-γb,* and the lesions themselves larger, though this expression was lost by 12 dpi in the plant co-infiltrated with that suppressor alone. For plants infiltrated with *Agrobacterium-hcpro*, the lesions remained vivid in infiltrated tissue through 14 dpi, though there was heavy tissue necrosis. *Agrobacterium-p19* gave enhanced GFP expression with increasing lesion size as the timecourse progressed, and the lesions were similar in appearance to those seen on RMJ-1 only inoculated plant. For plants infected with RMJ-3 and combinations of the *Agrobacterium*- silencing suppressors, plants infiltrated with γb in combination with another suppressor displayed a visible GFP signal at an earlier time-point, though this treatment seemed to display the most tissue necrosis (Fig. 4.6B). The HcPro/P19 combination and all the silencing suppressors co-expressed gave the most vivid signal and largest lesions (Fig 4.6B). This experiment is currently undergoing more repetitions.

Discussion

The goal of this work was to extend and enhance the amount of foreign protein transiently produced in a plant using RNAi silencing suppressors. The titer and expression of transiently expressed proteins has been shown to decrease over time due to the silencing of mRNA (Voinnet et al., 2003). The main hypothesis of the present study was that as silencing suppressors operate at different steps in the RNAi pathway (Mlotshwa et al., 2005; Rakitina et al., 2006; Scholthof, 2006), their combined use allows

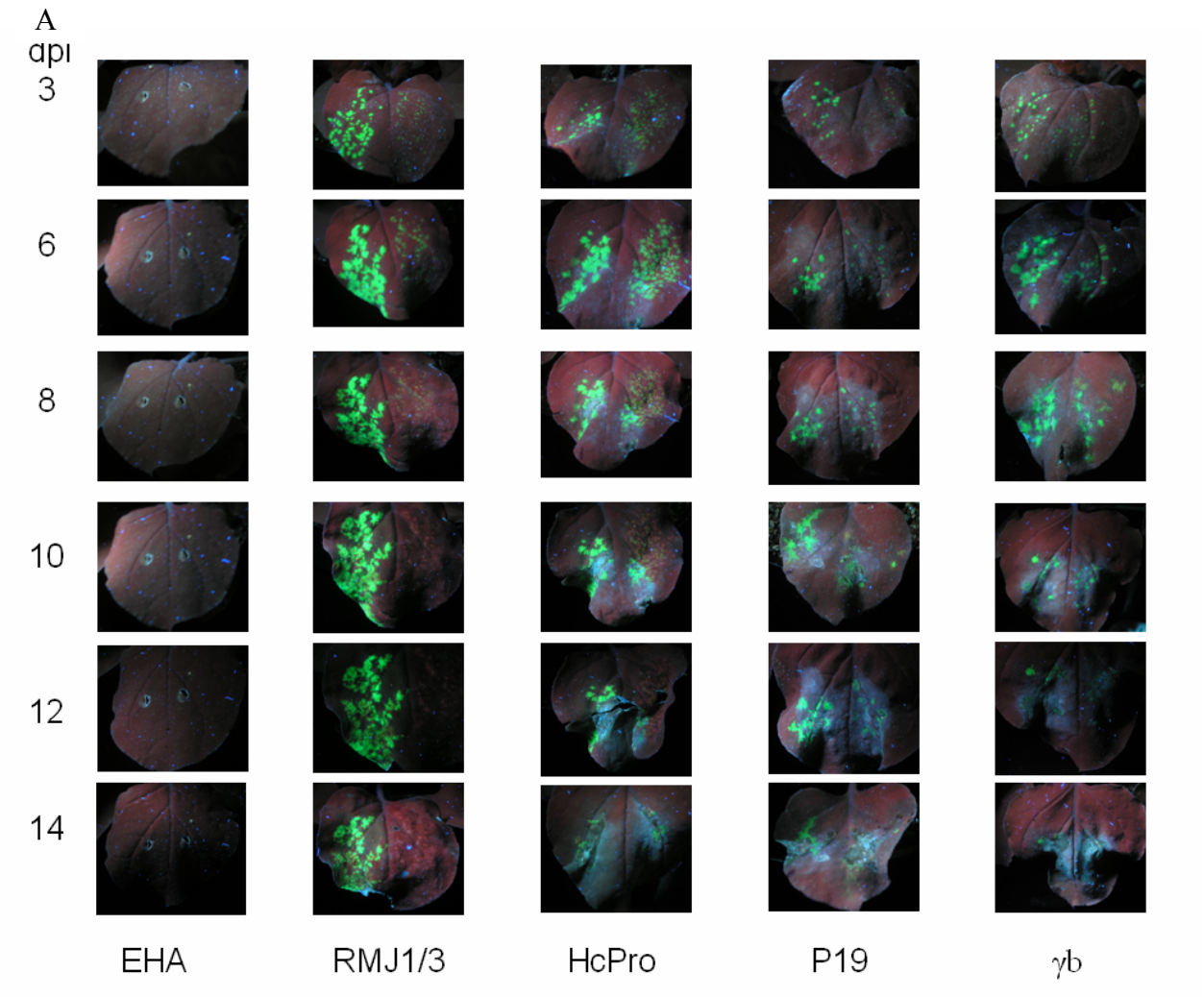

Fig. 4.6 *Agrobacterium*-vectored silencing suppressors and virus vectors. TBSV vector RMJ-1 (expressing P19) and RMJ-3 (lacking P19 expression) both carry *gfp*. Three week-old *N. benthamiana* plants were infiltrated with *Agrobacterium*-mediated GFP and silencing suppressors at an optical density of 0.8, mixed as indicated. The plants were then photographed at each time point indicated under a 488 nm wavelength UV light with a 4 second exposure, no flash, to monitor levels of visible GFP expressed.

A.) The plants in the first column, labeled EHA, are those infiltrated with untransformed *Agrobacterium*, as a negative control. The plants in the second column are those inoculated with RMJ-1 on the left half and RMJ-3 on the right half. The plants in the later lanes were inoculated with RMJ-1 and RMJ-3 plus 0.125 ml of one of the silencing suppressors, plus *A. tumafaciens* EHA to raise the correct volume each leaf was inoculated with to 0.5 ml *Agrobacterium* culture.

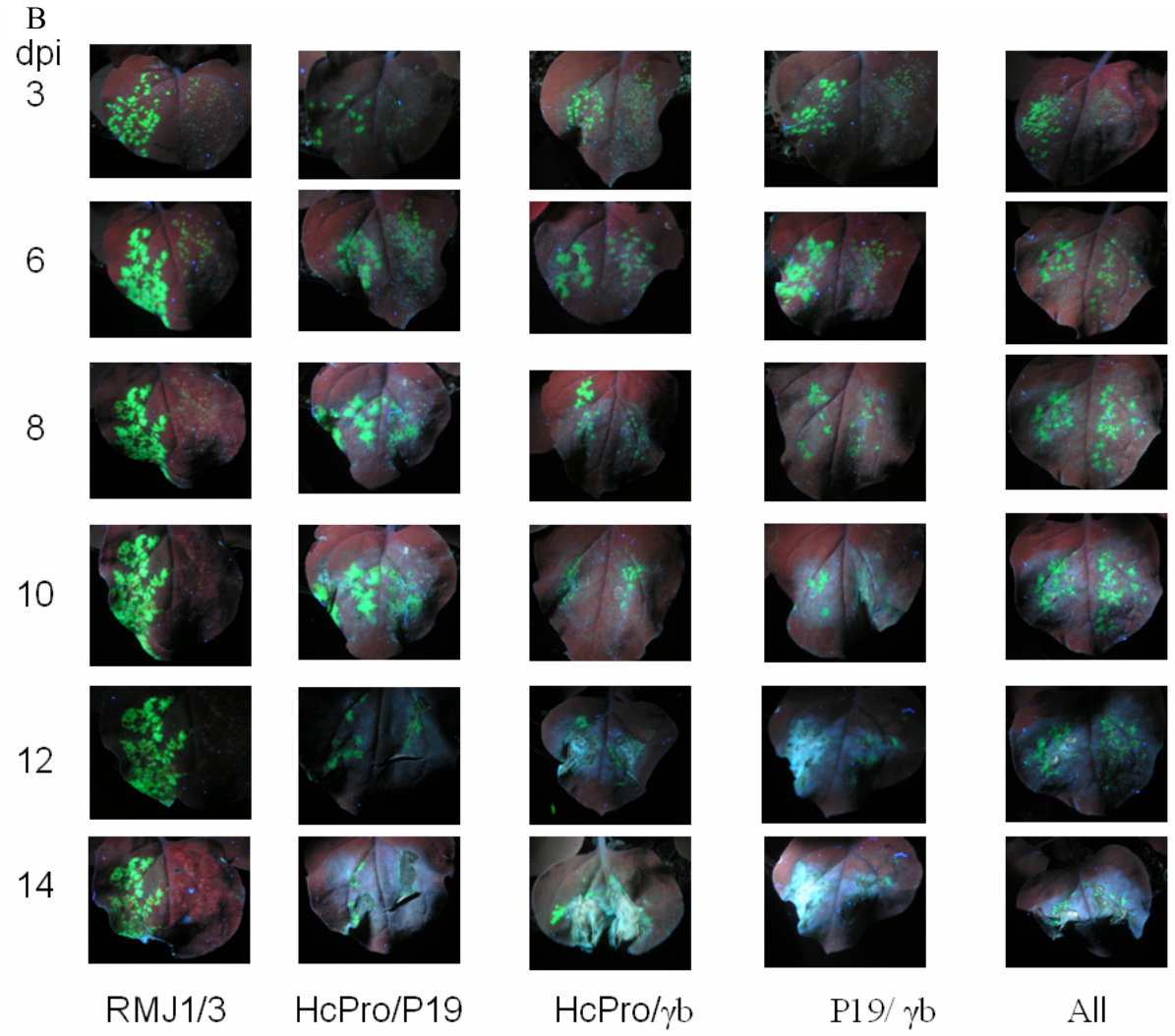

Fig. 4.6 Continued
B.) The plants in the first column, labeled EHA, are those infiltrated with untransformed *Agrobacterium*, as a negative control. The plants in columns 2-4 are inoculated with RMJ-1 and RMJ-3, plus 0.125 mls each of the other silencing suppressors, and 0.125 *Agrobacterium EHA*. The plants in the 5th column are inoculated with 0.125 ml each of *Agrobacterium-hcpro, Agrobacterium-p19,* and *Agrobacterium-γb*. These combinations were mixed in this manner to ensure each leaf was infiltrated with 0.5 ml *Agrobacterium*.

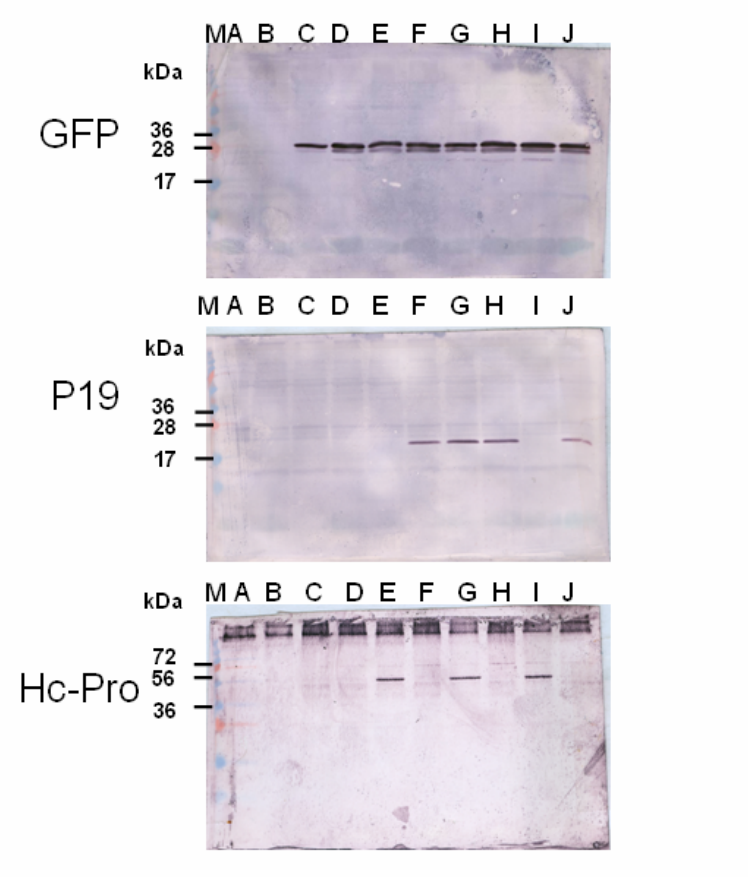

Fig. 4.7 Western blots from protein extractions of plants infiltrated with low OD cultures of *Agrobacterium* .The blots were probed with antibodies against the silencing suppressors indicated.
Centimeter-square sections were processed as for 4.4.
Lanes are marked as follows: M- low molecular weight protein marker,
A – healthy, B – A*grobacterium EHA*, C – *Agrobacterium-gfp*, D - *Agrobacterium-gfp and -γb,* E – *Agrobacterium-gfp and -hcpro,* F – *Agrobacterium-gfp and - p19,* G – *Agrobacterium- gfp, - p19, -hcpro,* H – *Agrobacterium-gfp, -p19 and -hcpro*, I – *Agrobacterium-gfp, -γb, and –hcp*, and J – *Agrobacterium-gfp, -hcpro, -p19, and γb.*
These samples were taken from infiltrated plants 3 dpi, to establish that the proteins were being produced at the start of the time course. Proteins were not extracted from later time points as their expression was correlated with enhanced and extended virus-vector related expression. The western blot for γb displayed only unspecific binding and was not shown, though plants infiltrated with the γb culture display evidence of silencing suppression (Fig. 4.5-6).

GFP to be produced for a longer length of time by synergistic hampering of the pathway when this foreign gene is expressed by a virus vector.

The results are fairly straightforward, and consistent for silencing suppressors expressed by *Agrobacterium* regardless of the GFP source, shown previously for agro-GFP but here demonstrated successfully for a *gfp*-TBSV viral vector. Visual signals of GFP alone are lost by 8 dpi, and the use of silencing suppressors extends both the length of time that these signals are visible, as well as enhancing the amount of GFP expressed (Fig. 4.3, 4.5). *Agrobacterium*-γb seems to enhance GFP expression early in the time-course. *Agrobacterium-p19 and Agrobacterium-hcpro* seem to enhance GFP expression later in the time-course, and extend the length of time that GFP is produced. When infiltrated in combination, the actions of the silencing suppressors in the RNAi pathway complement each other, and the GFP signal is correspondingly affected. For instance, γb affects GFP expression earlier in the time-course. This early activity is complemented by other suppressors and their action at later time points, resulting in the γb enhanced expression extending longer. Furthermore, co-infiltrations involving P19 and HcPro show an extended GFP visible signal, though the co-infiltration of HcPro and P19, sans γb, do not display as visible a GFP signal at earlier time points as do those in presence of γb.

The results are consistent with my hypothesis. These silencing suppressors are thought to act at different steps in the RNAi pathway; γb is thought to bind to RNA and interfere with silencing (Fig. 4.1D), HcPro possibly modifies Dicer and binds to dsRNAs (Fig. 4.1A, C), and P19 has been shown to sequester siRNA duplexes before they are loaded onto RISC (Fig. 4.1C). In the context of this experiment, the results are semi-logical. While unexpected, early enhancement of the GFP signal by γb might be caused by binding of the silencing suppressor to ssRNA, which would protect it from elements of the RNAi pathway. However, while it does enhance the GFP signal, this activity seems temporally out of place. Previous characterization of γb suggest that an RNA-binding domain contributes to its function as a silencing suppressor (Donald and Jackson, 1996; Yelina et al., 2002; Rakitina et al., 2006), as γb has been shown to bind to ssRNA in a sequence unspecific manner. This mode of silencing suppression would place it downstream of the pathway where P19, which binds dsRNAs, and HcPro, which is thought to both bind siRNAs and modify Dicer (Mlotshwa et al., 2005; Lakatos et al.,

2006). The data indicate that γb acts earlier in the pathway than HcPro and P19. This might be due more to the known role of this protein as a replication enhancer; it is possible that the early enhancement is due to the fact that γb does not have to compete with plant proteins and can act immediately upon expression to protect the co-expressed ssRNA, and this effect is not seen later in the infection because ssRNA is being targeted heavily by RISCs. The later suppression activities by HcPro and P19 might require the presence of siRNAs in the cell, and lag of silencing suppression activity, as compared to that of γb, would be explained by necessity of siRNAs accumulation, which would take more time. The combined synergistic effect of all three silencing suppressors, early in the time course, plus extending the length of time that GFP is produced by about a week, indicates that the suppressors constitute a valuable addition to transient protein expression designs.

In the design and execution of these experiments, there are several issues to take into consideration. It is exceedingly difficult to quantify levels of GFP expression visually, and nearly as difficult to accomplish this using other protein-assaying techniques while conducting a time-course due to the destruction of the GFP-expressing tissue. This study aimed to make conditions for the plants as identical as possible to avoid introducing any other outside variables that would interfere with protein expression. This was at odds with collection of tissue for western assays, as removal of leaves or infiltrated tissue from the plants might stimulate plant defenses that could affect protein expression and accumulation. Thus, visualization of GFP and detection of protein levels at only 2 points in each experiment seemed the best method to determine extension and enhancement of GFP expression.

Other experimental aspects were at odds during this study. *Agrobacterium* has been shown to elicit a necrotic response in certain hosts, with some hosts more sensitive than others to the bacterium. This has been shown for agroinfiltration of tomato, as well as members of the Solanaceous species (Wroblewski et al., 2005; Lindbo, 2007). As illustrated with varying the starting OD of the infiltrated *Agrobacterium* constructs, more turbid ODs negatively impacted the experiments with the stimulation of leaf chlorosis. However, in theory and as determined experimentally based on comparison of GFP pictures as well as GFP detection by western blotting, that more *Agrobacterium* used to

infiltrate the plant gave a higher expression of GFP, earlier in the time-course. This observation would have resonance based on the reason necessitating protein expression in an industrial setting. If the goal is to produce as much protein in a short amount of time, a higher infiltration OD would be appropriate. If extension of the length of time that the protein is expressed is the objective, I would recommend using a lower infiltration OD to avoid negative effects on the infiltrated tissue. These two factors would need to be adjusted in each case to best fit needs.

Additionally, while plants infiltrated with low starting ODs of the *Agrobacterium* constructs (including GFP) did not display tissue necrosis, the added stress of a virus vector rendered a necrotic response in co-infiltrated and rub-inoculated tissues at about 2-weeks post inoculation. There are several possible reasons for this. It has been shown that silencing suppressors interfere with regular RNAi pathways in plants (Chapman et al., 2004). This might interfere with the way proteins are processed, as mRNAs accumulate or regular plant cellular activities are interrupted, or it is possible that the combination *Agrobacterium*/virus infections might trigger an overwhelming defensive response within the cell, resulting in necrosis. To counter such a response, this study aimed to minimize necrosis by using a less virulent *Agrobacterium*, as well as diluting the optical density of the infiltrate. It may be speculated that the necrosis is a result of harsh inoculation practices; however, the entire leaf was rub-inoculated and the only necrotic tissue was in areas in which the silencing suppressor and virus-vector were both present, ruling out inoculation as the cause of necrosis.

An observation not addressed above was that plant age seemed to play a role for protein expression with agro-infiltration. *N. benthamiana* that were inoculated 1 week later, at 4 weeks, as opposed to 3 wks, did not seem to experience the same amount of chlorosis that the 3-wk old plants did following agro-infiltration. However, this is offset by the fact that older plants are much less susceptible to infection by a virus (Hull, 2002), and their use in this experiment would be deleterious in that regard.

Furthermore, silencing suppressors have been shown to act at different efficiencies in the RNAi pathway, and interact with potential hosts differently (Voinnet, 2005; Martin-Hernandez and Baulcombe, 2008). This has implications while comparing the response of HcPro and P19. While HcPro seemed to have a enhanced effect of GFP

when compared to P19, it is important to consider the toxic effect of P19 in *N. benthamiana* (Chapman et al., 2004; Siddiqui et al., 2008), in addition to the fact that the virus vector used expresses P19 as the native silencing suppressor. This may impact comparisons of the responses of P19 and HcPro, and so this was avoided here. However, it is important to note that HcPro, when used as a heterologous suppressor in a TBSV virus vector, acts to enhance foreign protein production as well, if not better, than TBSV P19, when both were expressed by agro-infiltration. This is consistent with the roles that suppressors work on conserved, virus non-specific steps, and furthermore, that it is certain that the use of a heterologous suppressor such as HcPro will not result in a recombined, complete virus vector.

To summarize the main points of this study, silencing suppressors can be used to extend and enhance a virus-vectored foreign protein in a plant host. The step at which the silencing suppressor works in the RNAi pathway impacts functionality; silencing suppressors which bind to dsRNAs or interfere with Ago might have a delayed response when compared to silencing suppressors that act in earlier in the RNAi pathway, like binding to RNA to prevent cleavage by Dicer. Other factors to consider include the starting optical density of the *Agrobacterium* culture; a greater starting OD produces a greater amount of protein more quickly, but also causes plant physiological issues and might impact protein accumulation. A lower starting OD extends the length of time that the protein is expressed by avoiding overload of the cell, though the initial amount of protein expressed is less. Collectively, the data suggest that early expression of any silencing suppressor combination may subsequently improve the performance of viral vectors for expression of value-added proteins in plants.

CHAPTER V
FINAL SUMMARY AND DIRECTIONS

In objective 1, *biochemical characterization of an RNAi response against TBSV in N. benthamiana,* TBSV-infected plant tissue was fractionated by column chromatography, and the resultant fractions were tested for anti-viral RNAi ribonucleases. These ribonucleases were present in the same fractions as viral siRNAs, were inhibited by treatment with EDTA, enhanced by the addition of Mn^{2+} and Mg^{2+}, and stable through further steps of column chromatography. When plants were inoculated with wt TBSV encoding a silencing suppressor, activity was inhibited. Additionally, ribonuclease activity eluted in Sephacryl S200 gel filtration fractions that would represent molecules or moieties of 500 kDa, possibly denoting a protein complex (RISC). The results support the model that following viral infection, a RNAi response is triggered which subsequently targets TBSV for degradation and eventual virus clearance.

Following other methods of column chromatography, individual proteins were found to be in the 100 kDa range (perhaps representing Ago). However, after isolation and sequencing of proteins after visualization by silver staining, those proteins known to be associated with RNAi were not detected. RISC is thought to be a multiple turnover complex, thus it would not be unreasonable to attribute difficulty in isolating the responsible catalytic proteins to the hypothesis that they are present in such low quantities. It was also shown that ribonuclease activity was inhibited by the addition of NaCl in work done after the conclusion of this chapter; because siRNAs are known to interact with the RISC Ago protein through ionic interactions, this finding was also in agreement with the proposed RNAi pathway.

To further identify the proteins present that might contribute to RNAi, antibodies were generated against a conserved region of the Piwi domain, a domain unique to the Ago family of proteins. Fractions displaying RNase activity and siRNAs were also shown to contain proteins with a Piwi-domain (unpublished data). Further characterization of the RISC proteins might include some sort of antibody-affinity column, or possibly a north-western (for antibodies and siRNAs) to help directly determine potential proteins. Preliminary data indicate that the RISCs can be reloaded with siRNAs, therefore it might

be possible to label these siRNAs before they are loaded onto the RISCs perhaps using a biotin molecule, crosslink the RNA to the ribonuclease once it associates, then use a detection method for the siRNAs to find the proteins responsible.

The material presented in the appendix, a description of a novel method of TBSV virion purification, is very straightforward. Hydroxyapatite column chromatography was used to isolate virions from TBSV-infected *N. benthamiana* plant tissue as well as TBSV-infected pepper plant tissue. The true identity of the virions was confirmed by re-inoculation of *N. benthamiana* by western blotting with antibodies for the CP of TBSV, by northern blotting of both the virions themselves and virion-infected plant tissue with a TBSV hybridization probe, and upon electron microscopy of the virions. Exploration of this virion purification method might involve the isolation of viruses with different capsid morphologies, to see if these also can be purified by this method. Regardless, this is a very useful method of isolating virions and maintaining stock for experimental use.

For *objective 2, determination of the antiviral response following infection of N. benthamiana with TRV, as well as examination of defense elements present following PMV and SPMV infection of monocots*, again, the results of these experiments are consistent with those seen for TBSV; an anti-viral ribonuclease with RISC-like characteristics, targeting only TRV-virus RNA, was isolated. To further clarify the TRV studies, it is unknown at this point whether the ribonucleases present in TRV fractions following hydroxyapatite and S200 gel filtration with 250 mM NaCl are targeting the total RNA from TBSV-infected plants due to the presence of siRNAs brought in with the total RNA. This might be resolved by somehow adding only genomic and subgenomic TBSV RNA, without small RNA fragments/siRNAs, to the fractions and then observing if degradation occurs.

Along with this, TRV infections might also stimulate other antiviral defenses, which then target and degrade all RNAs. An alternative theory is that the ribonuclease present, instead of being programmed with siRNAs against a particular virus, simply targets all RNA of a particular size. To support this theory, in many of the experiments above, it appears that the ribonuclease seems to prefer TBSV genomic RNA (Fig 2.13B, particularly), and for total RNA extracted from plants, ribosomal RNAs around 2000 bp are also targeted. Other literature has shown that RISC is programmed with ribosomal

RNA in some instances, but it is interesting that the ribonuclease seems to prefer larger strands of ssRNA. At this time, it is unknown how RISC finds viral RNA in the cell; the target ssRNA might need to be a certain length for recognition, as was also found for the anti-TBSV RISC.

Other interesting results not addressed in the chapter indicate that it is difficult to 'reprogram' RISCs from TRV-infected tissue with siRNAs purified from the fractionation of TBSV-infected plants. This might be due to some sort of modification required upon binding to RISC, and following dissociation, these siRNAs can no longer re-associate. To address this, viral siRNAs might need to be purified directly from infected plants, and used for 'reprogramming'.

It is also hypothesized that TRV produces less siRNAs than does TBSV; TRV does not seem to produce nearly as much viral dsRNA intermediates as TBSV. This might help explain why detection of siRNAs following gel filtration after hydroxyapatite is a challenge. At this time, I suggest this might be due to RNA used as a target for the hybridization probe. Current efforts are investigating this by using hybridization probes against TRV-RNA1 in addition to TRV-RNA2 to probe these membranes, and finally tie siRNAs directly to the fractions containing ribonuclease activity and Piwi-containing proteins.

The PMV and SPMV-infected plant tissue hydroxyapatite fractions need to be subjected to another type of column chromatography, probably gel filtration, to further study the anti-viral defense in monocots more in depth. This set of experiments also needs to be repeated an additional time.

In conclusion, this work further supports the RNAi model that an anti-viral RISC is triggered upon virus infection; TRV-infected plant extracts and possibly PMV/SPMV infected plant tissues harbor a virus-specific ribonuclease with properties that agree with the RISC model.

In *objective 3, determining the effect of silencing suppressors HcPro, P19, and γb on the performance of a virus-vectored GFP gene plants*, it was found that the silencing suppressors did enhance GFP signal and extend the length of time that the signal was visible. Furthermore, it was hypothesized that as these silencing suppressors are thought to act in different steps of the RNAi pathway, their use in combination would have a

synergistic effect. This hypothesis was upheld by the data to an extent; the use of γb enhanced the signal earlier in the infection, but did not seem to have any effect of the length of time that GFP is produced. HcPro and P19 did not enhance GFP expression until later in infection, but co-infection with these extended the length of GFP signal visibility by about a week for both the *Agrobacterium*-vectored GFP, and the RMJ-*gfp* viral vectors. However, plants inoculated with the *Agrobacterium*-silencing suppressors and the virus vectors resulted in necrotic tissue, seen in two iterations of the project. Studies are ongoing to examine if the necrotic leaves are due to an overwhelming amount of silencing suppressors, or simple damage to the plant. Other projects might examine if these silencing suppressors have a similar effect on other foreign proteins. Additionally, it was observed that older plants do not display quite the same tissue chlorosis seen for younger plants; the age of plants might be adjusted to manipulate the system for maximal protein expression.

In summary, silencing suppressors can be used to enhance and extend the length of time a foreign gene is expressed from a virus vector. This has valuable implications for use in pharming, and expression of proteins in plants for use in biotechnology.

REFERENCES

Ameres, S.L., Martinez, J., and Schroeder, R. (2007). Molecular basis for target RNA recognition and cleavage by human RISC. Cell **130,** 110-112.

Batten, J., Desvoyes, B., Yamamura, Y., and Scholthof, K.-B.G. (2006). A translational enhancer element on the 3′-proximal end of the Panicum mosaic virus genome FEBS Lett. **580,** 2591-2597.

Batten, J.S., Yoshinari, S., and Hemenway, C. (2003). Potato virus X; a model system for virus replication, movement, and gene expression. Mol. Plant Path. **4,** 125-131.

Baulcombe, D. (2004). RNA silencing in plants. Nature **431,** 356-363.

Baumberger, N., and Baulcombe, D.C. (2005). Arabidopsis ARGONAUTE1 is an RNA slicer that selectively recruits microRNAs and short interfering RNAs. Proc. Natl. Acad. Sci. USA **102,** 11928-11933.

Baumberger, N., Tsai, C.-H., Lie, M., Havecker, E., and Baulcombe, D.C. (2007). The polerovirus silencing suppressor P0 targets Argonaute proteins for degradation. Curr. Biol. **17,** 1609-1614.

Bennasser, Y., and Jeang, K.-T. (2006). HIV-I Tat interaction with Dicer: requirement for RNA. Retrovirology **3**.

Bernstein, E., Caudy, A.A., Hammond, S.M., and Hannon, G.J. (2001). Role for a bidentate ribonuclease in the initiation step of RNA interference. Nature **409,** 363-366.

Borsani, O., Zhu, J., Verslues, P.E., Sunkar, R., and Zhu, J.K. (2005). Endogenous siRNAs derived from a pair of natural *cis*-antisense transcripts regulate salt tolerance in *Arabidopsis*. Cell **123,** 1279-1291.

Bortolamiol, D., Pazhouhandeh, M., Marrocco, K., Genschik, P., and Ziegler-Graff, V. (2007). The poleovirus F Box protein P0 targets Argonaute1 to suppress RNA silencing. Curr. Biol. **17,** 1615-1621.

Bragg, J.N., and Jackson, A.O. (2004). The C-terminal region of the Barley stripe mosaic virus gamma b protein participates in homologous interactions and is required for suppression of RNA silencing. Mol. Plant Pathol. **5,** 465-482.

Brigneti, G., Voinnet, O., Li, W.-X., Ji, L.-H., Ding, S.-W., and Baulcombe, D.C. (1998). Viral pathogenicity determinants are suppressors of transgene silencing in *Nicotiana benthamiana*. EMBO J. **17,** 6739-6746.

Brodersen, P., and Voinnet, O. (2006). The diversity of RNA silencing pathways in plants. Trends Genet. **22,** 268-280.

Burch-Smith, T.M., Anderson, J.C., Martin, G.B., and Dinesh-Kumar, S.P. (2004). Applications and advantages of virus-induced gene silencing for gene function studies in plants. Plant J. **39,** 734-746.

Burch-Smith, T.M., Schiff, M., Liu Y., and Dinesh-Kumar, S.P. (2006). Efficient virus-induced gene silencing in *Arabidopsis*. Plant Physiol. **142,** 21-27.

Carmell, M.A., and Hannon, G.J. (2004). RNase III enzymes and the initiation of gene silencing. Nat. Struct. Mol. Bio. **11,** 214-218.

Cerutti, L., Mian, N., and Bateman, A. (2000). Domains in gene silencing and cell differentiation proteins: the novel PAZ domain and redefinition of the Piwi domain. Trends Biochem. Sci. **25,** 481-482.

Chao, J.A., Lee, J.H., Chapados, B.R., Debler, E.W., Schneemann, A., and Williamson, J.R. (2005). Dual roles of RNA-silencing suppression by Flock House virus protein B2. Nature Struct. Biol. **12,** 952-957.

Chapman, E., Prokhnevsky, A.I., Gopinath, K., Dolja, V.V., and Carrington, J.C. (2004). Viral RNA silencing suppressors inhibit the microRNA pathway at an intermediate step. Genes Dev. **18,** 1179-1186.

Chendrimada, T.P., Gregory, R.I., Kumaraswamy, E., Norman, J., Cooch, N., Nishikura, K., and Shiekhattar, R. (2005). TRBP recruits the Dicer complex to Ago2 for microRNA processing amd gene silencing. Nature **436,** 740-744.

Chiba, M., Reed, J.C., Prokhnevsky, A.I., Chapman, E.J., Mawassi, M., Koonin, E.V., Carrington, J.C., and Dolja, V.V. (2005). Diverse suppressors of RNA silencing enhance agroinfection by a viral replicon. Virology **346,** 7-14.

Deleris, A., Gallego-Bartolome, J., Bao, J., Kasschau, K.D., Carrington, J.C., and Voinnet, O. (2006). Hierarchical action and inhibition of plant dicer-like proteins in antiviral defense. Science **313,** 68-71.

Desvoyes, B., Faure-Rabasse, S., Chen, M.-H., Park, J.-W., and Scholthof, H.B. (2002). A novel plant homeodomain protein interacts in a functionally relevant manner with a virus movement protein. Plant Physiol. **129,** 1521-1532.

Desvoyes, B., and Scholthof, H.B. (2002). Host-dependent recombination of a *Tomato bushy stunty virus* coat protein mutant yields truncated capsid subunits that form virus-like complexes which benefit systemic spread. Virology **304,** 434-442.

Donaire, L., Barajas, D., Martinez-Garcia, B., Martinez-Priego, L., Pagan, I., and Llave, C. (2008). Structural and genetic requirements for the biogenesis of Tobacco rattle virus-derived small interfering RNAs. J. Virol. **82,** 5167-5177.

Donald, R.G.K., and Jackson, A.O. (1996). RNA-binding activities of barley stripe mosaic virus γb fusion proteins. J. Gen. Virol. **77,** 879-888.

Eulalio, A., Behm-Ansmant, I., Schweizer, D., and Izaurralde, E. (2007). P-body formation is a consequence, not the cause of RNA-mediated gene silencing. Mole. Cell Biol. **27,** 3970-3981.

Fields, B.N., Knipe, D.M., Howley, P.M., Griffin, D.E., Lamb, R.A., Martin, M.A., Roizman, B., and Straus, S.E. (2007). Fields Virology. (Boston, MA: Lippincott Williams and Wilkins).

Filipowicz, W. (2005). RNAi: the nuts and bolts of the RISC machine. Cell **122,** 17-20.

Fire, A., Xu, S., Montgomery, M.K., Kostas, S.A., Driver, S.E., and Mello, C.C. (1998). Potent and specific genetic interference by double-stranded RNA in *Caenorhabditis elegans*. Nature **391,** 806-811.

Gagnon, P., Frost, R., Tunon, P., and Ogawa, T. (1996). CHT Ceramic hydroxyapatite - a new dimension in chromatography of biological molecules. (Technote: Bio-Rad).

Goodin, M.M., Dietzgen, R.G., Schichnes, D., Ruzin, S., and Jackson, A.O. (2002). pGD vectors: versatile tools for the expression of green and red fluorescent protein fusions in agroinfiltrated plant leaves. Plant J. **31,** 375-383.

Grimsley, N., Hohn, B., Hohn, T., and Walden, R.M. (1986). "Agroinfection", an alternative route for viral infection of plants by using the Ti plasmid. Proc. Nat. Acad. Sci. USA **83,** 3282-3286.

Gunawardane, L.S., Saito, K., Nishida, K.M., Miyoshi, K., Kawamura, Y., Nagami, T., Siomi, H., and Siomi, M.C. (2007). A slicer-mediated mechanism for repeat-associated siRNA 5' end formation in *Drosophila.* Science **315,** 1587-1590.

Hammond, S.M., Boettcher, G., Caudy, A.A., Kobayashi, T., and Hannon, G.J. (2001). Argonaute2, a link between genetic and biochemical analyses of RNAi. Science **293,** 1146-1150.

Hannon, G.J. (2002). RNA interference. Nature **418,** 244-251.

Heaton, L.A. (1992). Use of agarose gel electrophoresis to monitor conformational changes of some small, spherical plant viruses. Phytopathology **82,** 803-807.

Hemmes, H., Lakatos, L., Goldbach, R., Burgyan, J., and Prins, M. (2007). The NS3 protein of Rice hoja blanca tenuivirus suppresses RNA silencing in plant and insect hosts by efficiently binding both siRNAs and miRNAs. RNA **13,** 1079-1089.

Hiraguri, A., Itoh, R., Kondo, N., Nomura, Y., Aizawa, D., Murai, Y., Koiwa, H., Shinozaki, K., and Fukuhara, T. (2005). Specific interactions between Dicer-like proteins and HYL1/DRB-family of dsRNA-binding proteins in *Arabidopsis thaliana*. Plant Mol. Biol. **57,** 173-188.

Hong, J., Na, W., Chalk, A., Wang, J., Song, Y., Yi, F., Qiao, R.P., Sonnhammer, E.L.L., Wahlestedt, C., Liang, Z., and Du, Q. (2008). Focusing on RISC assembly in mammalian cells. Biochem. Biophys. Res. Commun. **368,** 703-708.

Hood, E.E., Helmer, G.L., Fraley, R.T., and Chilton, M.-D. (1986). The hypervirulence of *Agrobacterium tumefaciens* A281 is encoded in a region of pTiBo542 outside of T-DNA. J. Bacteriol. **168,** 1291-1301.

Hooykaas, P.J.J., and Schilperoort, R.A. (1992). *Agrobacterium* and plant genetic engineering. Plant Mol. Biol. **19,** 15-38.

Hull, R. (2002). Matthews' Plant Virology. (London: Academic Press).

Hutvagner, G., and Simard, M.J. (2008). Argonaute proteins: key players in RNA silencing. Nature Rev. Mol. Cell Biol. **9,** 22-32.

Jaskiewicz, L., and Filipowicz, W. (2008). Role of Dicer in posttranscriptional RNA silencing. In RNA interference. Current Topics in Microbiology and Immunology., P.J. Paddison, and P.K.Vogt, eds. (Berlin: Springer-Verlag.) pp.77-97.

Ji, X. (2008). The mechanism of RNase III action: how Dicer dices. In RNA interference. Current topics in Microbiology and Immunology., P.J. Paddison, and P.K. Vogt, eds. (Berlin: Springer-Verlag.) pp. 99-116.

Jones, L., Keining, T., Eamens, A., and Vaistij, F.E. (2006). Virus-induced gene silencing of *Argonaute* genes in *Nicotiana benthamiana* demonstrates that extensive systemis silencing requires *Argonaute1*-like and A*rgonaute4*-like genes. Plant Physiol. **141,** 598-606.

Jones-Rhoades, M.W., Bartel, D.P., and Bartel, B. (2006). MicroRNAs and their regulatory roles in plants. Annu. Rev. Plant Biol. **57,** 19-53.

Katiyar-Agarwal, S., Morgan, R., Dahlbeck, D., Borsani, O., Villegas Jr., A., Zhu, J.K., Staskawicz, B., and Jin, H. (2006). A pathogen-inducible endogenous siRNA in plant immunity. Proc. Nat. Acad. Sci. USA **103,** 18002-18007.

Lacroix, B., Tzfira, T., and Vainstein, A.C., V. (2006). A case of promiscuity: Agrobacterium's endless hunt for new partners. Trends Genet. **22,** 29-37.

Lakatos, L., Csorba, T., Pantaleo, V., Chapman, E.J., Carrington, J.C., Liu, Y.P., Dolja, V.V., Calvino, L.F., Lopez-Moya, J.J., and Burgyan, J. (2006). Small RNA binding is a common strategy to suppress RNA silencing by several viral suppressors. EMBO J. **25,** 2768-2780.

Lecellier, C.H., and Voinnet, O. (2004). RNA silencing: no mercy for viruses. Immunol. Rev. **198,** 285-303.

Leuschner, P.J., Ameres, S.L., Kueng, S., and Martinez, J. (2006). Cleavage of the siRNA passenger strand during RISC assembly in human cells. EMBO Rep **7,** 314-320.

Li, F., and Ding, S.W. (2006). Virus counterdefense: diverse strategies for evading the RNA-silencing immunity. Ann. Rev. Microbiol. **60,** 503-531.

Lindbo, J.A. (2007). High-efficiency protein expression in plants from agroinfection-compatbile *Tobacco mosaic virus* expression vectors. BMC Biotechnol. **7,** 52.

Liu, J., Carmell, M.A., Rivas, F.V., Marsden, C.G., Thompson, J.M., Song, J.-J., Hammond, A.M., Joshua-Tor, L., and Hannon, G.J. (2004). Argonaute 2 is the catalytic engine of mammalian RNAi. Science **305,** 1437-1441.

Liu, Q., Rand, T.A., Kalidas, S., Du, F., Kim, H.E., Smith, D., and Wang, X. (2003). R2D2, a bridge between the inititaion and effector steps of a *Drosophila* RNAi pathway. Science **301,** 1921-1925.

Liu, X., Jiang, F., Kalidas, S., Smith, D., and Liu, Q. (2006). Dicer-2 and R2D2 coordinately bind siRNA to promote assembly of the siRISC complexes. RNA **12,** 1514-1520.

Liu, Y., Schiff, M., and Dinesh-Kumar, S.P. (2002a). Virus-induced gene silencing in tomato. Plant J. **31,** 777-786.

Liu, Y., Schiff, M., Marathe, R., and Dinesh-Kumar, S.P. (2002b). Tobacco Rar1, EDS1 and NPR1/NIM1 like genes are required for N-mediated resistance to Tobacco mosaic virus. Plant J. **30,** 415-429.

MacFarlane, S.A. (1999). Molecular biology of the tobraviruses. J. Gen. Virol. **80,** 2799-2807.

MacRae, I., Ma, E., Zhou, M., Robinson, C.V., and Doudna, J.A. (2007). *In vitro* reconstitution of the human RISC-loading complex. Proc. Nat. Acad. Sci. USA **105,** 512-517.

MacRae, I., Zhou, K., Li, F., Repic, A., Brooks, A.N., Cande, W.Z., Adams, P.D., and Doudna, J.A. (2006). Structural basis for double-stranded RNA processing by Dicer. Science **311,** 195-198.

Martin-Hernandez, A.M., and Baulcombe, D.C. (2008). Tobacco rattle virus 16K encodes a suppressor of RNA silencing that allows transient viral entry into meristems. J. Virol. **82,** 4064-4071.

Martinez, J., Patkaniowska, A., Urlab, H., Luhrmann, R., and Tuschl, T. (2002). Single-stranded antisense siRNAs guide target RNA clevage in RNAi. Cell **110,** 563-574.

Matsuo, K., Hong, J.-S., Tabayashi, N., Ito, A., Masuta, C., and Matsumura, T. (2007). Development of *Cucumber mosaic virus* as a vector modifiable for different host species to produce therapuetic proteins. Planta **225,** 277-286.

McCormick, A.A., Reinl, S.J., Cameron, T.I., Vojdani, F., Fronefield, M., Levy, R., and Tuse, D. (2003). Individualized human scFv vaccines produced in plants:

humoral anti-idiotype responses in vaccinated mice confirm relevance to the tumor Ig. J. Immunol. Methods **278,** 95-104.

Meister, G., Landthaler, M., Patkaniowska, A., Dorsett, Y., Teng, G., and Tuschl, T. (2004). Human Argonaute2 mediates RNA cleavage targeted by miRNAs and siRNAs. Mol. Cell **15,** 185-197.

Mlotshwa, S., Schauer, S.E., Smith, T.H., Mallory, A., Herr-Jr., J.M., Roth, B.M., Merchant, D.D., Ray, A., Bowman, L.H., and Vance, V. (2005). Ectopic DICER-LIKE1 expression in P1/HC-Pro Arabidopsis rescues the phenotypic anomalies but not the defects in microRNA and silencing pathways. Plant Cell **17,** 2873-2885.

Moissiard, G., Parizotto, E.A., Himber, C., and Voinnet, O. (2007). Transitivity in Arabidopsis can be primed, requires the redundant action of the antiviral Dicer-like 4 and Dicer-like 2, and is compromised by viral-encoded suppressor proteins. RNA **13,** 1268-1278.

Napoli, C., Lemieux, C., and Jorgensen, R.A. (1990). Introduction of a chimeric chalcone synthase gene into petunia results in reversible co-suppression of homologous genes *in trans*. Plant Cell **2,** 279-289.

Nelson, D.L., and Cox, M.M. (2005). Lehninger's Principles of Biochemistry. (New York: Freeman and Company).

Nykanen, A., Haley, B., and Zamore, P.D. (2001). ATP requirements and small interfering RNA structure in the RNA interference pathway. Cell **107,** 309-321.

Omarov, R.T., Ciomperlik, J.J., and Scholthof, H.B. (2007). RNAi-associated ssRNA-specific ribonucleases in *Tombusvirus* P19 mutant-infected plants and evidence for a discrete siRNA-containing effector complex. Proc. Natl. Acad. Sci. USA **104,** 1714-1719.

Omarov, R., Qi, D., and Scholthof, K.-B.G. (2005). The capsid protein of satellite panicum mosaic virus contributes to systemic invasion and interacts with its helper virus. J. Virol. **79,** 9756–9764.

Omarov, R., Sparks, K., Smith, L., Zindovic, J., and Scholthof, H.B. (2006). Biological relevance of a stable interaction between the tombusvirus-encoded P19 and siRNAs. J. Virol. **80,** 3000-3008.

Pantaleo, V., Szittya, G., and Burgyan, J. (2007). Molecular bases of viral RNA targeting by viral small interfering RNA-programmed RISC. J. Virol. **81,** 3797-3806.

Park, J.-W., Faure-Rabasse, S., Robinson, M.A., Desvoyes, B., and Scholthof, H.B. (2004). The multifunctional plant viral suppressor of gene silencing P19 interacts with itself and an RNA binding host protein. Virology **323,** 49-58.

Parker, J.S., Roe, S.M., and Barford, D. (2005). Structural insights into mRNA recognition from a PIWI domain-siRNA guide complex. Nature **434,** 663-666.

Qi, D., and Scholthof, K.-B.G. (2008). Multiple activities associated with the capsid protein of satellite panicum mosaic virus are controlled separately by the N- and C-terminal regions. Mol. Plant-Microbe Interact. **21,** 613-621.

Qiu, W., and Scholthof, K.-B.G. (2004). Satellite panicum mosaic virus capsid protein elicits symptoms on a nonhost plant and interferes with a suppressor of virus-induced gene silencing. Mol. Plant-Microbe Interact. **17,** 263-271.

Qiu, W., and Scholthof, H.B. (2007). Tomato bushy stunt virus derived gene vectors. Curr. Prot. Microbiol. **7,** 16In14.12-16In14.16.

Qiu, W.P., Park, J.-W., and Scholthof, H.B. (2002). Tombusvirus P19-mediated suppression of virus induced gene silencing is controlled by genetic and dosage features that influence pathogenicity. Mol. Plant-Microbe Interact. **15,** 269-280.

Qu, F., and Morris, T.J. (2002). Efficient infection of *Nicotiana benthamiana* by *Tomato bushy stunt virus* is facilitated by the coat protein and maintained by p19 through suppression of gene silencing. Mol. Plant-Microbe Interact. **15,** 193-202.

Rakitina, D.V., Yelina, N.E., and Kalinina, N.O. (2006). Zinc ions stimulate the cooperative RNA binding of hordeiviral γb protein. FEBS Lett. **580,** 5077-5083.

Rand, T.A., Ginalski, K., Grishin, N.V., and Wang, X. (2004). Biochemical identification of Argonaute 2 as the sole protein required for RNA-induced silencing complex. Proc. Natl. Acad. Sci. USA **101,** 14385-14389.

Ratcliff, F., Martin-Hernandez, A.M., and Baulcombe, D. (2001). Tobacco rattle virus as a vector for anaylsis of gene function by silencing. Plant J. **25,** 237-245.

Robb, G.B., and Rana, T.M. (2007). RNA helicase A interacts with RISC in human cells and functions in RISC loading. Mol. Cell **26,** 523-527.

Romano, N., and Macino, G. (1992). Quelling: transient inactivation of gene expression in *Neurospora crassa* by transformation with homologous sequences. Mol. Microb. **6,** 3343-3353.

Rossi, J.J. (2005). RNAi and the P-body connection. Nat. Cell Biol. **7,** 643-644.

Ruiz-Ferrer, V., and Voinnet, O. (2007). Viral suppression of RNA silencing: 2b wins the golden fleece by defeating Argonaute. BioEssays **29,** 319-323.

Ryu, C.-M., Anand, A., Kang, L., and Mysore, S. (2004). Agrodrence: a novel and effective agroinoculation method for virus-induced gene silencing in roots and diverse Solanaceous species. Plant J. **40,** 322-331.

Sambrook, J., Fritsch, E.F., and Maniatis, T. (1989). Molecular Cloning: A Laboratory Manual, 2nd ed. (Cold Spring Harbor, N.Y.: Cold Spring Harbor Laboratory Press).

Scholthof, H.B. (2005). Plant virus transport: motions of functional equivalence. Trends Plant Sci. **10,** 376-382.

Scholthof, H.B. (2006). The *Tombusvirus*-encoded P19: from irrelevance to elegance. Nature Rev. Microbiol. **4,** 405-411.

Scholthof, H.B. (2007). Heterologous expression of viral RNA interference suppressors; RISC management. Plant Physiol. **145,** 1110-1117.

Scholthof, H.B., Desvoyes, B., Kuecker, J., and Whitehead, E. (1999a). The biological activity of two tombusvirus proteins translated from nested genes is influenced by dosage control via context-dependent leaky scanning. Mol. Plant-Microbe Interact. **12,** 670-679.

Scholthof, H.B., Morris, T.J., and Jackson, A.O. (1993). The capsid protein gene of tomato bushy stunt virus is dispensable for systemic movement and can be replaced for localized expression of foreign genes. Mol. Plant-Microbe Interact. **6,** 309-322.

Scholthof, H.B., Scholthof, K.-B.G., and Jackson, A.O. (1996). Plant virus gene vectors for transient expression of foreign proteins in plants. Annu. Rev. Phytopathol. **34,** 299-323.

Scholthof, H.B., Scholthof, K.-B.G., Kikkert, M., and Jackson, A.O. (1995a). Tomato bushy stunt virus spread is regulated by two nested genes that function in cell-to-cell movement and host-dependent systemic invasion. Virology **213,** 425-438.

Scholthof, K.-B.G. (1999). A synergism induced by satellite panicum mosaic virus. Mol. Plant-Microbe Interact. **12,** 163-166.

Scholthof, K.-B.G., Jones, R.W., and Jackson, A.O. (1999b). Biology and structure of plant satellite viruses activated by icosahedral helper viruses. Curr. Top. Microbiol. Immunol. **239,** 123-143.

Scholthof, K.-B.G., Mirkov, T.E., and Scholthof, H.B. (2002). Plant viral gene vectors: biotechnology applications in agriculture and medicine. Genet. Eng. **24,** 67-86.

Scholthof, K.-B.G., Scholthof, H.B., and Jackson, A.O. (1995b). The tomato bushy stunt virus replicase proteins are coordinately expressed and membrane associated. Virology **208,** 365-369.

Scholthof, K.-B.G., Scholthof, H.B., and Jackson, A.O. (1995c). The effect of defective interfering RNAs on the accumulation of tomato bushy stunt virus proteins and implications for disease attenuation. Virology **211,** 324-328.

Schroder, E., Jonsson, T., and Poole, L. (2005). Hydroxyapatite chromatography: altering the phosphate-dependent elution profile of protein as a function of pH. Anal. Biochem. **313,** 176-178.

Schwartz, D.S., Hutvagner, G., Du, T., Xu, Z., Aronin, N., and Zamore, P.D. (2003). Assymmetry in the assembly of the RNAi enzyme complexes. Cell **115,** 199-208.

Schwarz, D.S., Hutvagner, G., Haley, B., and Zamore, P.D. (2002). Evidence that siRNAs function as guides, not primers, in the *Drosophila* and human RNAi pathway. Mol. Cell **10,** 537-548.

Schwarz, D.S., Tomari, Y., and Zamore, P.D. (2004). The RNA-induced silencing complex is a Mg^{2+}-dependent endonuclease. Curr. Biol. **14,** 787-791.

Shams-Bakhsh, M., Canto, T., and Palukaitis, P. (2007). Enhanced resistance and neutralization of defense responses by suppressors of RNA silencing. Virus Res. **130,** 103-109.

Sheth, U., and Parker, R. (2003). Decapping and decay of messanger RNA occur in cytoplasmic processing bodies. Science **300,** 805-808.

Siddiqui, S.A., Sarmiento, C., Trueve, C., Lehto, H., and Lehto, K. (2008). Phenotypes and functioanl effects caused by various viral RNA silencing suppressors in transgenic *Nicotiana benthamiana* and *N. tabacum*. Molec. Plant Microbe Interact. **21,** 178-187.

Silhavy, D., and Burgyan, J. (2004). Effects and side-effects of viral RNA silencing suppressors on short RNAs. Trends Plant Sci. **9,** 76-83.

Singh, D.P., Moore, C.A., Gilliland, A., and Carr, J.P. (2004). Activation of multiple antiviral defense mechanisms by salicylic acid. Mol. Plant Pathol. **5,** 57-63.

Song, J.J., and Joshua-Tor, L. (2006). Ago and RNA - getting into the groove. Curr. Opin. Biol. Rev. **16,** 5-11.

Song, J.-J., Smith, S.K., Hannon, G.J., and Joshua-Tor, L. (2004). Crystal structure of Argonaute and its implications for RISC slicer activity. Science **305,** 1434-1437.

Tabara, H., Yigit, E., Siomi, H., and Mello, C.C. (2002). The dsRNA binding protein RDE-4 interacts with RDE-1, DCR-1, and a DExH-box helicase to direct RNAi in *C. elegans*. Cell **109,** 861-871.

Toila, N.H., and Joshua-Tor, L. (2007). Slicer and the Argonauts. Nat. Chem. Biol. Rev. **3,** 36-43.

Tomari, Y., Du, T., and Zamore, P.D. (2007). Sorting of *Drosophila* small silencing RNAs. Cell **130,** 299-308.

Tomari, T.Y., Matranga, C., Haley, B., Martinez, N., and Zamore, P.D. (2004). A protein sensor for siRNA assymetry. Science **306,** 1377-1380.

Tomari, Y., and Zamore, P.D. (2005). Perspective: machines for RNAi. Gene Dev. **19,** 517-529.

Turina, M., Desvoyes, B., and Scholthof, K.-B.G. (2000). A gene cluster encoded by Panicum mosaic virus is associated with virus movement. Virology **266,** 120-128.

Turina, M., Maruoka, M., Monis, J., Jackson, A.O., and Scholthof, K.-B.G. (1998). Nucleotide sequence and infectivity of a full-length cDNA clone of panicum mosaic virus. Virology **241,** 141-155.

Turina, M., Omarov, R., Murphy, J.F., Bazaldua-Hernandez, C., Desvoyes, B., and Scholthof, H.B. (2003). A newly identified role for the *Tomato bushy stunt virus* P19 in short distance spread. Mol. Plant Pathol. **4,** 67-72.

Tzfira, T., and Citovsky, V. (2002). Partners-in-infection: host proteins involved in transformation of plant cells by *Agrobacterium*. Trends Cell Biol. **12,** 121-129.

Tzfira, T., and Citovsky, V. (2006). Agrobacterium-mediated genetic transformation of plants: biology and biotechnology. Curr. Opin. Biotechnol. **17,** 147-154.

Vagin, V.A., Sigova, A., Li, C., Seitz, H., Gvozdev, V., and Zamore, P.D. (2006). A distinct small RNA pathway silences selfish genetic elements in the germline. Science **313,** 320-324.

Vasquez, F., Vaucheret, H., Rajagopalan, R., Lepers, C., Gasciolli, V., Mallory, A., Hilbert, J., Bartel, D.P., and Crete, P. (2004). Endogenous *trans*-acting siRNAs regulate the accumulation of *Arabidopsis* mRNAs. Mole. Cell **16,** 69-79.

Voinnet, O. (2005). Induction and suppression of RNA silencing: Insights from viral infections. Nat Rev Genet. **6,** 206-220.

Voinnet, O., and Baulcombe, D.C. (1997). Systemic signaling in gene silencing. Nature **389,** 553.

Voinnet, O., Pinto, Y.M., and Baulcombe, D.C. (1999). Suppression of gene silencing: a general strategy used by diverse DNA and RNA viruses of plants. Proc. Natl. Acad. Sci. USA **96,** 14147-14152.

Voinnet, O., Rivas, S., Mestre, P., and Baulcombe, D. (2003). An enhanced transient expression system in plants based on suppression of gene silencing by the p19 protein of tomato bushy stunt virus. Plant J. **33,** 949-956.

Wagner, B., Fuchs, H., Adhami, F., Ma, Y., Scheiner, O., and Breiteneder, H. (2004). Plant virus expression systems for transient production of recombinant allergens in *Nicotiana benthamiana*. Methods **32,** 227-234.

White, K.A. (1996). Formation and evolution of Tombusvirus defective interfering RNAs. Sem. Virol. **7,** 409-416.

Wingard, S.A. (1928). Hosts and symptoms of ringspot, a virus disease of plants. J. Agric. Res. **37,** 127-153.

Wroblewski, T., Tomczak, A., and Michelmore, R. (2005). Optimization of Agrobacterium-mediated transient assays of gene expression in lettuce, tomato and Arabidopsis. Plant Biotechnol. J. **3,** 259-273.

Xie, Z., Johansen, L.K., Gustafson, A.M., Kasschau, K.D., Ellis, A.D., Zilberman, D., Jacobsen, S.E., and Carrington, J.C. (2004). Genetic and functional diversification of small RNA pathways in plants. PLoS Biol. **2,** E104.

Yamamura, Y., and Scholthof, H.B. (2005). Pathogen profile: Tomato bushy stunt virus: A resilient model system for studying virus-plant interactions. Mol. Plant Pathol. **6,** 491-502.

Ye, K., Malinina, L., and Patel, D. (2003). Recognition of small interfering RNA by a viral suppressor of RNA silencing. Nature **426,** 874-878.

Yelina, N.E., Savenkov, E.I., Solovyev, A.G., Morozov, S.Y., and Valkonen, J.P. (2002). Long-distance movement, virulence, and RNA silencing suppression controlled by a single protein in hordei- and potyviruses: complementary functions between virus families. J. Virol. **76,** 12981-12991.

Yuan, Y.R., Pei, Y., Chen, H.Y., Tuschl, T., and Patel, D. (2006). A potential protein-RNA recognition event along the RISC-loading pathway from the structure of A. aeolicus Ago with the externally bound siRNA. Structure **14,** 1557-1565.

Zaitlin, M. (1998). The discovery of the causal agent of the Tobacco mosaic disease. In Discoveries in Plant Biology, S.D. Kung and S.F. Yang, eds (Hong Kong: World Publishing Co., Ltd), pp. 105-110.

Zhang, X., Henderson, I.R., Lu, C., Green, P.J., and Jacobsen, S.E. (2007). Role of RNA polymerase IV in plant small RNA metabolism. Proc. Nat. Acad. Sci. USA **104,** 4536-4541.

Zhang, X., Yuan, Y.R., Pei, Y., Lin, S.S., Tuschl, T., Patel, D.J., and Chua, N.H. (2006). Cucumber mosaic virus-encoded 2b suppressor inhibits Arabidopsis Argonaute1 cleavage activity to counter plant defense. Genes Dev. **20,** 3255-3268.

APPENDIX
TBSV VIRION PURIFICATION BY COLUMN CHROMATOGRAPHY

Introduction

Tomato bushy stunt virus (TBSV) serves as a common model virus for plant systems. It is a single-stranded, positive-sense RNA virus with an iscosahedral capsid structure. The particles are reported to be 33 nm in diameter (Hull, 2002; Yamamura and Scholthof, 2005). TBSV is also of research importance as it produces the highly effective silencing suppressor P19, routinely used in RNAi studies (Scholthof, 2006). Traditional methods of purification for *Tomato bushy stunt virus* (TBSV) and other viruses involve isolation of the virions by centrifugation gradients with sucrose and cesium chloride (Fields et al., 2007). These protocols are time consuming and require multiple steps. In this section, I address the possibility for the use of hydroxyapatite as an alternative to purify virions; it is rapid, inexpensive to assemble, and economical as the column media can be regenerated for multiple uses.

Hydroxyapatite is a calcium phosphate ceramic, $Ca_{10}(PO_4)_6(OH)_2$ (Gagnon et al., 1996), coincidentally used in the medical field as a biomaterial filler for teeth and bones and as a covering to promote growth of bones into prosthetic implants. As a column chromatography medium, it separates by a 'mixed-modes' or pseudo-affinity means of ion exchange. The positively-charged calcium ions and negatively-charged phosphate ions allow for interaction with both positively charged amino acids of proteins, and negatively charged carbonyls of DNA groups, or carboxylate residues on protein surfaces (Schroder et al., 2005). This allows for differential separation via functional group electrostatic interactions with the column media, and elution through application of buffer with an increasing gradient of phosphates (Gagnon et al., 1996; Schroder et al., 2005).

Here, a method is reported to quickly purify TBSV and possibly other virions from infected plant crude extract following centrifugation and column application. When crude plant extract was applied to the column, it is demonstrated that virions comprise the only contents of the flowthrough buffer, without further purification steps. These virions are present in high concentration and purity, and are suitable for rub inoculation with up to a thousand-fold dilution. Resultant infections are identical to those of plants that have

been inoculated with TBSV RNA-transcripts, or inoculated with infected tissue. Virion purification via hydroxyapatite chromatography may be preferable to other methods in that it is more economical than generating RNA-transcripts in vitro, and deleterious effects of defective interfering RNAs, seen in passaged TBSV infections (Scholthof et al., 1995c; White, 1996), are not a concern.

Materials and Methods

Infection of plants with TBSV.

Infectious TBSV RNA transcripts were generated in vitro using a Fermentas T7 transcription kit (1 µl linearized DNA, 16 µl dd-water, 5 µl 5X transcript buffer, 2.5 µl 5 mM rNTP mix, 2 µl 0.1 mM DTT, 0.25 µl Ribolock RNase inhibitor, and 0.5 µl T7 RNA polymerase (Fermentas, Glen Burnie, MD). To confirm transcription, 3 µl of transcripts were mixed with 1 µl loading dye and electrophoresied on a 1% agarose gel and stained with ethidium bromide. These transcripts were then mixed in a 1:4 dilution with cold RNA inoculation buffer (50 mM KH_2PO_4, 50 mM Glycine, pH 9.0, 1% celite, 1% bentonite), and 3 leaves of 3 week-old *N. benthamiana* plants were rub-inoculated with 20 µl of the dilution apiece. A week was allowed for establishment of the infection, then plant tissue was harvested by grinding upper leaves with 50 ml of 10 mM sodium phosphate buffer, pH 6.8, by mortar and pestle. This crude extract was then centrifuged at 4000 rpm, 4°C, for 20 min. with a Beckman S4180 rotor to remove insoluble proteins. The supernatant was filtered through cheesecloth into conical-bottomed tubes, and further clarified by centrifugation at 10,000 rpm, 4°C, for 20 min. in a Beckman F0630 rotor, and the supernatant placed on ice for application to the column.

Hydroxyapatite column preparation and virion purification

The chromatographic arrangement involved a 30 x 2.5 cm chromatographic column attached to a peristaltic pump for elution purposes. The column was packed with 40 ml of CHT ceramic hydroxyapatite media (Bio-Rad, Hercules, CA) according to manufacturer's directions, briefly reviewed as follows: 80 ml of 200 mM dibasic sodium phosphate buffer was applied to the column, followed by 80 ml 200 mM sodium phosphate buffer, pH 6.8, to rapidly lower the pH. A 10 mM sodium phosphate buffer,

pH 6.8, was used to equilibrate the column and as running buffer; the column was washed extensively (~200 ml) with this buffer before application of the plant extract. Once the column was packed, the extract was applied to the column at a flow rate of about 1.3 ml/min. Flowthrough containing virions was collected (usually about 50-100 ml). This preparation was either used immediately to inoculate plants, or frozen at (-) 20° C for later use.

Additionally, *Capsicum annuum* (pepper) plants were inoculated with wt TBSV, and a small (about 10 ml) hydroxyapatite column was used for chromatography of 5 grams of plant tissue. The flowthrough was collected, and concentrated using a vacuum dehydrator. The concentration of potential virions was determined by staining a 1% agarose electrophoresis gel before submitting the sample for electron microscopy.

Verification of virions

Column flowthrough was used to inoculate three week-old *N. benthamiana* plants. For this, 100 µl of the flowthrough was mixed with RNA inoculation buffer as described in Table A.1. Plants were incubated at room temperature, and checked for infection.

Table A.1 Virion dilution for *N. benthamiana* plant assays.

	I	Ii	Iii	iv	V
Virions soln.	0.1 µl	1.0 µl	10 µl	50 µl	100 µl
Virus inoculation buffer	200 µl	199 µl	190 µl	150 µl	100 µl

Additionally, flowthrough was inspected by transmission electron microscopy. A sample (2 µl) was stained with uranyl acetate, and viewed at high magnification. (Electron microscopy performed by E. Ann Ellis, Microscopy and Imaging Center, Texas A&M University).

Results

Upon column chromatography of extracts from TBSV ΔP19 infected plants, proteins can be visualized as a single band at about 41 kDa with Coomassie and silver staining ($AgNO_3$) techniques (Fig. A.1A). Using an antibody generated against TBSV CP, western blot analysis (Fig. A.1B) verified the presence of TBSV CP, as well as another band around 85 kDa (possibly CP aggregates). Following northern blotting of SDS-treated crude extracts and virion-containing column flowthrough (Fig. A.1C), hybridization probes specific for TBSV demonstrate the presence of RNA. Additionally, a native (whole virus) gel displays the presence of a discrete band in the flowthrough column, slightly smaller than that in the crude extracts column, representative of virions (Fig. A.1D).

The column flowthrough was diluted out in 0.25, 0.05, 0.005, and 0.0005 dilutions (Table A.1), and all were used to rub inoculate 3 week-old *N. benthamiana* plants. Plants infected with virion-containing column flow-through displayed typical TBSV symptoms (Fig. A.2), with curled, crinkled upper leaves. Following one week post inoculation, all plants showed evidence of infection, indicating a very high concentration. To determine if the symptoms present were the result of a true TBSV infection, about 0.5 grams (1 leaf) infected tissue was removed from the plants. RNA was extracted from the tissue, and analyzed by northern blotting with a TBSV-specific probe. These northern blots from virion-infected plants displayed ample genomic and subgenomic RNA signals when probed with a TBSV hybridization probe (Fig. A.3), indicating a TBSV infection results upon inoculation of *N. benthamiana* with the virions purified with hydroxyapatite. It is interesting to note that it appears that equal amounts of TBSV RNA are present for all dilutions.

Virions were also visualized with transmission electron microscopy. Following staining with uranyl acetate and magnification, spherical virions about 35 nm in size were seen isolated from TBSV and TBSV ΔP19 infected plants (Fig. 2.S.4A- B). These were present in what appeared to be a high titer, and the sample looked clear of any cellular

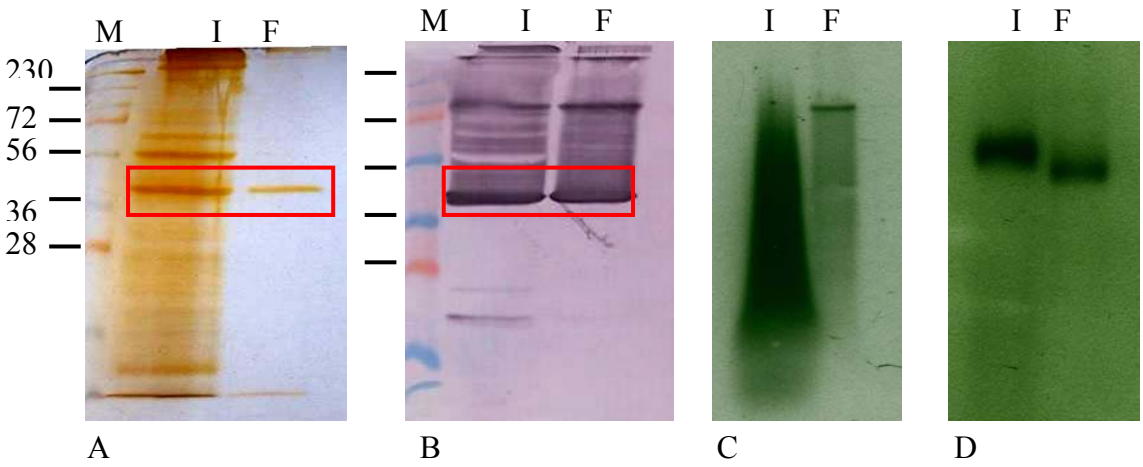

Fig. A.1 Visualization of TBSV virions. M is Protein ladder, I indicates crude extract prior to application to column (the input), F is flow-through elution from column during washing with 10 mM sodium phosphate buffer. A.) The single band present in F (flowthrough) lane is TBSV coat protein (CP). B.) Western blot probed with antibodies against TBSV coat protein. C.) Northern blot hybridization following treatment of samples with 10% SDS to disrupt capsid and release nucleic acid, probed for TBSV; D. northern blot of a native gel, probed for TBSV. (lines indicate marker size, as denoted on the left side, and boxes enclose the ~ 41 kDa CP bands).

Fig. A.2 Virion-inoculated *N. benthamiana*. *N. benthamiana* inoculated with a thousand-fold dilution of hydroxyapatite column flowthrough containing only virions for a TBSV 19-defective mutant. Infection demonstrates typical TBSV symptoms for the TBSV mutant.

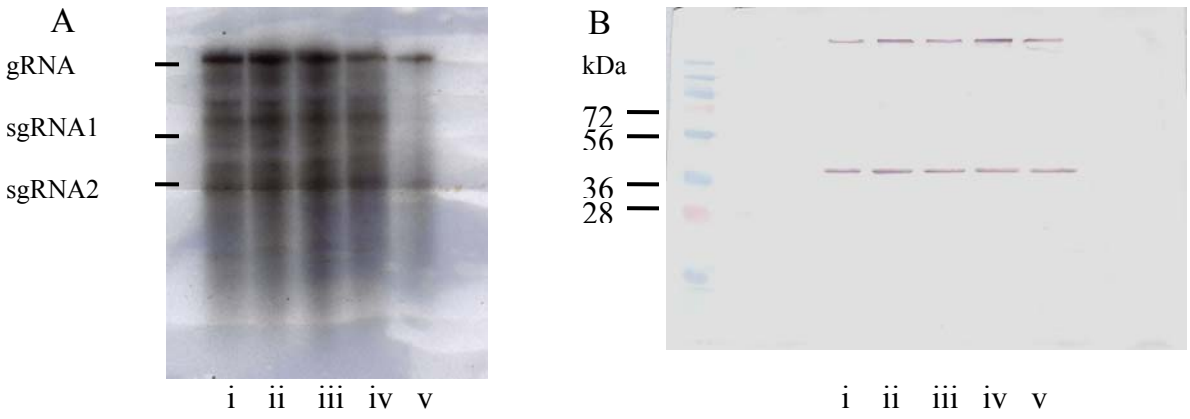

Fig. A.3 Blots from plants infected with dilutions of the virions. These were assayed for A.) TBSV RNA (indicated as genomic or subgenomic) by a northern blot with a hybridization probe for TBSV, and B.) CP with a western blot. Dilutions of virions are i.) 0.1 / 200; ii.) 1/200; iii.) 1/20; iv.) 0.25; and v.) 0.5.

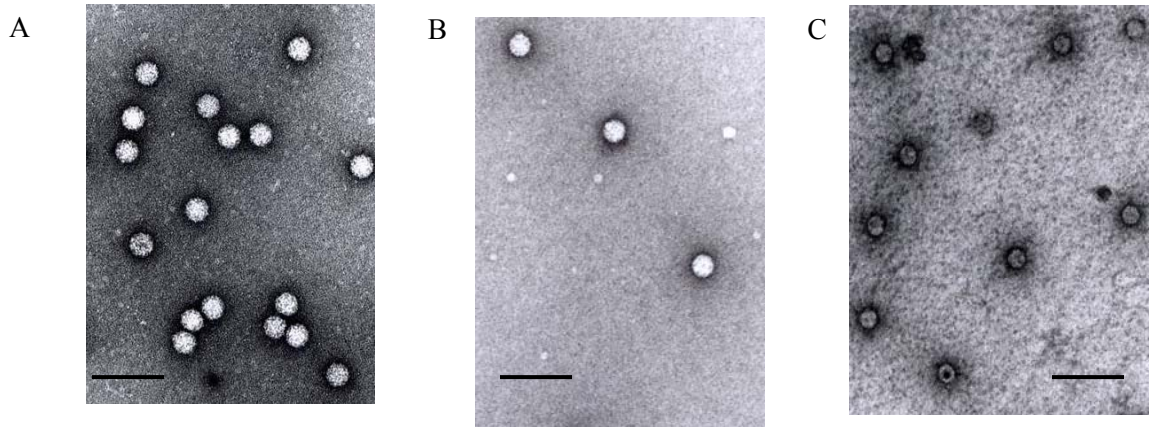

Fig. A.4 Virions visualized by electron microscopy. A.) wt TBSV virions and B.) TBSV Δ P19 virions, isolated from *N. benthamiana.* C.) wt TBSV virions isolated from *C. annuum* (pepper) plants, and concentrated prior to visualization. (Bar indicates approx. size of 100 nm) .

Slightly smaller virions, ~33 nm in size, were found in the flowthrough of wt TBSV infected peppers plants (Fig. 2.S.4C). These virions were present in a much more dilute quantity, and required concentration by vacuum centrifugation before visualization. The sample from infected pepper tissue also contains what appears to be slight cellular debris, most likely due to the necessary concentration, or possibly effects of a different host on hydroxyapatite chromatography.

Discussion

This set of experiments was performed following the observation of a discrete protein band for about 42 kDa in the flowthrough of TBSV-infected plant tissue crude extract after hydroxyapatite chromatography. Following silver staining, northern blotting, and detection of CP with western blotting, it was shown that the protein band represents CP and that the flowthough contains complete virions. However, following a native whole gel analysis by northern blotting, the flowthrough bands were smaller than that observed for the crude plant extract; this might be interpreted as the virions not being associated with any cellular elements after purification.

Based on EM visualization, it appears that the method yields a remarkably pure isolation of virions, eliminating need of further purification steps. This method also works for various TBSV mutants in the lab, provided that they form complete virions. One of the few limitations to this method of virion purification seem to be due to storage. It has been observed that following several rounds of thawing and refreezing, virions stored at - 20°C lose infectivity. This is most likely due to the damage associated with freezing and thawing, and virions viewed by EM seem to exhibit capsid damage. Different methods of storage are recommended, such as in a 25% glycerol buffer.

Tissue from proso millet (*Panicum miliaceum* L.) plants infected with a PMV/SPMV mixed infection were also subjected to hydroxyapatite column chromatography, and the flowthrough was examined for the presence of virions. Virions were not detected in the flowthrough (data not shown). There are several possible explanations for this; virions might be associated with different cellular components, and not as easily purified by grinding tissue. There might be less virions present, leading to undetectable amount by staining. To test this, these samples would need to be inoculated

on proso millet, and see if an infection is established. Alternately, the flowthrough could be concentrated, and re-assayed.

Additionally, to further explore if virions can only be purified in this manner due to host specificity, a 2 week-old pepper plant was inoculated with TBSV. Following establishment of infection, extract from the upper leaves was subjected to column chromatography. There appears to be a band present at about the correct size after staining with ethidium bromide (data not shown), and electron microscopy was done to further verify that virions were present (Fig. 2.S.4). The presence of virions in flowthrough from pepper indicate that this method of TBSV virion purification is not host specific. This might imply that it is possible to purify virions in this manner for other icosahedral viruses of a similar size. Future experiments to develop this method of virion purification would include purifying virions from plant tissue infected with viruses that have differently shaped capsids; ideal for this would be *Tobacco mosaic virus* with a rigid rod shape, or the flexuous rod-shaped *Potato virus X*, as well as possibly determining if viruses can be purified for insect or animal systems.

The concept of using hydroxyapatite to isolate virions from infected plant tissue is not necessarily that surprising; *Tobacco mosaic virus* was originally purified from infected plant tissue using porcelain filters (Zaitlin, 1998), and hydroxyapatite medium forms a ceramic column. However, cellular debris is removed by centrifugation before column application, and all other cellular and unassociated viral elements most likely remain bound to the mixed affinity matrix of the column before elution with a higher concentration of sodium phosphate, leaving only virions to pass through.

The size difference between virions isolated from the tissues of different plants (Fig. 2.S.4) might be due to swelling of the virus particle. This has been observed upon removal of divalent cations like calcium from the particles of several different viruses, such as *Brome mosaic virus, Turnip crinkle virus,* and *Cowpea chlorotic mottle virus*, (Heaton, 1992). It is reasonable to assume something similar might occur during purification (as illustrated in the differences between band sizes as observed in Fig. 2.S.1.D, with a native gel assay). However, this has no bearing on infectivity, as seen in Fig. 2.S.2.

In conclusion, this report shows that TBSV virions can be quickly and simply purified from infected plant tissue using a hydroxyapatite chromatography column. Following centrifugation to remove insoluble plant tissue, crude plant extract can be applied to a column, and virions are present in the flowthrough wash. This produces a clear source of inoculum that might be preferable to current methods. For instance, sucrose density centrifugation is time consuming and requires multiple steps, the in vitro generation of TBSV RNA transcripts using T7 polymerase is expensive, and using crude extract from infected plants has detrimental effects to the infection due to the co-infection with TBSV DIs (Scholthof et al., 1995c; White, 1996). The method reported here yields virions that are the correct size and morphology, and are readily infectious, and therefore provides a rapid, inexpensive, and reliable alternative.

VITA

Jessica J. Ciomperlik

2132 TAMU
College Station, TX 77843-2132
Telephone: (979) 845-7831
Fax: 979-845-6483

email: jciomp@gmail.com

Education

2006 Texas A&M University, College Station
Bachelor of Science – Biology
2008 Texas A&M University, College Station
Master of Science – Plant Pathology and Microbiology

Publications, Presentations and Abstracts

Omarov, R.T**., Ciomperlik, J.**, and Scholthof, H.B. (2007) An RNAi-associated siRNA-containing ribonuclease complex in *Tombusvirus* P19 mutant-infected plants Annual Meeting of American Society for Virology, Corvallis, OR, July, 2007.

Omarov, R.T., **Ciomperlik, J.J.**, and Scholthof, H.B. (2007) RNAi-associated ssRNA-specific ribonucleases in *Tombusvirus* P19 mutant-infected plants and evidence for a discrete siRNA-containing effector complex. Proc. Natl. Acad. Sci USA**. 104**, 1714-1719.

Ciomperlik, J., and Scholthof, H.B. (2007) Characterization of siRNA-associated complexes generated by different viruses and their contribution potential anti-viral RNAi. Annual Plant Virology meeting, Noble Foundation, Ardmore, OK, April, 2007.

Ciomperlik, J. (2006) Isolation and Characterization of an anti-viral RISC in plants. Senior thesis, Texas A&M University, May 2006.http://handle.tamu.edu/1969.1/3653

Ciomperlik, J., Omarov, R., and Scholthof, H.B. (2006). A virus-activated RNA-induced silencing complex (RISC) in plants. Annual Plant Virology meeting, Noble Foundation, Ardmore, OK, April 2006.

Ciomperlik, J., Omarov, R., and Scholthof, H.B. (2006). A virus-activated RNA-induced silencing complex (RISC) in plants. Texas A&M University student research week, March 2006.